A Rapid Lipid-based Approach for Normalization of Quantum Dot-detected Biomarker Expression on Extracellular Vesicles in Complex Biological Samples

by

Meryl Rodrigues

A Dissertation Presented in Partial Fulfillment
of the Requirements for the Degree
Doctor of Philosophy

Approved June 2019 by the
Graduate Supervisory Committee:

Tony Hu, Chair
Mehdi Nikkhah
Samira Kiani
Barbara Smith
Haiyong Han

ARIZONA STATE UNIVERSITY

August 2019

ABSTRACT

Extracellular Vesicles (EVs), particularly exosomes, are of considerable interest as tumor biomarkers, since tumor-derived EVs contain a broad array of information about tumor pathophysiology including its metabolic and metastatic status. However, current EV based assays cannot distinguish between EV biomarker changes by altered secretion of EVs during diseased conditions like cancer, inflammation, etc. that express a constant level of a given biomarker, stable secretion of EVs with altered biomarker expression, or a combination of these two factors . This issue was addressed by developing a nanoparticle and dye-based fluorescent immunoassay that can distinguish among these possibilities by normalizing EV biomarker level(s) to EV abundance, revealing average expression levels of EV biomarker under observation. In this approach, EVs are captured from complex samples (e.g. serum), stained with a lipophilic dye and hybridized with antibody-conjugated quantum dot probes for specific EV surface biomarkers. EV dye signal is used to quantify EV abundance and normalize EV surface biomarker expression levels. EVs from malignant (PANC-1) and nonmalignant pancreatic cell lines (HPNE) exhibited similar staining, and probe-to-dye ratios did not change with EV abundance, allowing direct analysis of normalized EV biomarker expression without a separate EV quantification step. This EV biomarker normalization approach markedly improved the ability of serum levels of two pancreatic cancer biomarkers, EV EpCAM and EV EphA2, to discriminate pancreatic cancer patients from nonmalignant control subjects. The streamlined workflow and robust results of this assay are suitable for rapid translation to clinical applications and its flexible design permits it to be rapidly adapted to quantitate

other EV biomarkers by the simple swapping of the antibody-conjugated quantum dot probes for those that recognize a different disease-specific EV biomarker utilizing a workflow that is suitable for rapid clinical translation.

DEDICATION

I am extremely happy and proud to dedicate this work to my family- my loving, caring and overly protective mumma, my strong and supportive papa and my courageous and motivating little sis without whom I wouldn't be where I am and the person I am today. I know how proud they are of me but I rarely get to say how grateful I am to be their kid and to have them believe in my dreams. They know very little about the work I do, but they have been there for me during each and every step of this journey; knowing that doing this makes me happy is all that matters to them. It surely wasn't an easy road to get here but I always knew that they were there for me and as my mom would say everything will be fine in the end, as long as I believe in myself and her prayers will do the rest. Your family is what God chooses for you and my friends are my family I have found far away from home. Varun, thank you for listening to me each day and always being there, night or day, I am very lucky to have someone like you in my life to be able to share the rest of it with. Rishabh, thank you being my family here, nothing could have brought me more happiness than sharing and finishing this journey with you.

In a Ph.D. student's life research is a 24x7 thing, if were aren't physically doing experiments, we most likely are mentally preparing for one. During this phase what helped me in maintaining my sanity and remaining under check were my friends. Each one played a significantly role in his or her way, the ones here at ASU and far away as well. I would like to thank Sam, Harpinder, Sandhya, Kalyani, Pallavi, Rohit, Mansa, Akash and Pouya for helping me have a life outside my research; I have enjoyed every moment of it. I could not have done this without the love and support from my family and all my friends. I am blessed to have you all in my life. Last I would like to dedicate this to my grandparents whom I love and miss so much, I know you are looking out for me and are proud of me.

ACKNOWLEDGMENTS

As a child, I always wondered what/how one needed to study to be a scientist and, back home in India, I never knew the answer to that. When most career paths were stereotypes that had been perpetuated through millennia, my parents backed me to break the shackles and go on a journey to live my dream at the expense of being far away from them. When I came to ASU, I was under the impression that I had enough knowledge to be on par with the research and innovation that happens here, little did I know that theoretical knowledge was far from having hands-on experience and being a part of something that can make an actual difference in improving human lives. This realization which gives my research meaning and purpose has been the biggest lesson of my graduate life, and I would like to take this opportunity to express my gratitude to everyone that has contributed to it.

First, I would like to thank my adviser, Dr. Tony Hu, for believing in me when I truly needed it the most. I still remember his first talk, where at the end he showed a picture of a group of happy kids who were suffering from HIV and he said that it reminded him of his kids and that is what inspired him to build transformative platforms that would not be relegated solely to the pages of a peer-reviewed journal but could be easily translated into the real world and have an impact where its most needed- the clinical setting. His passion and drive are the key attributes that pushed me towards achieving my goals and finishing my Ph.D. with results that I am proud of. I have learnt a lot from him about focusing on the right research question, maintaining collaborations and mentoring young future scientists. I would not have been able to achieve what I have in the last two years if it hadn't been for his constant guidance, support and belief in my work.

Next, I would like to thank Dr. Christopher Lyon for his continuous input, expertise, and scientific rigor that helped me in designing robust experiments and asking the right questions. You helped me look at research in a way that optimized my time at the bench and by understanding what was required to tackle a problem effectively and efficiently.

I am very grateful to all the members who have been a part of my committee: Dr. Mehdi Nikkhah, Dr. Samira Kiani, Dr. Barbara Smith, and Dr. Haiyong Han for their insightful comments, expertise and guidance in driving my research in the right direction.

It has been the best years of my Ph.D. life working in Dr.Hu's lab and I am thankful for having had the opportunity to work with such passionate and hardworking fellow researchers. I would like to thank Nicole Richards- it has been a pleasure mentoring you and I am grateful for all the hard work and dedication you have shown towards this project. Thank you Dr. Qingbo Shu, and Dr. Xiangxing Kong for all the insightful and exciting discussion we have had over science. Thank you Devika for being so kind and helpful. I am grateful to The Biodesign Institute for the platform it has provided me with; it holds a special place in my heart, having worked here for 7 years now, it surely feels like home. I would like to thank all my faculty and staff at the School of Biological and Health Systems Engineering department for the constant help and support, both Laura and Dr. Buneo

Finally, I would like to acknowledge the support provided by NIH (U01CA214254, R01HD090927, R01AI122932, R01AI113725, and R21Al126361-01) and the Arizona Biomedical Research Commission (ABRC) young investigator award through which most of the work in this dissertation was funded. I sincerely apologize if I have forgotten to acknowledge anyone.

TABLE OF CONTENTS

CHAPTER Page

CHAPTER Page

CHAPTER Page

LIST OF TABLES

Table Page

LIST OF FIGURES

Figure Page

Figure Page

Figure Page

Figure Page

Figure Page

Figure Page

Figure Page

Figure Page

PREFACE

This dissertation includes original research and review articles previously published by the primary author. Chapter 1 focuses on the background and role of EVs in infectious disease and cancer and Chapter 7 which discusses the future work of the quantum dot assay in detection of bacteria related EVs (Rodrigues, M., J. Fan, C. Lyon, M. H. Wan, and Y. Hu (2018). "Role of Extracellular Vesicles in Viral and Bacterial Infections: Pathogenesis, Diagnostics, and Therapeutics." Theranostics 8(10): 2709-2721, Copyright ©2019 Ivyspring International Publisher). Chapter 2 discusses the release of EV in cancer vs normal cells, Chapter 3 focuses on the use of a lipid dye to measure the number of EVs in a sample, Chapter 4 emphasizes on the use of the two pancreatic cancer-specific markers to distinguish between cancer and normal EVs, Chapter 5 discusses about the design and development of the quantum dot assay with Chapter 7 covering the clinical validation of the assay (Reprinted with permission from Rodrigues, Meryl; Richards, Nicole; Ning, Bo; Lyon, Christopher; Hu, Tony, "Rapid lipid-based approach for normalization of quantum dot-detected biomarker expression on extracellular vesicles in complex biological samples", Nano Letters Article ASAP, DOI:10.1021/acs.nanolett.9b02232, Copyright © 2019, American Chemical Society)

CHAPTER

1 BACKGROUND AND RESEARCH OBJECTIVES

1.1. Introduction

Extracellular vesicles (EVs), particularly exosomes, have gained attention for their potential as disease biomarkers and therapeutic agents. EVs are exosomes released by the endocytic pathway that range from 30-100 nm in diameter, and contain host (and pathogen)-derived nucleic acid, protein and lipid cargos. Microvesicles (also known as shedding vesicles, ectosomes or microparticles), are a distinct type of exosome that forms by the outward budding of the plasma membrane and are 100-1000 nm in diameter. These EV types are distinct in their subcellular site of origin and physical parameters, but the size overlap of exosomes and microvesicles and differences in exosome isolation and handling procedures can lead to confusion, despite ongoing efforts by the International Society for Extracellular Vesicles (ISEV) to standardize and harmonize these methods (Witwer, Buzas et al. 2013, Lener, Gimona et al. 2015).

1.1.1. Exosome biogenesis

Exosomes are formed is a multistep process which includes four stages: initiation, endocytosis, multivesicular bodies formation (MVBs) and exosome secretion (Zhang, Yuan et al. 2015). It begins with inward invagination of the cellular plasma membrane to form an early endosome. The early endosome undergoes several changes as it matures to form a late endosome. The limiting membrane of the late endosome undergoes a series of inward invaginations resulting in accumulation of intraluminal vesicles (ILVs) and formation of MVBs that eventually fuse with the plasma membrane to release exosomes into the extracellular space. Recent research in the field has brought to light that exosomes

may represent a vehicle for intercellular communication. In fact, exosomes may deliver proteins, soluble factors, nucleic acids and RNAs (mRNA and miRNA) and modulate protein expression in recipient cells (Rodrigues, Fan et al. 2018). This appears to be of great importance for maintaining normal homeostasis of the body and the pathogenesis of the disease, including tumors. Studies revealed that Rab guanosine triphosphates (GTPase) play a critical role in the regulation of exosome secretion. Studies show that Rab27a/b affects the size and localization of MVBs, while Rab3 regulates MVB docking and tethering at the plasma membrane (Zhang, Yuan et al. 2015). Apart from Rab GTPase playing a role in exosome secretion, there is evidence that accumulation of intracellular Ca^{2+} results in an increase in exosome secretion (Savina, Furlan et al. 2003). Soluble factors (e.g., nucleic acids, proteins, carbohydrates, and other factors), are captured from the cytosol during endosomal membrane invagination, but these components can be preferentially enriched by interaction with endosomal membrane factors, including the endosomal sorting complexes required for transport (ESCRTs) which recognize ubiquitinylated proteins. Despite much progress in the field, there are significant gaps in the understanding of the mechanisms responsible for sorting proteins into internal vesicles of multivesicular compartments and, hence, to exosomes (Whiteside 2016, Rodrigues, Fan et al. 2018) (Figure 1A).

1.1.2. Exosomal Cargo

EVs carry an imprint of their parent cell, which includes nucleic acids, proteins, enzymes, lipids, cytokines and other soluble factors but do not completely resemble the parent cell (van der Pol, Boing et al. 2012, Raposo and Stoorvogel 2013). Due to their endosomal origin, EVs carry components of the endosomal-sorting complex required for

transport (ESCRT) along with other ESCRT-associated molecules (Colombo, Moita et al. 2013). EV membranes are enriched for several broadly expressed tetraspanins proteins , including CD9, CD63, and CD81 - molecules used as EV markers confirming the endocytic origin of the vesicles (Andreu and Yanez-Mo 2015). EVs express molecules involved in MVB biogenesis such as TSG101 and ALIX, proteins that participate in signal transduction such as protein kinase, metabolic enzymes, heat shock proteins (HSP70, HSP 90), and lipid raft proteins like flotillin-1. They contain membrane trafficking proteins like Annexin and Rab family proteins, cytoskeleton proteins like actin and tubulin, and various transmembrane proteins (De Toro, Herschlik et al. 2015, Whiteside 2016) (Figure 1B).

Furthermore, EV-specific protein molecules may be subjected to the cell type or tissue birthplace from which the EV originates and may differ based on any physiological changes or stimulations the cell underwent. An example of this is the presence of major histocompatibility class (MHC) I and II complexes on EVs derived from antigen-presenting cells such as B-cells or dendritic cells (DCs), or presence of tumor antigens in tumor-derived EVs (Rodrigues, Fan et al. 2018). Because of their endosomal origin, nuclear, or mitochondrial proteins have not been found in EVs (De Toro, Herschlik et al. 2015). Further studies have revealed the presence of messenger RNA (mRNA) and microRNA (miRNA) in EVs, in addition to other RNA species like transfer RNA, long non-coding RNA and even viral RNA.

1.1.3. EV trafficking and uptake

Secreted EVs are detectable in most body fluids, including plasma, urine, saliva, broncheoalveolar and cerebrospinal fluids, and can interact with cells close to their site of origin or at distant anatomical sites after transport through the circulation. Interactions

between membrane factors on circulating and target cells appear to control EV uptake selectivity. Such uptake primarily occurs phagocytosis, which requires dynamin 2 and phosphatidyl inositol-3-kinase, and relies heavily upon surface molecules specific to certain cell types (e.g. T-cell membrane protein 4) as well as EV surface proteins, including integrins, annexins, galectin, and intercellular adhesion molecule 1 (Pant, Hilton et al. 2012). However, EV uptake by these recipient cells can alter their gene expression levels to alter future EV uptake through the transfer of regulatory mRNAs, miRNAs and lncRNAs, cytoplasmic proteins and cell-specific receptors (Matsuo, Chevallier et al. 2004). The presence of different types of RNA in EVs can affect the transcriptome of recipient cells (Ratajczak, Miekus et al. 2006, Valadi, Ekstrom et al. 2007). EV-derived factors can thus alter gene transcription and translation, and regulate signaling cascades to alter transcript and protein modifications, protein localization, key enzymatic reactions to impact overall cellular homeostasis, with interactions among factors supplied by the EV donor and recipient cell determining which molecular mechanisms will predominate (Pant, Hilton et al. 2012). The presence of different types of RNA in EVs can affect the transcriptome of recipient cells (Ratajczak, Miekus et al. 2006, Valadi, Ekstrom et al. 2007).

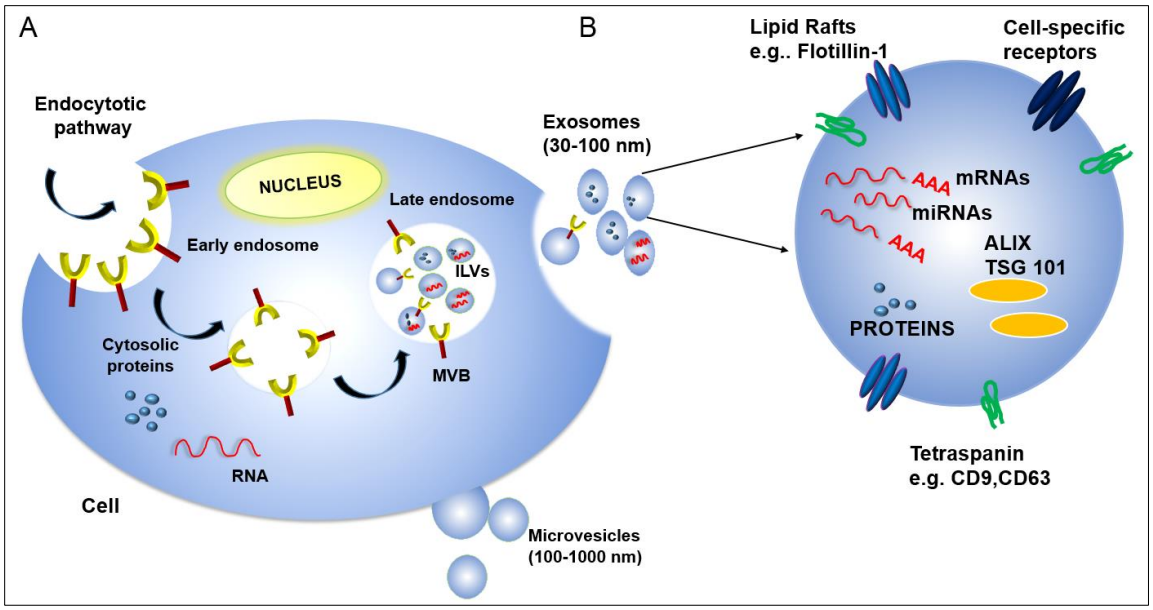

Figure 1. (A) Exosome biogenesis begins with the invagination of the plasma membrane to generate early endosomes. These endosomes can then invaginate to form intraluminal vesicles (ILVs). This process creates multi-vesicular bodies (MVBs) that can then fuse with the plasma membrane to release mature ILVs, now called EVs, into the extracellular space. (B) Exosomes contain proteins, nucleic acids (including mRNAs, miRNAs, and DNA fragments), and lipids, and these cargos can reflect selective incorporation during exosome formation in a process controlled by lipid raft proteins, ESCRT accessory proteins (e.g., ALIX and TSG101) and tetraspanin proteins. The cytosolic release of these contents upon EV uptake can alter the phenotype of the recipient cells.

1.2. Role of EVs in viral and bacterial infections

Most cells secrete EVs, but EVs produced during pathogen infections can reveal differences in their composition to reflect their origin from infected cells and the overall state of the infection. Studies have revealed multiple ways by which viruses and bacteria can manipulate EV synthesis to enhance their transmission and pathogenesis (reviewed in (Raab-Traub and Dittmer 2017)). Conversely, EVs produced by immune cells play an important role in host responses to infection. One early example of this role was the finding that EVs from B lymphocytes contained class II major histocompatibility (MHCII)-antigen complexes that could activate CD4+ T cells in an antigen-specific manner (Raposo, Nijman

et al. 1996). Subsequent studies found that EVs of dendritic cells contained class I major histocompatibility (MHCI)-peptide complexes that could stimulate cytotoxic CD8+ T cell responses, identified cell-dependent and independent mechanisms for the antigen presenting activity, and identified receptor and cytokine/chemokine effects to regulate multiple cells involved in the adaptive immune response (Hwang, Shen et al. 2003, Nolte-'t Hoen, Buschow et al. 2009, Mittelbrunn, Gutierrez-Vazquez et al. 2011). Notably, EVs derived from cells infected with either viral or bacterial pathogens demonstrate several mechanisms to mediate the immune system, including effects to inhibit host EV effects to promote adaptive immune responses, indicating that better understanding of these mechanisms is important to improve therapeutic approaches used to treat these pathogens. EVs carrying pathogen-derived factors are also of interest as biomarkers of infection, since these factors should be more stable than soluble factors in circulation that are exposed to circulating hydrolase activities. EVs are also stable in circulation, are capable of packaging a broad array of biomolecules and small molecule drugs, and exhibit potential as selective targeted biogenic carriers (Clayton, Harris et al. 2003, Morse, Garst et al. 2005, Admyre, Bohle et al. 2007, Sun, Zhuang et al. 2010, Alvarez-Erviti, Seow et al. 2011, Tian, Li et al. 2014, Fuhrmann, Neuer et al. 2017). Based on these properties, this review describes current knowledge of EV actions to promote disease and regulate host immunity, and the potential of these EVs as disease biomarkers and future therapeutic agents.

1.2.1. EV regulation of immune responses

EVs derived from immune cells carry proteins that can regulate important aspects of host immunity, including T-cell activation (e.g., MHCI and MHCII, lymphocyte function-associated antigen-1, and intercellular adhesion molecule-1, depending on the parent cell)

(Lee, El Andaloussi et al. 2012). MHC I and MHC II and immunomodulatory proteins are enriched on EVs of antigen-presenting cells (APCs; e.g., dendritic cells (DCs) and macrophages) (Raposo, Nijman et al. 1996) and these EVs appear capable of activating T cells by transferring antigens or MHC-antigen complexes to conventional APCs, or by directly presenting MHC-antigen complexes to T cells as APC surrogates (Thery, Duban et al. 2002, Hwang, Shen et al. 2003, Segura, Amigorena et al. 2005, Montecalvo, Shufesky et al. 2008, Qazi, Gehrmann et al. 2009).

For the first mechanism, evidence suggests that immature DCs that do not support robust immune responses secrete EVs that can transfer MHC-antigen complexes, or antigens, to mature DCs to activate CD4+ and CD8+ T-cell responses (Thery, Duban et al. 2002, Andre, Chaput et al. 2004). In the so-called "cross-dressing" model, intact MHC-antigen complexes are transferred from inactive to active DC populations (Thery, Duban et al. 2002, Andre, Chaput et al. 2004, Chaput, Schartz et al. 2004, Segura, Amigorena et al. 2005), whereas in the "cross-presentation" mechanism, mature DCs present peptides derived from captured EVs on their own MHC molecules (Montecalvo, Shufesky et al. 2008, Qazi, Gehrmann et al. 2009).

There is also evidence that APC-derived EVs can directly activate CD4+ and CD8+ T cells (Utsugi-Kobukai, Fujimaki et al. 2003, Admyre, Johansson et al. 2006, Luketic, Delanghe et al. 2007), and stimulate both previously activated and memory T cells (Admyre, Bohle et al. 2007, Muntasell, Berger et al. 2007). APC-derived EVs are also able to directly activate naïve CD8+ T cells *in vitro* (Hwang, Shen et al. 2003), although they appear to be 10- to 20-fold less efficient than APCs, suggesting that EVs may not have a direct effect on naïve T cell activation *in vivo*. Similar studies indicate that EVs of B cells

can also directly present antigens to induce T cell responses (Admyre, Bohle et al. 2007), although with less efficiency than their parental B cells. Receptor aggregation between interacting T cells and DCs also creates an extended "immunological synapse" where DC-derived EVs can directly interact with adjacent T cells in a LFA-1 (lymphocyte function-associated antigen 1) dependent manner to promote their activation (Nolte-'t Hoen, Buschow et al. 2009).

However, while evidence indicates that EVs can directly and indirectly regulate *in vitro* CD4+ and CD8+ T cell responses, it is unclear to what extent they affect these responses *in vivo*.

1.2.2. EV roles in infectious diseases

EVs released by infected cells contain pathogen- and host-derived factors, and play key roles in pathogen-host interactions, including pathogen uptake and replication and regulation of the host immune response (reviewed in (Mittelbrunn, Gutierrez-Vazquez et al. 2011, Schorey and Harding 2016)). For example, studies have shown that multiple viruses—including human immunodeficiency virus 1 (HIV-1), hepatitis viruses B, C and E (HBV, HCV, and HEV), and multiple members of the human herpesvirus (HHV) family—utilize EV ESCRT machinery for viral transmission (Pawliczek and Crump 2009, Sadeghipour and Mathias 2017). HIV-1, in particular, has developed several EV-mediated strategies to manipulate the behavior of its target cells (Garcia, Pion et al. 2005), including a Nef-regulated mechanism that alters EV protein trafficking in CD4+ T cells. Hepatitis A virus (HAV), HCV and HEV employ the EV biogenesis machinery to produce enveloped virions that allow the virus to avoid immune surveillance (reviewed in (Alenquer and Amorim 2015)). HHVs, which are responsible for a broad range of important pathologies,

employ endosomes to evade anti-viral immune responses through several distinct mechanisms that differ among these viruses (Sadeghipour and Mathias 2017). In the following sections, we describe how several viruses subvert the EV biogenesis machinery for their replication and infectivity. Much less is known about how bacteria employ the EVs of their host to favor their growth and survival, and most studies focus on the behavior of *Mycobacterium tuberculosis* (*Mtb*), an important intracellular pathogen. We will therefore summarize current knowledge on how *Mtb* regulates cellular and systemic processes to favor active and latent *Mtb* infections, and how these processes overlap with those of other bacterial pathogens (Figure 2).

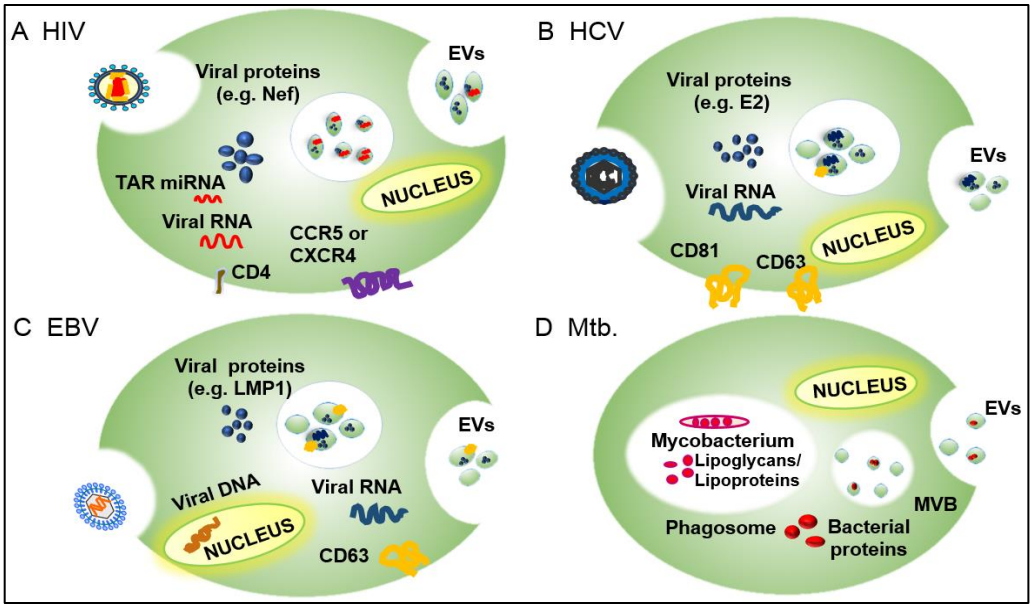

Figure 2. Overview of the EV incorporation of pathogen-derived factors by the EVs of their host cells, including pathogen receptors and regulatory factors, to promote infection and pathogenesis. (A) EVs of HIV-infected cells express the HIV receptor target proteins CCR5 and CXCR4 and regulatory factors, including the HIV protein Nef and TAR RNA, among others. (B) EVs of HCV-infected cells express E2 and CD81, which promote HCV uptake, as well as viral RNA and host proteins (e.g., CD63) that promote HCV infections. (C) EVs of HBV-infected cells contain EBV RNA and proteins (e.g., LMP1) and host proteins (e.g., EGFR and FGF2) that promote EBV infectivity and pathogenesis. (D) EVs of Mtb-infected cells contain Mtb-derived glycolipids (LAM) and lipoproteins (LpqH) that regulate innate and acquired immune responses to promote infection.

1.2.3. EVs facilitate viral and bacterial pathogenesis

Viral and bacterial pathogens can subvert EV functions to promote pathogen replication, survival, or pathology. Cells employ EVs to transfer regulatory factors that modulate the response of local and distant cells and systemic responses. In cells with active viral or bacterial infections, the EV machinery can also package pathogen-derived factors that alter the phenotype of EV recipient cells. Many pathogen factors that are packaged into EVs interact with ESCRT proteins or related factors, suggesting that pathogens have evolved to exploit this intercellular transport and signaling pathway, using it to promote infection and repress anti-pathogen host responses. We discuss several examples of these interactions in the following sections.

1.2.3.1. Viruses

Functional overlaps between EV biogenesis and viral budding: Mechanisms involved in EV and enveloped virus budding share common features. Many retroviruses are reported to interact with ESCRT complex and ESCRT-related proteins involved in EV biogenesis through conserved protein motifs, referred to as late domains since their deletion or mutation leads to the arrest of virus assembly at late stages of virion synthesis (Pawliczek and Crump 2009). For example, HIV-1 virion interactions with TSG101, ALIX, and other host proteins are similar to those employed to package host proteins during EV formation (Gould, Booth et al. 2003). Similarities between the EV and HIV-1 packaging mechanisms led to the statement of "the Trojan EV hypothesis", which proposes that HIV-1 evolved to utilize EV biogenesis proteins to package its capsid, while also exploiting EV uptake mechanisms to allow cell infection in the absence of viral envelope proteins that normally direct HIV-1 uptake (Gould, Booth et al. 2003). Mounting evidence suggests that several

human viruses hijack proteins involved in EV biogenesis to package their capsids. Human herpesvirus (HHV) family members exploit proteins that regulate EV biogenesis for their virion production. HHV-1 (herpes simplex virus 1; HSV-1) structural proteins contain potential TSG101 (ESCRT-I complex) and ALIX (ESCRT-I associated) binding motifs. Dominant-negative and siRNA expression studies also indicate that HHV-1 does not employ TSG101 or ALIX, but requires functional expression of CHMP (ESCRT-III complex) and VPS4 (ESCRT-III associated) proteins for the formation of its virion envelope (Pawliczek and Crump 2009, Sadeghipour and Mathias 2017). HHV-5 (human cytomegalovirus; HCMV) also appears to utilize a similar packaging mechanism, since inhibition of either CHMP1A or VPS4, but not ALIX, interferes with its virion packaging. Neither HHV-4 (Epstein-Barr virus; EBV) nor HHV-8 (Kaposi Sarcoma-associated herpesviruses) appear to require exosomal protein interactions for their secretion (Sadeghipour and Mathias 2017).

Despite these functional interactions, it is not clear how all of these viruses employ EV proteins in their packaging and secretion. While components of multiple viruses have been shown to associate with MVBs, there is little evidence that these viruses localize within MVBs and are secreted by MVB fusion with the plasma membrane. Only one HHV study appears to provide data consistent with an MVB release mechanism, reporting that HHV-6 virions localize within MVBs in infected cells (Sadeghipour and Mathias 2017), although these virions (~200 nm) would be much larger than EVs (30-100 nm).

All members of the hepatitis virus family are reported to employ EV-related proteins to form enveloped virions. HBV envelope proteins colocalize with MVB proteins ALIX and VPS4B, and dominant-negative versions of either of these proteins block the release

of enveloped HBV virions (Watanabe, Sorensen et al. 2007). HCV interacts with Hrs (ESCRT-0 complex) to promote apparent MVB uptake of viral capsids (Tamai, Shiina et al. 2012) and EVs isolated from HCV-infected hepatoma cell lines and sera of patients with chronic HCV infections contain HCV core and envelope proteins and full-length HCV RNA (Bukong, Momen-Heravi et al. 2014). HAV and HEV are shed as naked viral particles in feces but circulate as membrane-enclosed virions, which are less infectious but are masked by the host's immune response (Sadeghipour and Mathias 2017). Recent evidence suggests that production of these circulating enveloped virions requires interaction with the exosomal sorting components CHMP2a (ESCRT-III complex), ALIX, and VSP4 (ESCRT-I and -III associated) for HAV (Feng, Hensley et al. 2013, McKnight, Xie et al. 2017) or Hrs (ESCRT-0 complex) for HEV (Nagashima, Jirintai et al. 2014). Similar to HHV, however, there is scarce evidence for MVB-mediated release of hepatitis family viruses, with only one study indicating that ~50 nm enveloped virions are detectable in MVBs of HEV-infected cells (Nagashima, Jirintai et al. 2014).

EVs can alter virus antigenicity and infectivity: Results suggest that some persistent viruses (e.g., HCV and HAV) employ EVs as a strategy to escape negative selective pressure from neutralizing antibodies and other immune responses that act to promote viral clearance (Dreux, Garaigorta et al. 2012, Feng, Hensley et al. 2013, Ramakrishnaiah, Thumann et al. 2013). MVB-mediated encapsulation may also allow a virus to spread beyond its normal range of cell hosts through the normal EV uptake process, as demonstrated by the ability of EVs containing HAV capsids to infect target cells using EV surface proteins instead of the EV-masked viral receptor proteins (reviewed in (Raab-Traub and Dittmer 2017)).

EVs can spread viral docking receptors to promote viral infectivity: HIV normally binds to CD4 and the chemokine receptors CCR5 or CXCR4 on target cells to mediate infection, and cells lacking these receptors, or with receptor mutations, are resistant to HIV infection. EVs secreted by HIV-infected cells contain CCR5 or CXCR4, however, and their uptake by cells lacking these receptors facilitates HIV infection of these otherwise HIV-resistant cells (Mack, Kleinschmidt et al. 2000, Rozmyslowicz, Majka et al. 2003). The widespread EV markers CD81 and CD63 colocalize with subgenomic HCV RNA and appear to promote its packaging into EVs. The HCV envelope glycoprotein E2 also colocalizes with CD81 and cells that internalize EVs containing this complex are more susceptible to HCV infection (Pileri, Uematsu et al. 1998, Ramakrishnaiah, Thumann et al. 2013). Interaction with this complex may also promote HCV uptake by EVs (Zhang, Randall et al. 2004, Chang, Hsu et al. 2017). Studies suggest that EV proteins may facilitate viral-receptor-independent transmission of HCV and HAV, and presumably other EV-enveloped viruses, to uninfected cells (Ramakrishnaiah, Thumann et al. 2013, Bukong, Momen-Heravi et al. 2014).

Regulatory actions of virus-associated EVs on host cells: EVs derived from virus-infected cells can also transfer viral proteins to influence viral pathogenesis. EVs from HIV-infected cells contain the HIV-1 protein Nef, which regulates endocytosis, cytoskeletal rearrangement, and organelle trafficking to increase the number of EVs released from HIV-infected cells (Ali, Huang et al. 2010, Raymond, Campbell-Sims et al. 2011), and may thus promote EV-mediated HIV infectivity. Nef-induction of EV-associated ADAM17 also

appears to promote HIV-infection of resting CD4+ T cells (Arenaccio, Chiozzini et al. 2014), while ADAM17 and TNFα together can activate latent HIV-1 infections in primary CD4+ T lymphocytes and macrophages (Arenaccio, Anticoli et al. 2015). Finally, EVs carrying Nef appear to exert complex effects to regulate HIV-1 infection and pathogenesis through actions on uninfected cells (Lenassi, Cagney et al. 2010, Gray, Gabuzda et al. 2011, Aqil, Naqvi et al. 2013), including the ability to alter the functions of import immune responses.

Human gammaherpesviruses, such as EBV, have complex effects to promote both viral infection and cancer. EVs derived from EBV-infected cells exploit the endosomal-exosomal pathway to enclose both EBV- and host-derived regulatory factors (Flanagan, Middeldorp et al. 2003, Meckes, Gunawardena et al. 2013). In EBV-infected cells, an interaction between the EV protein CD63 and the viral protein LMP1 appears to promote LMP1 incorporation into EVs (Verweij, van Eijndhoven et al. 2011, Hurwitz, Nkosi et al. 2017) and EVs that contain LMP1 can deliver important signaling proteins to uninfected cells (Meckes, Gunawardena et al. 2013). LMP1 also induces the expression of both epidermal growth factor receptor (EGFR) and fibroblast growth factor 2 (FGF2), which are also packaged in LMP-1-marked EVs (Ceccarelli, Visco et al. 2007, Meckes, Shair et al. 2010), suggesting that EV-mediated transfer of these receptors may stimulate the growth of recipient cells with a potential to promote EBV-mediated tumor development.

Effects of virus-associated EVs to inhibit anti-viral responses: Viruses employ several EV-mediated strategies to attenuate host immune responses. EVs of HIV-infected macrophages deliver Nef to recipient cells to alter their immune function. Nef is associated with

intracellular sorting and trafficking pathways that promote the lysosomal degradation of CD4 and MHCI to reduce their surface expression (Schaefer, Wonderlich et al. 2008, Gray, Gabuzda et al. 2011), rendering cells that express Nef less susceptible to cytotoxic immune responses. Evidence also indicates that Nef+ EVs facilitate HIV pathogenesis by conditioning their target cells to undergo apoptosis, promoting CD4+ T cell depletion and HIV-mediated immune suppression to reduce immune clearance of HIV-infected cells (Nguyen, Booth et al. 2003, Lenassi, Cagney et al. 2010, Lenassi, Cagney et al. 2010).

The major EBV oncoprotein LMP1, which is carried by EVs of EBV-infected cells, plays an important role in EBV infection (reviewed in (Raab-Traub and Dittmer 2017)). LMP1 expression has an important function to activate B cells; however, recent work suggests that EVs carrying LMP1 may also promote B cell activation and proliferation (Gutzeit, Nagy et al. 2014) and can inhibit proliferation of T cells and the ability of natural killer (NK) cells to exert cytotoxic effects. (Flanagan, Middeldorp et al. 2003, Meckes, Shair et al. 2010). EBV also encodes a number of miRNAs that can modify the transcriptome of infected cells, and non-infected cells via EV transfer (Pfeffer, Zavolan et al. 2004, Yang, Huang et al. 2013). EBV-infected cells release EVs containing EBV miRNAs that suppress EBV target genes, including CXCL11, an immunoregulatory gene involved in antiviral activity (Pegtel, Cosmopoulos et al. 2010). EVs released by EBV-infected cells also contain the host-derived protein galectin-9, which is known to induce apoptosis of EBV-specific CD4+ T cells through an interaction with immunoglobulin mucin-3, and to negatively regulate both macrophage and T cell activation (Klibi, Niki et al. 2009).

Viruses thus appear to employ multiple EV-based mechanisms to suppress the clearance of their host cells by the immune system to promote continued viral infections; however, the in vivo relevance of these mechanisms is not clear.

Viral transfer through immune cell EVs: In addition to actions to inhibit the antiviral activity of immune cells, virus-derived EVs can also use these cells to promote viral transfer to new host cells. HIV-1 virions captured by immature DCs and exocytosed in association with the DC cell's EVs can trans-infect CD4+ T cells (Wiley and Gummuluru 2006). *The Trojan horse hypothesis* of HIV-1 trans-infection (Gould, Booth et al. 2003, Izquierdo-Useros, Naranjo-Gomez et al. 2010) takes this further, suggesting that HIV-1 virions are retained in the MVB compartment of mature DCs and trans-infect CD4+ T cells in lymph nodes by following the same trafficking pathway that DC EVs use to disseminate antigens (Gould, Booth et al. 2003, Izquierdo-Useros, Naranjo-Gomez et al. 2010, Narayanan, Iordanskiy et al. 2013).

1.2.3.2. Bacteria

Regulatory actions of bacterial-associated EVs on host cells: Bacterial pathogens can be classified based on the nature of their interactions with their host, including whether they prefer or require an intracellular or extracellular niche to initiate and maintain active infections. Both extracellular and intracellular bacteria can display complicated lifecycles, but intracellular bacteria have several unique options to subvert cellular processes, including the EV pathway, to promote their growth and survival. *Mycobacterium tuberculosis* is perhaps the best studied of these pathogens with respect to its EV effects due to its significant worldwide impact on public health, although several other

intracellular pathogens are responsible for significant human diseases. *M. tuberculosis* (*Mtb*) evades the innate immune response by stably infecting phagocytic cells, such as macrophages, which are primarily responsible for clearance of microbial pathogens. *Mtb* lipoproteins and lipoglycans inhibit phagosome maturation, generating a stable intracellular niche for the engulfed *Mtb bacilli* and blocking MHCII-antigen complex cycling to the cell surface to inhibit the host response to *Mtb*-derived antigens (Beatty and Russell 2000, Beatty, Ullrich et al. 2001). *Mtb*-derived factors can also promote EV release and it is hypothesized that some mycobacterial proteins contain signals that direct them to MVBs to promote their incorporation into EV (Giri, Kruh et al. 2010).

Mtb-related EVs play important roles in regulating the phenotypes of both infected and uninfected cells and likely contribute to the overall pathogenesis of *Mtb* infections (Beatty and Russell 2000, Beatty, Ullrich et al. 2001). EVs of *Mtb*-infected macrophages can stimulate non-infected macrophages to secrete chemokines to induce the migration of naïve T-cells and macrophages (Singh, Smith et al. 2012). Mice intranasally injected with EVs from *Mtb* and *M. bovis* BCG, revealed increased TNFα and IL-12 production, as well as the recruitment of macrophages and neutrophils to the lung (Bhatnagar, Shinagawa et al. 2007), suggesting that these EVs could recruit non-infected target cells to promote disease progression. Macrophages infected with *M. avium* also revealed increased EV secretion, which leads to a pro-inflammatory response in non-infected macrophages while simultaneously downregulating a number of IFN-γ-inducible genes in naïve cells to inhibit the inducible expression of MHC-II and the CD64 immunoglobulin receptor (Bhatnagar and Schorey 2007). Macrophages infected with *M. avium* and *M. smegmatis* exhibited increased EV secretion and increased EV expression of HSP70 to promote *in vitro*

macrophage activation and TNFα expression (Anand, Anand et al. 2010). EVs of *Mtb*-infected cells also contain the 19 kDa lipoprotein LpqH, which can promote inflammation and stimulate *in vitro* macrophage activation and TNF-α expression via the Toll-like receptor/MyD88 pathway (reviewed in (Schorey and Bhatnagar 2008)). These results suggest that EVs from mycobacterium-infected cells can both activate and recruit immune cells, and may therefore influence innate and acquired immune responses during mycobacterial infection (Bhatnagar, Shinagawa et al. 2007), although the relative impact of such putative effects on the overall immune response is not clear.

Effects of bacterial-associated EVs to inhibit anti-bacterial immune responses: EVs released by macrophages infected with *Mtb* bacilli contain protein cargos that regulate both innate and adaptive immune responses. EVs from *Mtb*-infected macrophages contain the glycolipid lipoarabinomannan (LAM) that inhibits T cell receptor signaling and T cell activation responses, which may induce immune suppressive mechanisms that promote the survival of *Mtb*-infected cells to maintain active *Mtb* infections (Mahon, Sande et al. 2012, Yang, Ruffner et al. 2012). EVs from *Mtb*-infected cells can partially suppress the ability of macrophages to respond to INF-γ to inhibit macrophage APC function (Harding and Boom 2010). EVs of macrophages infected with *M. avium* can also downregulate a number of IFN-γ-inducible genes in naïve cells to inhibit the inducible expression of MHC-II and the CD64 immunoglobulin receptor (Bhatnagar and Schorey 2007).

These results suggest that exosomes from mycobacterial-infected cells can promote both the recruitment and the activation of the immune cells, and thus may play a key role in the innate and acquired immune responses during mycobacterial infection (Bhatnagar, Shinagawa et al. 2007).

1.3. The emergency of liquid biopsy in cancer diagnostics

Tumor biopsy is considered the gold standards for detection and routine monitoring of cancer progression. However, their invasiveness, along with tumor sampling brings about challenges with studying tumor heterogeneity and evolution, making it an unlikely process for regular monitoring (Vaidyanathan, Soon et al. 2019). Recently, liquid biopsy samples, including plasma/serum, saliva, and urine, are of great interest as a means to reduce barriers to the rapid evaluation and treatment of diseases, including most cancers, where it is not feasible to obtain biopsies or repeat biopsies from the disease site. Such biopsies methods have influenced the development of several therapies that require routine measurements of essential biomarkers (Sharma, Zuniga et al. 2017, Vaidyanathan, Soon et al. 2019). Circulating tumor DNA (ctDNA) and circulating tumor cells (CTCs) are biomarkers present in blood known to be released from cells within the primary tumor and play a key role in metastasis. However, their low availability (1–10 circulating tumor cells [CTCs]/mL of blood) and difficulty in enrichment makes them an unfavorable candidate for cancer detection and prognosis (Herreros-Villanueva and Bujanda 2016).

EVs on the other hand, are stable membraneous vesicles , ranging from 30-100 nm in diameter released by cells and present in all bodily fluids with concentrations of $> 10^{10}$ vesicles / mL in blood, (Keller, Ridinger et al. 2011, Lee, Fraser et al. 2018), making EVs highly abundant and easily available biomarkers (Nuzhat, Kinhal et al. 2017, Rajagopal and Harikumar 2018, Rodrigues, Fan et al. 2018, van Niel, D'Angelo et al. 2018). Critical information is stored in the molecular profile of the exosomal cargo and surface expression due to their endocytotic biogenesis from parent tumor cells making them favorable for studying tumor microenvironment (Kalluri 2016). However, being smaller than cells (10-

30μm) and larger than proteins makes it very difficult to isolate these EVs (Vaidyanathan, Soon et al. 2019). The conventionally available analytical tools are time-consuming, require extensive pre-treatments like (ultracentrifugation), quantification (Nanosight) , have low yield and hard to optimize, making it difficult for its use in clinical EV research environment (Thery, Amigorena et al. 2006, Dragovic, Gardiner et al. 2011) . Current new technologies are able to circumvent the conventional process for EVs isolation and purification by developing methods that can improve isolation efficiency and specificity from bodily fluids but have a lower throughput which needs to be addressed to have a more practical use (Shao, Im et al. 2018).

1.4. Variable abundance of EVs in diseased conditions

There are several studies focusing on how EVs release rate changes based on different pathological conditions, and how not only the total protein levels but also the contents of individual proteins in EVs can play a role in providing prognostic information (Whiteside 2016). Thus having knowledge of the amount of EVs present in plasma or serum acts as crucial information during biomarker readout as it can influence the absolute measurement of the expression levels of markers under consideration. For instance, findings suggested that plasma EVs levels were increased in HIV-positive subjects which correlated with increased oxidative stress and decreased polyunsaturated fatty acids. On further evaluation, they did not see any clear relationship to virological and immunological parameters in treated patients with suppressed viral load (Chettimada, Lorenz et al. 2018), likewise another study revealed increased levels of plasma EV- associated alpha-synuclein (α-syn) in Parkinson's disease which could reflect a mechanism to release α-syn under conditions of cellular stress and relatively increased α-syn concentrations (Shi, Liu et al.

2014). A number of studies in cardiovascular-related disorders have demonstrated increasing levels of circulating EVs in insulin-resistant patients, patients with type-2 diabetes along with a further increase in these levels with microvascular complications. There are studies showing increased levels of EVs are an indication of cardiovascular disorders including, atherosclerosis, hypertension and following a stroke or myocardial infarction (Charlotte, Jose et al. 2016).

In cancer alone, the EVs release can be affected by several underlying conditions present in tumor microenvironment such as hypoxia, change in intracellular to intercellular pH levels, or even overexpression of an enzyme such as heparanase (Parolini, Federici et al. 2009, King, Michael et al. 2012, Thompson, Purushothaman et al. 2013, Zhang, Yuan et al. 2015). EVs are also increased in many inflammatory conditions, there were studies focusing on the relationship between inflammation and kidney diseases which revealed that in mice with acute and chronic kidney injury showed an increase in levels of exosomes carrying the inflammatory chemokine mRNA in mice (Console, Scalise et al. 2019). Apart from underlying pathological conditions impacting the release rate of EVs, this change is even observed in normal healthy pregnancy. The number of EVs present in the maternal plasma increased significantly in the gestational age across the first trimester of pregnancy. Along with observations wherein there were increased concentrations of EVs in women with full-term pregnancies that those from pregnancies delivery pre-term (Sarker, Scholz-Romero et al. 2014). Further emphasizing how a change in the number of EVs in a sample could influence the expression levels of biomarkers under observation.

1.5. Influence of marker expression levels in EVs

Over the past decade surface protein expression levels on circulating tumor EVs are of particular interest in providing valuable information in regards to the physiological states of parental cells, along with playing a significant role in developing prognosis for potential metastasis and decision making for deciding the route for treatment (Xu, Rai et al. 2018). While performing these measurements there is an increasing need to know whether there is a significant change in exosomal marker expression levels, either overexpression or suppressed expression in individual EVs. A recent study on exosomal PD-L1 expression demonstrated increased levels in circulating EVs that correlated with tumor size. Further investigations revealed that stimulation with interferon-γ (IFN-γ) increased the amount of PD-L1 on EVs, which suppresses the functions of CD8 T cells and promotes tumor growth. A similar increase was observed in patients with metastatic melanoma and varied during the course of anti-PD-1 therapy. This increase during early stages of treatment indicates how this information could be used as an indicator for disease detection and monitoring. To strengthen the point there were making, they showed that there was no or only marginal difference in the number of circulating EVs, and the increase in levels of PD-L1 was a change in the expression levels of the marker on these EVs (Chen, Huang et al. 2018).

There were other studies that revealed exosomal uptake by organ-specific cells can prepare pre-metastatic niches based on the distinct EVs integrin expression levels and could help in predicting organ-specific metastasis. They study integrins $\alpha_6\beta_4$ and $\alpha_6\beta_1$ were associated with lung metastasis, while exosomal integrin $\alpha_v\beta_5$ was linked to liver metastasis. Additionally, they showed these integrin expression levels could

predict lung and liver metastasis and that exosomal integrin expression did not reflect cellular expression, thus emphasizing how exosomal integrin expression alone could help predict organ-specific metastasis.(Hoshino, Costa-Silva et al. 2015).

A recent study focused on the effects of increased endogenous levels of transcription factor Hypoxia-inducible factor-1α (HIF-1α) in nasopharyngeal carcinoma associated latent membrane protein 1(LMP1) positive EVs. HIF-1α mediates cellular responses to hypoxia and transcriptionally regulate over 40 genes that are involved in tumor development and progression, along with increased proliferation rate and invasiveness. Whereas, LMP1 is the oncoprotein of Epstein - Barr virus (EBV) that drives oncogenic processes by promoting tumor progression by enhancing the expression of invasion and metastatic factors. They showed that LMP1 positive EVs containing HIF-1 α can have reciprocal changes in the expression factors associated with the epithelial-mesenchymal transition (EMT) pathways , along with pro-metastatic effects in recipient cells by making non-malignant nasopharyngeal cells more invasive (Aga, Bentz et al. 2014, Sarker, Scholz-Romero et al. 2014).

These above studies accentuate the increasing need to know EV protein expression levels, and how that information can help understand tumor progression, metastatic niches, and responses to treatment. Therefore, in order to understand the expression change of markers in EVs, we need to have a way to understand the starting sample population and take that into consideration when measuring biomarker readout, as absolute readout could blind us and fail to understand the underlying process and its effects in a diseased condition.

1.6. Motivation and Significance

Circulating levels of a disease-associated EV biomarker can thus reflect both the release rate of disease-associated EVs from the target tissue and their relative expression of the target biomarker, which are regulated by different processes. This critical difference is not addressed by standard EV analyses unless a study protocol also quantifies the number of target EVs in an analysis sample. As part of my doctoral work, we tried to tackle the problem of quantifying EVs in sample and measuring the relative expression levels of markers in EVs by developing a fluorescence-based assay that can measure the number of EVs and the total protein readout of EV surface markers.

We established a method where EVs derived from two pancreatic cell lines were captured and immobilized on the surface of a 96-well plate with an antibody specific for the common EV membrane protein CD81 (Kowal, Arras et al. 2016) and stained the EV population with a lipophilic dye that labeled the EV lipid bilayer to provide a quantitative readout reflecting the total number of EVs in the sample. These EVs were then hybridized with quantum dot-labeled antibody probes specific to target EV biomarkers and signal from the bound probes was normalized to the lipophilic dye signal to determine the mean EV expression of these biomarkers in the analyzed sample. This novel assay utilized multiplexed fluorescent signals from specific antibody-labeled quantum dots to measure EV expression of two cancer-associated biomarkers – epithelial cell adhesion molecule (EpCAM) and Ephrin type-A receptor 2 (EphA2) – on pancreatic cancer cell-derived EVs (Figure 3). The approach revealed linearity for the sample between normal and cancer cell lines for both EpCAM and EphA2 expression. Furthermore, the normalized signal showed a similar protein expression level for EVs from the same cell

type. This approach circumvents the need for separate EV isolation, purification and quantification steps, which are time-consuming, low-throughput, require expensive and specialized equipment, and are difficult to optimize, rendering them unsuitable for clinical translation (Thery, Amigorena et al. 2006, Dragovic, Gardiner et al. 2011)

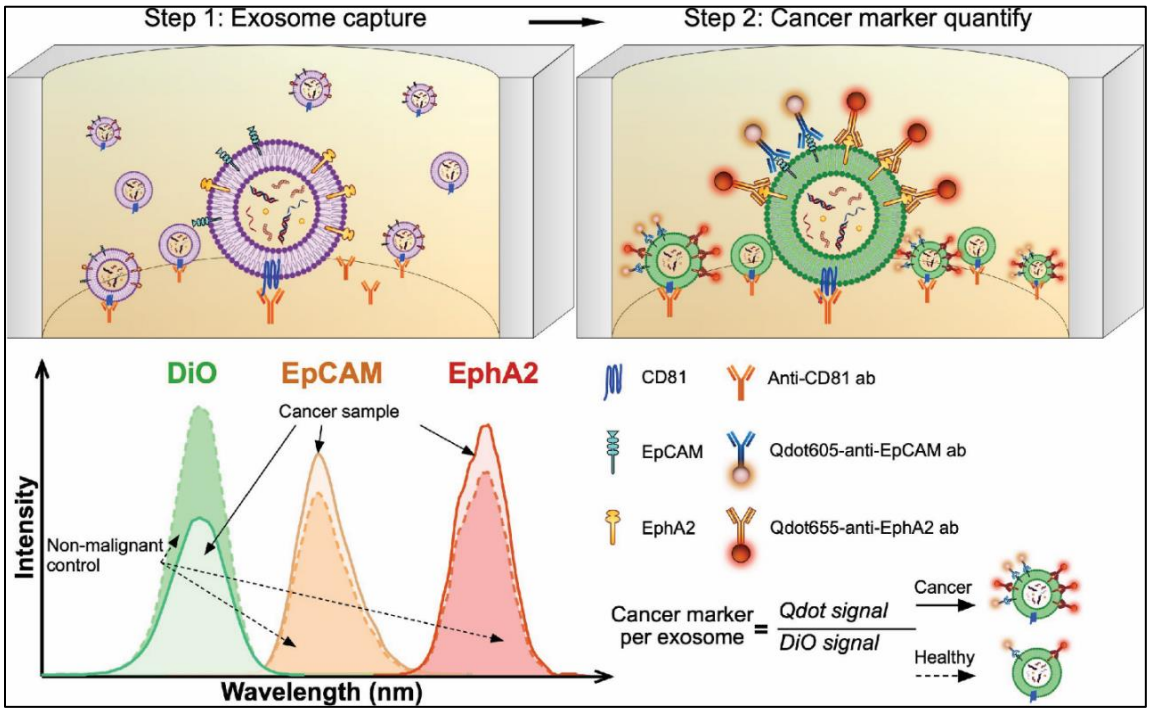

Figure 3. Schematic of the quantum dot (Qdot Assay). EVs captured by an antibody to an EV-specific surface are stained with the lipophilic fluorescent dye DiO and then hybridized with antibody-conjugated quantum dot probes specific for biomarker targets on the EV membrane (e.g., EpCAM and EphA2). DiO signal from the captured EVs functions as a surrogate marker of EV abundance and allows direct normalization of quantum dot probe signal to permit quantification of mean biomarker levels in a captured population without the need for an independent EV isolation and quantitation procedure. This allows direct comparison of relative EV biomarker levels among different cohorts for disease diagnosis (e.g., cancer patients vs. non- cancer).

We further performed clinical validation on two cancer cohort. One comprised of plasma samples collected and tested for a pancreatic cancer cohort (n=74; Control =21, Stage I\II = 11, Stage III = 21 , Stage IV=21) which revealed robust sensitivity and linearity for the detection of individual EV expression levels, which distinguished cancer and

normal subjects for both markers – EpCAM and EphA2. The second consisted of serum samples collected for pancreatic cancer cohort (n= 20; Non-Cancer = 7, Cancer = 9 and Metastasis = 4) showing significant difference for the two marker EpCAM and EphA2 for cancer vs non- cancer group , which further significantly increased after normalizing the signal of the markers to the number of EVs present. Notably, this assay approach analyzes EVs directly captured from serum/plasma without the need for purification steps or quantification, utilizing a fluorescence-based workflow that is suitable for clinical translation, and employs a format in which disease specificity can be altered by shifting the detection probe (quantum dots) specificity.

1.7. Organization of the dissertation

The aim of the dissertation was to design and develop and immuno-based fluorescent assay which allows EV capture, followed with quantifying the number of EV and finally measuring the total expression of two cancer specific surface markers on the EVs. Finally, the signal from the bound probes for EV biomarker was normalized to the lipophilic dye signal to determine the mean EV expression of these biomarkers. The dissertation captures the proposed concept as follows:

i. Normalization using fluorescent dye : Demonstrating the use of a fluorescent lipophilic lipid membrane dye (DiO) to measure EV abundance in different sample populations.

Chapter 2 will focus on variable abundance of EVs as observed in cancer cells and the need to know the number of EVs in a sample when studying the total expression levels of surface markers. In chapter 3, we focus on developing a method that will label the EVs and measure the qualitative signal for the total amount of EVs in a sample. We

used a fluorescent lipid dye which would bind to the membrane of the capture EVs on a 96-well black plate. Labeling EVs bound to a solid substrate eliminates the need for sample washing and ultracentrifugation to get rid of unbound dye.

ii. Analytical Validation : Development and analytical validation of the quantum dot assay (Qdot Assay) for multiplexed detection of cancer-specific surface markers on EVs

Chapter 4 focuses on testing and validating the two markers, EpCAM and EphA2 to help distinguish between normal and cancer-derived EVs. Followed with chapter 5, where we, determine the detection probes in our assay by conjugating the quantum dots with EpCAM and EphA2. In addition to testing the assay for multiplexed detection of the total protein levels by measuring the total quantum dot signal. Finally, we present our proof of concept, by normalizing our total protein signal with the DiO signal for total EVs to measure individual EV protein expression levels.

iii. Clinical Validation : Performing the quantum dot assay on a clinically relevant cancer cohort

Chapter 6 is the clinical validation of the assay where we test the significance of the Qdot assay in two different clinically relevant pancreatic cancer/ cancer cohort. In the first study, we analyzed DiO-normalized anti-EpCAM-QD605 and anti-EphA2-QD655 probe signal on CD81-captured EVs from serum samples drawn from a cohort of 35 subjects that included non-cancer control subjects having other disease conditions like liver injury, pancreatitis and cholangitis (n=14) and pancreatic cancer patients (n=21). In the second study, we tested in total 74 subjects that included healthy non-malignant control

subjects, and pancreatic cancer patients with stage I/II, III, or IV tumors (11 – 21 subjects/group).

1.8 Significant Contributions

Manuscripts under review:

- Rodrigues, Meryl; Richards, Nicole; Ning, Bo; Lyon, Christopher; Hu, Tony, " A rapid lipid-based approach for normalization of quantum dot-detected biomarker expression on extracellular vesicles in complex biological samples", Nano Letters
- Amrollahi, Pouya; Rodrigues, Meryl; Lyon, Christopher J; Goel, Ajay, Han, Haiyong; Hu, Tony Ye ;"Ultra-Sensitive Detection of Cancer: Methodology, Mechanism, and Applications" , Frontiers in Genetics

Published Manuscript:

- Rodrigues, Meryl; Fan, Jia; Lyon, Christopher J; Wan, Meihua, Ye Hu, "Role of Extracellular Vesicles in viral and bacterial infections: Pathogenesis, Diagnosis and Therapeutics," Theranostics, 2018; 8 (10):2709–2721. Published 2018 Apr 9. doi:10.7150/thno.20576

Conference presentations:

- Meryl Rodrigues, Liang K, Liu F, Fan J, Sun D, Liu C, Lyon CJ, Bernard DW, Li Y, Yokoi K, Katz MH, Koay EJ, Zhao Z, Hu Y, "Nanoplasmonic Quantification of Tumor-Derived Extracellular Vesicles in Plasma Microsamples for Diagnosis and Treatment Monitoring" World Pharma Week, Boston, Poster presentation

CHAPTER 2 VALIDATING THE HYPOTHESIS OF VARIABLE ABUNDANCE OF EVS DERIVED FROM CANCER CELLS

2.1 Introduction

EV biogenesis in enhanced in cancer, where tumor cells produce and secrete more EVs than normal proliferating cells (Atay and Godwin 2014) . EV levels in plasma and other body fluids of patients with cancer are frequently elevated (Melo, Sugimoto et al. 2014, Melo, Luecke et al. 2015, Kalluri 2016). This shows that EV biogenesis is enhanced in cancer; and especially that tumor cells can produce and secrete many more EVs than normal proliferating cells (Taylor and Gercel-Taylor 2008, Dabitao, Margolick et al. 2011, Melo, Luecke et al. 2015). The underlying reason for this increase in EV release is still unclear, however, it is speculated that one reason could be the altered cellular physiology during pathological conditions like cancer (Kalluri 2016).

Several studies have been performed to understand the underlying reasons for the increase in the number of EVs released in cancer. There are studies showing that stress, including hypoxia prevalent in a tumor microenvironment, accounts for an increase in EV secretion by tumor cells (King, Michael et al. 2012). Additionally, intracellular and intercellular pH can affect EV release rate. Low pH condition is a hallmark of tumor malignancy. It is observed that when the microenvironmental pH is low, EV secretion and uptake by recipient cells is increased (Parolini, Federici et al. 2009). There is evidence that oncogenes and tumor suppressors regulate EV secretion in cancer. It was demonstrated that p53- regulated protein tumor suppressor-activated pathway 6 (TSAP6) induces EV secretion under stressed conditions (Yu, May et al. 2005, Yu, Harris et al. 2006).

Heparanase, an enzyme overexpressed in many tumor cell lines, was reported to regulate EV secretion (Thompson, Purushothaman et al. 2013). Although there are many insights suggesting several different mechanisms that may be involved in EV release, it seems that it may depend heavily on the cancer type and its aggressiveness. Several studies show that the number of EVs released can increase as time increases, but the reason behind it is still unknown. There are studies showing that EV concentration has been elevated in the systemic circulation of patients with ovarian, breast, and pancreatic cancer. However, one must account for the fact that in these studies, there were instances when EVs increased as tumor size increased, or the EV concentration increased as a natural extension of cancer stage progression (Taylor and Gercel-Taylor 2008, Melo, Luecke et al. 2015).

2.2. Materials and Methods

We designed an experiment to culture and quantify the number of EVs released from normal vs cancer cells. In this study, we collected EVs from two pancreatic cell lines, pancreatic cancer cell line (PANC1) and a normal pancreatic cell line (HPNE)

1. Cell Culture. The human pancreatic cancer cell line PANC-1 and the non-malignant human pancreas cell line HPNE were obtained from American Type Culture Collection (Manassas, VA). PANC1 and HPNE cell lines were grown at 37^{o}C in a humidified 5% CO_2 incubator in RPMI-1640 (Gibco, Life Technologies) or DMEM (Gibco, Life Technologies) medium, respectively, and supplemented with 10% fetal bovine serum (FBS), penicillin (1U), and streptomycin (1 μg/mL).
2. EV Isolation, and quantification. Cells were incubated with media containing 10% FBS for a minimum of 48 hours prior, then washed twice with PBS (pH 7.0), and incubated

in FBS-free media for 48 hours, after which the media was collected and centrifuged at 400 g for 20 minutes and the resulting supernatant was passed through a 0.45 µm filter to remove cell debris. This sample was then concentrated with a 100k MWCO filter (Merck Millipore Ltd.), centrifuged at 110,000 g for 2 hours, and the EV pellet was suspended in PBS and stored at 4^{o}C until use (< 2 weeks). EV size distributions and EV concentrations of HPNE and PANC-1 EV samples were analyzed using a NanoSight LM10 instrument and Nanoparticle Tracking Analysis Software (Malvern Instruments).

2.3 Results and discussions

We performed a comparative study on the number of cells vs the number of EVs released from PANC-1 and HPNE cell lines at three different time points. All culture conditions between the two populations were maintained in order to have a fair comparison. The data was collected after the cells had reached 90% confluency, where in the culture media was then replaced with serum-free media for EV collection. Following the standard protocol for the EV isolation, purification, and isolation, both cells and EVs were collected at three-time points 24 h, 48 h and 72 h. The total number of cells was calculated using a cell counter and the number of EVs using the nanosight instrument.

The same number of cells were seeded during the start of the experiment and by monitoring the growth of these cells, we managed to have the same number of cells at the three-time points for both HPNE and PANC-1., we can see there is no significant difference between the total number of cells collected at the three time points, stating that we could

now perform a comparative study on the number of EVs that would be released from these cells (Figure 4).

The EVs were isolated from cell culture supernatants by ultracentrifugation and analyzed by NanoSight, nanoparticle tracking analysis at 24, 48 and 72 h. respectively. The NanoSight instrument reveals number of vesicles along with the size distribution for each sample. HPNE shows EVs being released post 24 h, and then there isn't an increase for the next 48 h. or 72 h. time point (Figure 5). However, in PANC1 cells, the EVs released is noticed at 24 h., but following that there is still an increase in the total number of EVs for 48 h. and 72 h. time points. On comparing the number of EVs at these time points, they were significantly higher in PANC-1 compared to HPNE , with p-values 0.0019 for 24 h, 0.0011 for 48 h and <0.001 for 72 h with 95% confidence interval.

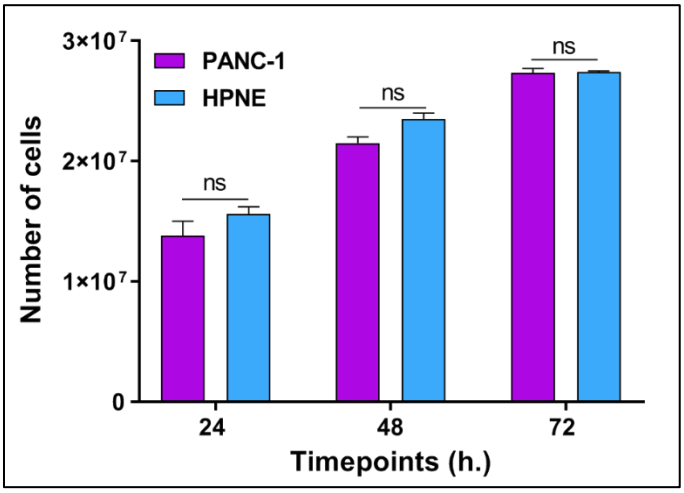

Figure 4. The comparison between the number of cells for both PANC-1 and HPNE at the three time points. There is no significant difference observed, stating that the number of EV collected from these samples comes from the same number of cells at 24, 48 and 72 h. respectively.

On further analyzing the data collected, we examined the per cell EV release (Figure 6), which suggests that the same number of cells in both populations can release different number of EVs which confirms the hypothesis that EV secretion rates are could be altered by multiple reasons, and that the number of EVs released can be different even after they adjust for the growth increase in total number of cells at that time.

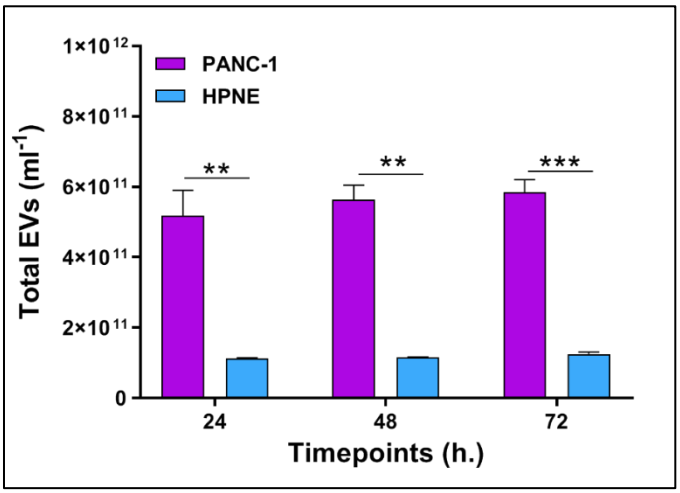

Figure 5.The total number of EVs released from same number of PANC-1is more than HPNE cells for the three different time points. (** p<0.01, *** p<0.001, *** p<0.001, ****p<0.0001 by Student's t-test)

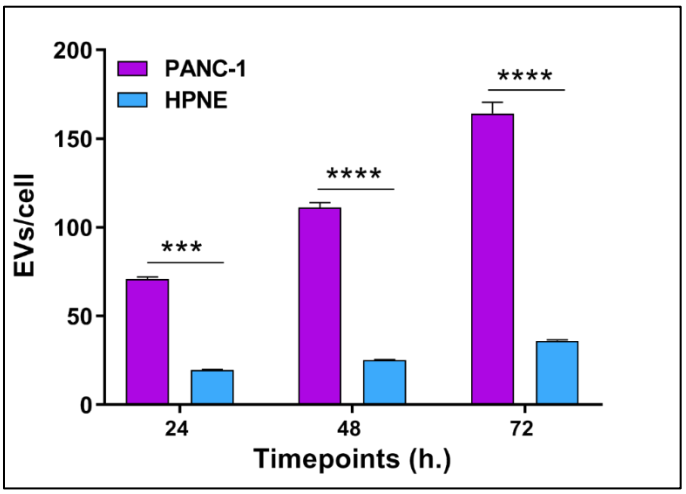

Figure 6. The per cell number of EVs released for PANC-1 is more than HPNE cells, and this difference increasing significantly as the time increases. (** p<0.01, *** p<0.001, *** p<0.001, ****p<0.0001 by Student's t-test)

CHAPTER

3 NORMALIZATION USING A FLUORESCENT LIPID DYE

3.1. Introduction

Despite increasing scientific and clinical interest in the potential of EVs for disease diagnosis, there are few standard procedures for their isolation, detection, characterization and quantification. The International Society for Extracellular Vesicles (ISEV) has emphasized the development and harmonization of standard protocols for specimen handling, isolation and analysis to facilitate comparison of results achieved within this fast-growing field (Witwer, Buzas et al. 2013, Lener, Gimona et al. 2015). EVs are too small to analyze by conventional optical detection methods, and their low refractive index and heterogeneous size and composition complicate such analyses, but recent advances now allow nanoparticle quantitation, which is useful for general EV analyses.

Current EV studies are focusing on quantifying the number of EVs when studying biomarker expression levels (Chen, Huang et al. 2018, Shao, Im et al. 2018). However, in-order to integrate it into the analysis platform, it needs a study protocol that would require to quantify the number of target EVs in an analysis sample. The quantification methods require purified sample, as there are abundant factors in serum, plasma, and other body fluids that interfere with these analyses along with large volume for sample preparation making it not practical for most clinical setting. Some of the current quantification methods is further discussed in the following section.

3.1.1. Technologies for quantifying EVs

3.1.1.1. Transmission electron microscopy (TEM)

Transmission electron microscopy can visualize EVs (Yuana, Koning et al. 2013) and analyze size and morphology, but not concentration, and overlap of the EV size range with those of several easily detectable contaminants (e.g., immune complexes, liposomes, calcium-phosphate micro precipitates and other particles) may introduce artifacts. This method is labor intensive and requires the use of procedures that are expensive and impractical for clinical use. More importantly, while it can potentially be conjugated with immune-gold staining to visualize specific EV sub-types, it cannot cope with the challenge of identifying and quantitating disease-associated EVs amidst the diverse population of EVs, particularly during early disease progression when these EVs should be extremely rare in the highly abundant circulating EV population.

3.1.1.2. Nanoparticle tracking analysis (NTA)

Nanoparticle tracking analysis (NTA) is an optical particle based tracking mechanism which employs a laser beam to illuminate all vesicles in a sample suspension, a light microscope to record the scattered light, and software to measure vesicle sizes as determined by the Brownian motion track of each particle (Dragovic, Gardiner et al. 2011, Vogel, Willmott et al. 2011). These instruments are commercially available and can measure the number and absolute size distribution of vesicles in a solution, and quantitate EVs based on their unique size profile but however need accurate camera and analysis setting to employ proper readings.

3.1.1.3. Tunable Resistive pulse sensing (RPS)

Resistive pulse sensing (TRPS) is another alternative method to the NTA, that can

determine the absolute size distribution of vesicles in sample suspensions via the Coulter principle (Kozak, Anderson et al. 2012), and at least one company has developed an instrument to exploit this approach. This system consists of two fluid cells divided by a non-conductive nanoporous membrane. A particle moving through one of these nanopores in response to a voltage applied across the cell membrane alters the ion flow, resulting in a brief "resistive pulse", which is recorded for calculation against a reference standard made with beads of known diameter and concentration (Vogel, Willmott et al. 2011, Kozak, Anderson et al. 2012).

3.1.1.4. Alternating current electrokinetic microarray chip (ACE)

Current technologies are trying to focus on integrating the isolation of these EVs on a single platform. In 2017, a group addressed this issue by developing alternating current electrokinetic (ACE) microarrays can isolate EVs from plasma samples followed with on-chip immunofluorescent detection of EV proteins and provide mRNA for downstream RT-PCR analysis (Ibsen, Wright et al. 2017), providing a potential means to isolate and analyze total EV populations without a separate EV isolation step. However, none of these approaches are yet available for clinical applications, but they demonstrate the potential of new chip technologies to rapidly profile disease-specific EVs from human samples after minimal sample preparation

3.1.2. Variable exosomal cargo – DNA, RNA, and proteins

To address this issue of quantifying EVs and bi-passing the conventional route, we focused on using fluorescent dyes to help quantitate the EVs in our study. There are several studies showing their use in exosomal localization, uptake and transfer studies (Hood, San et al. 2011, Chen, Wang et al. 2013, Kanwar, Dunlay et al. 2014, Mendt, Kamerkar et al.

2018). Fluorescent labeling of EV cargo components such as RNA, DNA, or protein could be used as a source for relative EV abundance in highly defined and homogeneous EV samples (Li, Zeringer et al. 2014, Williams, Rodriguez-Barrueco et al. 2014, Xu, Rai et al. 2018), such as purified cell culture-derived EVs samples. However, in 2014 a group focused on studying the presence of double-stranded DNA in tumor-derived EVs (Thakur, Zhang et al. 2014). They revealed that this exosomal DNA represent the entire genome and emulate the mutations seen in parental tumor cells. Furthermore, they looked at the exosomal DNA contents from various cancer cell lines including melanoma, breast, and lung, prostate and pancreatic cancer. They saw variable amounts of exosomal DNA, where in these levels were lowered in pancreatic and lung cancer cell lines, suggesting difference in exosomal DNA packaging among different cancer models. Exosomal cargo is known to contain RNA that play a role in wide range of biological functions, right from cell to cell communication to different signaling pathways. Another recent study revealed variable amounts of RNA present on EV isolated from serum versus urine EVs (Li, Zeringer et al. 2014). They studied the amount of RNA present in these EVs and noted that the theoretical values did not match the values observed for these EVs, suggesting that EVs have a very heterogeneous population with variable RNA contents based on packaging of these molecules and hence some EV might contain substantially lower amount of RNA in comparison to other EVs.

Comprehensive protein profiling studies revealed the difference in the cargo between EVs, suggesting that during biogenesis there is selective enrichment of these molecules in EVs. To sum it up EV biogenesis is a complex process and several underlying processes that are either parent cell related or other signaling and pathological stimuli that the cell

could undergo can influence exosomal cargo (van Niel, D'Angelo et al. 2018) further stating that labelling these biomolecules is not feasible with EV populations found in complex biological samples and body fluids, since changes in the relative abundance of EVs with different cargo compositions can skew such normalizations. Looking back at EV biogenesis process which occurs via endocytosis for majority of the cell types, which includes the dual invagination processes, first by the inward budding of the plasma membrane followed with invagination of the early endosome membrane, states that the plasma membrane is the universally present characteristic feature within all EVs (Xu, Rai et al. 2018). We exploited this common feature where the mean EVs lipid content of a mixed population should significantly change only in response to a marked change in the mean EV diameter of the sample. Since lipophilic dyes have been employed in EV localization, uptake and transfer studies (Hood, San et al. 2011, Chen, Wang et al. 2013, Kanwar, Dunlay et al. 2014, Mendt, Kamerkar et al. 2018), we hypothesized that quantifying the signal from EVs stained with such a dye could serve as a surrogate marker of EV abundance.

3.2. Material and methods

The experiments were designed to test and validate the use of lipophilic lipid dye as a normalizer for the assay. The goal of the experiments was to culture, isolate and quantitate purified EVs using the nanosight, followed with labeling known amounts of both HPNE and PANC-1 EVs to measure the labeling efficiency of the lipid dye. Once we confirmed the use of the dye as a normalizer, we then incorporated the dye with the quantum dot assay using by testing it on the 96-well black plate.

3.2.1. EV Isolation, and quantification

Cells were incubated with media containing 10% FBS for a minimum of 48 hours prior, then washed twice with PBS (pH 7.0), and incubated in FBS-free media for 48 hours, after which the media was collected and centrifuged at 400 g for 20 minutes and the resulting supernatant was passed through a 0.45 μm filter to remove cell debris. This sample was then concentrated with a 100k MWCO filter (Merck Millipore Ltd.), centrifuged at 110,000 g for 2 hours, and the EV pellet was suspended in PBS and stored at 4^{o}C until use (< 2 weeks). EV size distributions and EV concentrations of HPNE and PANC-1 EV samples were analyzed using a NanoSight LM10 instrument and Nanoparticle Tracking Analysis Software (Malvern Instruments). Figure 7-8 reveal the results for purified PANC-1 and HPNE EVs samples isolated by ultracentrifugation demonstrating similar size distributions with similar mean diameters.

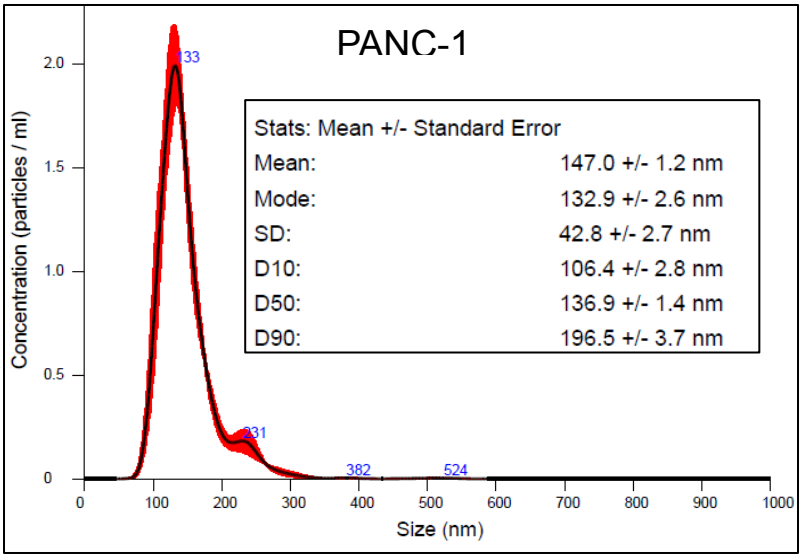

Figure 7. NanoSight analysis of PANC-1 EV size distribution profiles. Summarized results indicate the mean ± SEM of three replicate measurements.

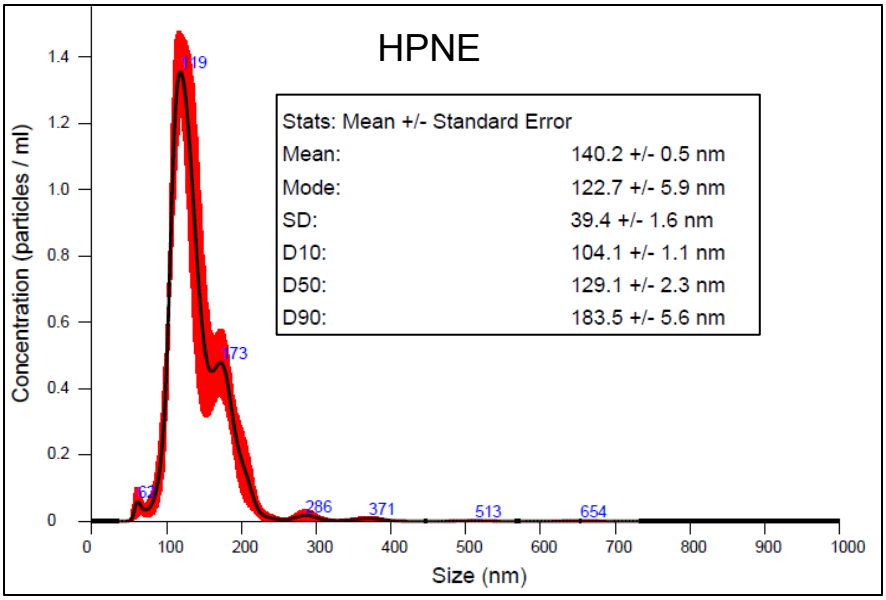

Figure 8. NanoSight analysis of PANC-1 EV size distribution profiles. Summarized results indicate the mean ± SEM of three replicate measurements.

3.2.2. EV Free Serum Preparation

Serum from healthy human subjects (Valley Biomedical Products & Services, Inc.) was centrifuged at 135 g for 15 minutes to allow lipid flotation, after which isolated serum samples were centrifuged at 9391 g for 45 minutes to precipitate insoluble debris and allow flotation of remaining lipid. This serum sample was then centrifuged at 110,000 g for 3 hours to precipitate EVs and the supernatant was collected and stored at -80^{o}C as EV-free serum

3.2.3. Fluorescent Lipophilic dye (DiO Dye)

Fluorescent lipophilic dyes are usually termed as membrane dyes. General membrane labeling with fluorescent lipophilic dyes has the advantages of being simple, rapid, and applicable for almost any type of cell. Since the EVs have a similar lipid membrane like the cells, these dyes can be used to label EVs as well. In this study we used Vybrant DiO cell-labeling solution (Invitrogen), DiO ($DiOC_{18}$ (3) or (3, 3′-dihexadecyloxacarbocyanine perchlorate)) also known as DiO dye for fluorescently labeling the EV membrane. The lipophilic carbocyanine dyes are known to be weakly fluorescent on water but are highly fluorescent, photostable and label membrane through lateral diffusion making them the right candidate for our study (Honig and Hume 1989). DiO was utilized for this analysis since it requires a one-step labeling process, unlike other fluorescent lipophilic dyes that have been used to stain EVs. For example, PKH dyes require extended incubation in an iso-osmotic mannitol solution, which can reduce EV yields and increase the variability of downstream EV analyses (Kanwar, Dunlay et al. 2014).

3.2.3.1 Determining the blocking buffer

One major issue with using the DiO dye was that this dye is mainly used to stain fixed cells or EVs for live cell imaging and EVs intake in cells. When using the dye in 96-well black polystyrene plate had several unseen problems.

The polystyrene plate being hydrophobic facilitates lipidic reactions causing the dye to bind to it resulting in a high background signal. The usual blocking buffer contains TWEEN-20 to get rid of these unbound hydrophobic regions. The buffer contains 5% BSA (Bovine serum albumin) in PBST (PBS +0.01% Tween 20) but it did not reduce the background signal.

The aim was to focus on getting rid of these hydrophobic regions that is available for the dye to bind to. Triton X 100, is a nonionic surfactant that has an uncharged hydrophilic head group of polyethylene oxide chain (on average it has 9.5 ethylene oxide units) and an aromatic hydrocarbon lipophilic or hydrophobic group tail, known to break lipid-lipid interactions rather than protein-protein interactions. This feature of Triton X can be exploited to get rid of the unbound hydrophobic region (Johnson 2013). We performed a study to test the blocking efficiency of three different blocking buffer followed with adding the DiO dye to a 96-well plate. The results revealed that blocking buffer with TritonX-100 showed low background signal in comparison to other blocking buffers (Figure 9).

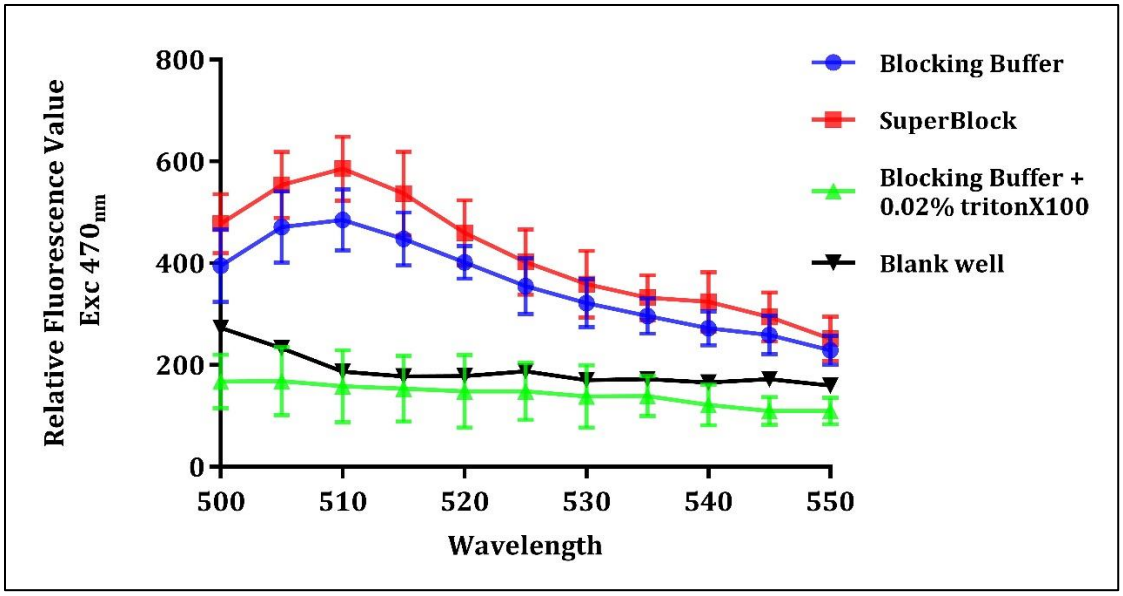

Figure 9. The fluorescence readout for the DiO dye after using three different types of blocking buffer , where blocking buffer consists of 5% BSA in PBST, SuperBlock™ (ThermoFisher Scientific) is a commercially available buffer and blocking buffer +0.02% tritonX-100

3.2.3.2. Determining Triton-X 100 concentration for wash step

Apart from being used in the blocking step, triton X100 is good at getting rid of unspecific binding and lipid-lipid interaction. However, Triton X 100 being a detergent is used to lyse cells, and studies have shown how different concentration of triton X 100 can cause EV lysis (Osteikoetxea, Sodar et al. 2015). The next aim was determining the right concentration of TritonX-100 in the wash buffer to get rid of unspecific binding of the dye along with not having any effect on the bound EVs. Three wash step for 10 minutes is equivalent to a total of 30 minutes interaction of the EVs with the wash buffer. The following experiment studied the influence of 5 different concentration of TritonX-100 on EVs incubated for 1 h and the EV content was then measured using the NanoSight

instrument. The study revealed that 0.01% tritonX-100 works best for the EV without damaging the integrity of the EVs and having the highest yield of 90.85% (Figure 10).

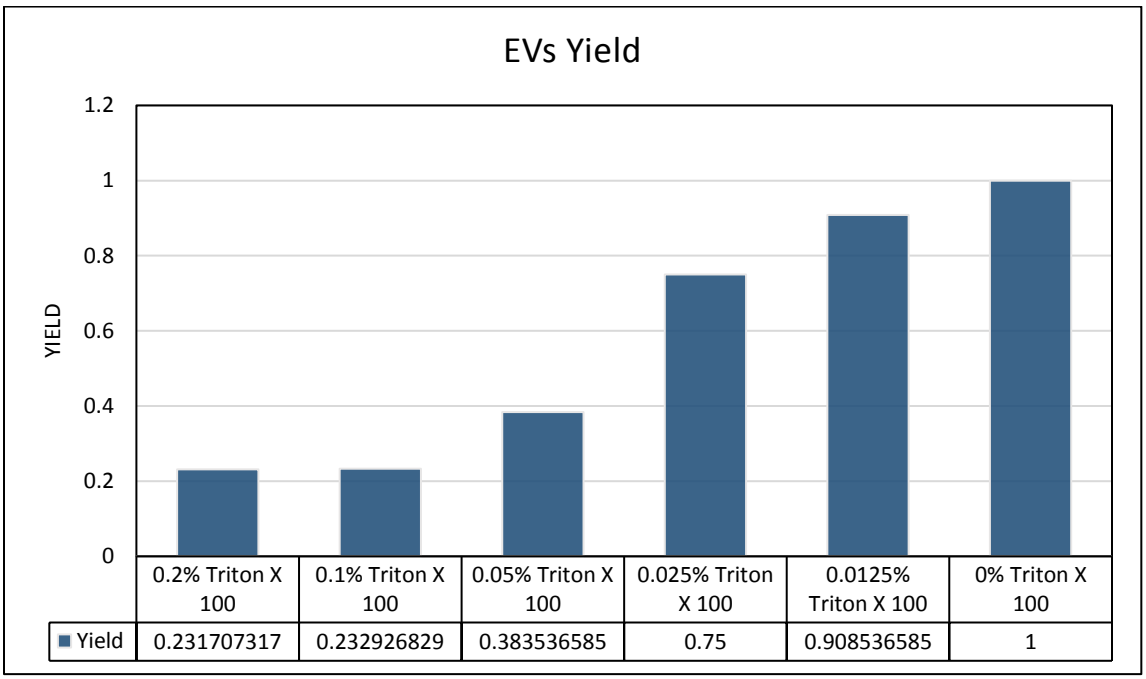

Figure 10.The influence of different concentrations of TrironX-100 on total EVs yield.

To summarize, the following procedure was developed to label the EVs:

1. High-binding 96-well black-walled, clear-bottom 96-well microplates (Corning 3601) were incubated with 100 µL/well of a 1:500 dilution of anti-CD81 (0.5mg/mL, BioLegend, Clone #5A6) antibody for 12 h at 4^{o}C
2. Wash twice with PBS Incubated with 200 µL/well of blocking (5% BSA in 0.02% TritonX-100, 0.05% Tween20 in PBS) buffer for 2 h at room temperature
3. Incubate the EVs for 12 h at 4^{o}C Add the 2.5 µL/ml Vybrant DiO cell-labeling solution (Invitrogen) diluted in PBS (100 µL/well) for 10 mins

4. Three 10 min washes with wash buffer (0.01% TritonX-100 and 0.05% Tween20 in PBS), and then read at 470 nm excitation on a fluorescence microplate reader to measure lipid labeling.

3.3 Results and discussions

The aim of this approach was to understand the feasibility of this technique, we designed an experiment to test the correlation of the lipid signal to the total number of EVs in the assay. For its accurate use as a normalizer in our assay, we labeled different known concentration of number of EVs for HPNE and PANC-1 with the DiO dye and performed a correlation study of the labeling of DiO for HPNE vs PANC-1 EVs.

A known concentration of EVs were first spiked into EV - free serum, followed with capture on the surface of a 96-well plate using a capture antibody, they were then labeled with the DiO, and the plate reader was used to measure the fluorescent signal at 470nm emission. Figure 11, represents the fluorescence signal for same number of EVs labeled in HPNE and PANC-1 populations. We performed linear regression analysis with 95% confidence intervals, which shows that PANC-1 EVs have a slope of 1.25 and R^2 = 0.88 and HPNE EVs have a slope of 1.099 with R^2 = 0.92. This suggests that there is a linear relationship of the binding of the dye to the number of EVs in a sample, irrespective of its cellular origin.

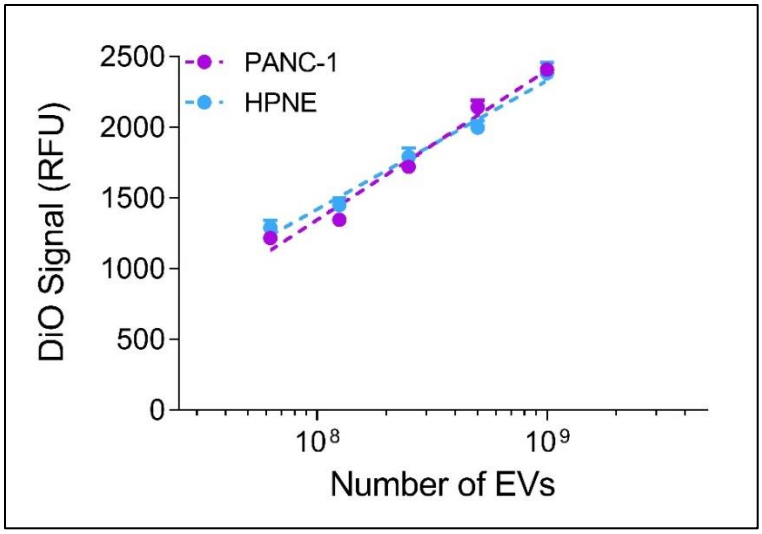

Figure 11. Standard curves of DiO-stained PANC-1 and HPNE EV standards. Data represent means ± SEM, n= 3 replicates/ sample

To further validate the data, we performed a correlation between the signal values for HPNE and PANC-1 EVs , Figure 12, represents the data showing a correlation with $R^2 = 0.97$. This approach exhibited robust performance to differentiate sequential 2-fold EV dilutions, with all HPNE samples and all but the lowest PANC-1 samples significantly differing from the next dilution sample. Thus indicating that any potential differences in membrane composition or EV size distributions did not affect DiO staining. HPNE and PANC-1 EVs stained with DiO demonstrated similar fluorescent intensity on confocal microscope images, which was distinct from the signal of a quantum dot probe bound to these EVs (Figure 13)

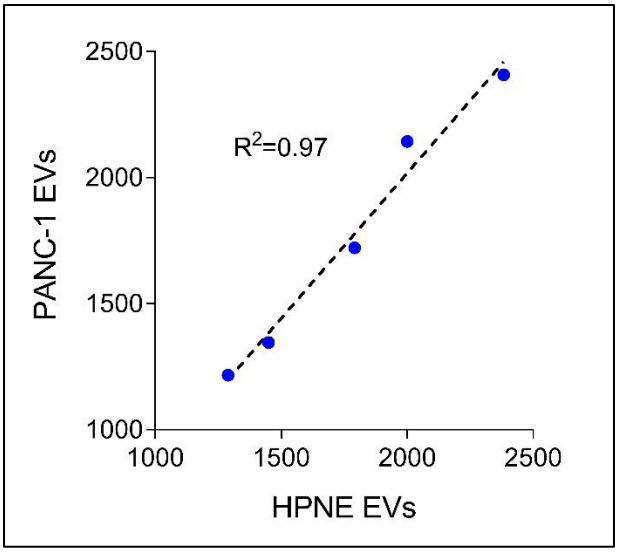

Figure 12. Correlation of DiO signal from PANC-1 and HPNE EV standards. Data represent means ± SEM, n= 3 replicates/ sample

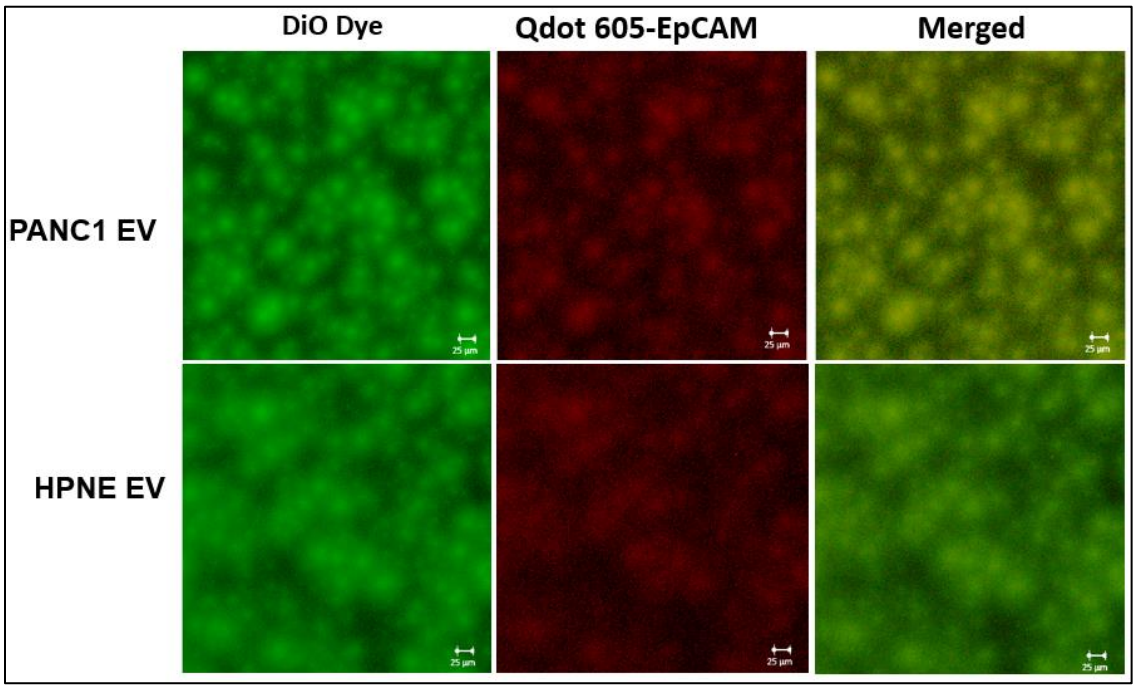

Figure 13. Confocal images of PANC-1 and HPNE EVs labeled with DiO and an EpCAM-specific quantum dot probe (Qdot 605-EpCAM). Scale bar = 25µm.

CHAPTER

4 Measuring the expression of cancer specific exosomal surface markers

4.1. Introduction

The American Cancer Society estimates close to 55,440 new cases of pancreatic cancer will be diagnosed in the US in 2018, comprising 3% of the total number of new cancer cases (Cancer Facts and Figures, 2018, American Cancer Society). However, the estimated number of deaths from pancreatic cancer is 44,330 in 2018, about 7% of all cancer deaths. With a 5-year survival rate of close to 8.5%, pancreatic cancer is the fourth leading cause of cancer in both men and women. One of the main reasons for this is the inability for proper diagnosis, which in turn leads to its poor prognosis.

The location of the pancreas in the body makes it difficult to see or feel early tumors (Cancer Facts and Figures, 2018, American Cancer Society). Majority of pancreatic cancers (PC) are known to progress to either locally advanced or metastatic disease before showing any symptoms, causing metastasis to be one of the most common causes of death in PC patients (Hidalgo 2010). Yachida et al. sequenced the genomes from seven pancreatic cancer metastatic samples to study the relationship between primary and metastatic cancer (Yachida, Jones et al. 2010). The novel insights from this study into the genetic information of pancreatic cancer progression revealed that it takes 5 years for the acquisition of metastatic ability after a parental tumor but the non-metastatic cell is detectable prior to this. This data established a broad time window of opportunity for early detection to prevent deaths from metastasis (Yachida, Jones et al. 2010, Herreros-Villanueva and Bujanda 2016)

Exocrine cancer is by far the most common type of pancreatic cancer, wherein about 95% of cancers are pancreatic adenocarcinoma (National Cancer Institute, Surveillance, Epidemiology and End Results Program, 2018). Pancreatic ductal adenocarcinomas (PDAC) are developed from three precursor lesions: pancreatic intraepithelial neoplasia (PanIN) lesions, intraductal mucinous neoplasm (IPMN) and mucinous cystic neoplasms (MCN) (Yachida, Jones et al. 2010). Diagnosis of PC is challenging due to the non-specific symptoms in patients which leads to late diagnosis. In fact, sometimes pancreatic masses are indistinguishable from chronic pancreatitis or benign pancreatic cysts when a biopsy is obtained , furthermore, pathological results can often be inconclusive (Yachida, Jones et al. 2010). Currently, there are no reliable markers that can accurately diagnose, classify and predict the biological behavior of pancreatic tumors. Therefore, it is imperative to focus on identifying and developing biomarkers, with high specificity and sensitivity that can help detect initial lesions in the early stages of pancreatic cancer (Herreros-Villanueva and Bujanda 2016, Nuzhat, Kinhal et al. 2017)

There are potential serum biomarkers for diagnosis, disease progression and monitoring of therapy (Hidalgo 2010). Carbohydrate antigen, CA19-9 is currently the most extensively studied biomarker and the only one approved by the FDA with demonstrated clinical usefulness (Goonetilleke and Siriwardena 2007). However, it has a major limitation of not being specific for pancreatic cancer with elevated levels in acute cholangitis, live cirrhosis, pancreatitis and obstructed jaundice (Loosen, Neumann et al. 2017). Furthermore, patients who are negative for Lewis antigen a or b, are unable to synthesize CA19-9 and have undetectable levels of serum CA19-9. CA19-9 levels are useful in

monitoring patients diagnosed with PC, but the use as a screening or diagnostic tool is still a concern (Hidalgo 2010, Loosen, Neumann et al. 2017)

4.2. EpCAM and EphA2 as pancreatic cancer specific markers

To test the ability of this approach to quantify the mean expression of EV biomarkers, we employed quantum dots labeled with antibodies specific to different EV membrane biomarkers associated with pancreatic cancer to analyze EVs isolated from PANC-1 and HPNE cell lines. We focused on two cancer-specific markers– Ephrin type-A receptor 2 (EphA2) and Epithelial cell adhesion molecule (EpCAM).

Ephrin type-A receptor 2 (EpHA2) , originally named epithelial cell kinase (Eck) is a transmembrane receptor tyrosine kinase, normally expressed at low levels in adult epithelial tissues (Lindberg and Hunter 1990). EphA2 is also an oncoprotein, with roles in the regulation of cell growth, survival, angiogenesis, and migration, along with an ability to confer malignant potential to non-transformed epithelial cells (Zelinski, Zantek et al. 2001). Studies have revealed that EphA2 is over-expressed in a number of human cancers, and increased levels of EphA2 are associated with aggressive disease and poor clinical outcomes (Duxbury, Ito et al. 2004, Mudali, Fu et al. 2006). In pancreatic cancers, EphA2 is over-expressed in pancreatic adenocarcinoma cell lines with higher metastatic potential, while suppression of EphA2 expression appears to lessen the invasive phenotypes of the same cell lines. This information enables EphA2 biomarkers to be used not only as a diagnostic tool but also helps provide support for EphA2 targeted therapies in cancer (Duxbury, Ito et al. 2004, Duxbury, Ito et al. 2004).

Epithelia cell adhesion molecule (EpCAM) is a surface glycoprotein of approximately 40 kDa that can play a role in cell adhesion and tissue plasticity, along with regulating cell proliferation and differentiation (Schnell, Cirulli et al. 2013). It is known to be expressed on a subset of normal epithelia and overexpressed in a variety of different tumors (Imrich, Hachmeister et al. 2012). EpCAM is a primary tumor marker, showing evidence of downregulation in circulating tumor cells during epithelial-to-mesenchymal transition (Duxbury, Ito et al. 2004, Duxbury, Ito et al. 2004, Visvader and Lindeman 2009). Studies have shown that pancreatic cancer EVs exhibit certain markers related to the cancer initiating cells, which include Tspan8, MET and EpCAM (Nuzhat, Kinhal et al. 2017). Several other studies unfolded higher expression levels of EpCAM that corresponded to poor prognosis in ovarian, breast and pancreatic cancer (Schnell, Cirulli et al. 2013).

4.3 Materials and methods

To validate the expression levels of these markers in HPNE and PANC-1 EVs we performed western blot analysis and ELISA using the same number of EVs for both cell types.

4.3.1 Western blot

Western blots (SDS-PAGE) were performed with 5 μg/sample HPNE and PANC-1 cells protein lysate as measured by Pierce™ BCA Protein Assay Kit (ThermoFisher Scientific) and same number of HPNE and PANC-1 EVs. The gel was transferred to the membrane using BioRad Trans-Blot Turbo. The membranes were blocked using 5% BSA/PBST blocking solution, and 1:1000 dilutions of the indicated primary antibodies

anti-human-EphA2 (Sigma-Aldrich , clone D7), anti-human EpCAM (ThermoFisher Scientific, clone #VU-1D9), anti-human TSG101 (Abcam, 4A10) and anti-human GM130 (Santa Cruz Biotechnology, B-10) and a 1:5000 dilution of HRP-labeled secondary antibody (goat anti-mouse, IgG H&L, Abcam, ab6789) in 5% BSA/PBST, with Clarity™ Western ECL substrate (Bio-Rad), and acquiring chemiluminescent images.

4.3.2. EV ELISA Assay

- Reduced surface area 96-well microtiter plates (Corning 3690) were incubated with 50 µL/well of a 1:500 dilution of anti-human CD81 (0.5 mg/mL, BioLegend, Clone #5A6) in PBS for 12 h at 4ºC.
- Plates were then washed twice with PBS for 5 min per wash, incubated with 5% BSA in PBS with 0.05% Tween-20 (PBST) for 2 h at room temperature (50 µL/well), then washed four times with PBST at a minimum of 5 min per wash.
- EV samples (25 µL/well) were added to the plate, which was then incubated overnight at 4ºC and then washed four times with PBST.
- The captured EVs were then incubated with biotin-labeled anti-human EpCAM (1µg/mL, ThermoFisher Scientific, clone #VU-1D9) and anti-human EphA2 biotin (1 µg/mL, R&D Systems) in 5% BSA/PBST for 1 h at 37ºC (50 µL/well), washed four times with PBST, and
- Then incubate with a 1:3000 dilution of HRP-conjugated streptavidin (1.25mg/mL, ThermoScientific Pierce) in 5% BSA/PBST for 1 h at room temperature (50 µL/well).
- Sample wells were then washed four times with PBST, incubated with 50 µL/well TMB reagent (ThermoScientific, Inc.) for 10-15 min at room temperature then

supplemented with 50 µL/well stop solution (2 M H_2SO_4) and read for absorbance at 450 nm on a microplate reader.

4.3.3. Statistical Analyses

GraphPad Prism version 8.0.2 (GraphPad Software) was used for all calculations. Statistical analyses were performed using Student's t-tests, one-way ANOVA with Tukey's multiple comparison test as determined by sample distribution and variance. Differences with p-values < 0.05 were considered statistically significant. Figures were prepared using GraphPad Prism 8.0.2 (GraphPad Software). All data points are derived from three biological or technical replicates as indicated for each experiment.

4.4 Results and discussions

Western blot analysis of cell lysates generated from HPNE and PANC-1 cells revealed that EphA2 and EpCAM expression were enhanced in PANC-1 versus HPNE cells, and further increased in equal numbers of EVs isolated from PANC-1 versus HPNE cells, stating that these two markers could further be used as targets for distinguishing normal vs cancer derived EVs (Figure 14) Cell lysate expression of the endosomal sorting complex required for transport (ESCRT) protein TSG101, an endosome-associated marker (Raiborg and Stenmark 2009, Willms, Johansson et al. 2016), was similarly expressed in both cell lysates but was less abundant in HPNE versus PANC-1 EVs, although the reason for this difference is not clear. Neither EV population appreciably expressed the Golgi marker GM130, which is not found in EV populations (Keerthikumar, Gangoda et al. 2015).

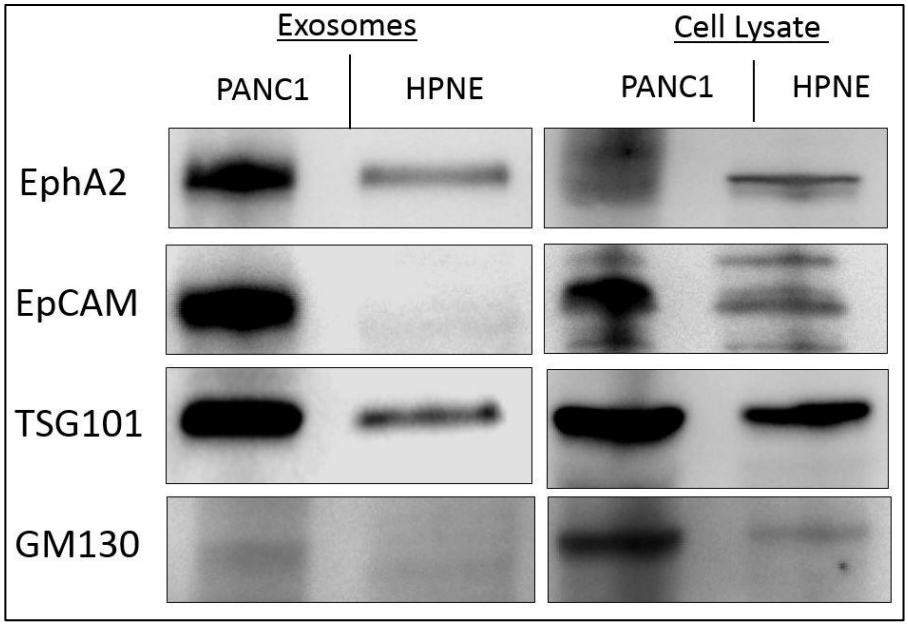

Figure 14. EphA2 and EpCAM are selectively expressed on PANC-1 vs. HPNE EVs. Western blot analysis of protein expression in equal numbers of PANC-1 and HPNE EVs and cell lysate. TSG101 as a positive marker for EVs and GM130 as a negative marker for EVs.

We then used the gold standard to quantify the expression of these markers on HPNE and PANC1 EVs. Similar EpCAM and EphA2 expression differences were also observed in EV ELISAs in which equivalent numbers of purified EVs isolated from these cell lines were captured with anti-CD81 antibody, a general EV marker (Kowal, Arras et al. 2016), and probed with EpCAM or EphA2 detection antibodies. The slopes of all these dilution curves were significantly different from zero, although ELISA signal from these two EV populations did not exhibit parallel increases with increasing EV numbers in the EphA2 EV ELISA, indicating an apparent weak detection efficiency for EphA2 expression on the HPNE-derived EVs.

Figure 15, linear regression analysis found that EpCAM signal demonstrated similar increases with increasing EV number (3×10^7 ~ 5×10^8 EVs) in EVs derived from both PANC-1 ($p<0.0001$, $R^2= 0.91$) and HPNE ($p = 0.0134$, $R^2 = 0.96$) cell cultures. In EphA2 signal also demonstrated trends to increase with increasing numbers of EVs from PANC-1 ($p <0.0001$, $R^2 = 0.85$), albeit with greater signal variability than observed in the EpCAM EV ELISA, but no significant trend to increase was observed in the HPNE samples ($p=0.4489$) (Figure 16) However, ELISA signal for both assays demonstrated poor sensitivity to discriminate differences in total EV expression of these biomarkers in sequential EV dilutions (Table.1-2), being unable to differentiate signal arising from 2-fold dilutions of most of these EV samples. Based on these results we selected EphA2 and EpCAM as our two candidate markers for detection and distinguishing of pancreatic cancer derived EVs from normal EVs.

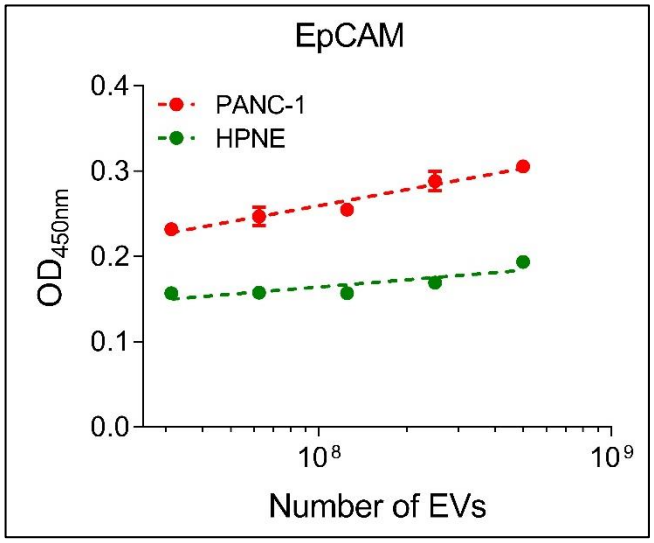

Figure 15. EpCAM signal from EV ELISAs of PANC-1 and HPNE EV concentration standards captured with anti-CD81 antibody. Data represent means ± SEM, n= 3 replicates/sample.

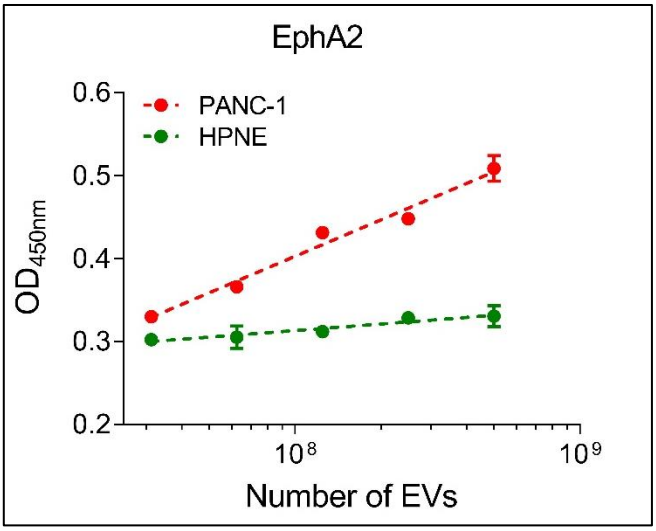

Figure 16. EphA2 signal from EV ELISAs of PANC-1 and HPNE EV concentration standards captured with anti-CD81 antibody. Data represent means ± SEM, n= 3 replicates/sample.

HPNE EV	3.13E+07	6.25E+07	1.25E+08	2.50E+08	5.00E+08
vs.					
PANC-1 EV	3.13E+07	6.25E+07	1.25E+08	2.50E+08	5.00E+08
P value	<0.0001	0.0012	<0.0001	0.0009	<0.0001
t, df	t=36.03, df=4	t=8.134, df=4	t=15.76, df=4	t=8.908, df=4	t=18.15, df=4

Table 1. Student's t-test analysis of EVs ELISA-measured for EpCAM expression from equal number of HPNE and PANC-1 EVs.

HPNE EV	3.13E+07	6.25E+07	1.25E+08	2.50E+08	5.00E+08
vs.					
PANC-1 EV	3.13E+07	6.25E+07	1.25E+08	2.50E+08	5.00E+08
P value	0.0272	0.0164	<0.0001	<0.0001	0.0009
t, df	t=3.403, df=4	t=3.982, df=4	t=18.61, df=4	t=26.68, df=4	t=8.853, df=4

Table 2. Student's t-test analysis of EVs in ELISA-measured for EphA2 expression from equal number of HPNE and PANC-1 EVs.

CHAPTER 5 NORMALIZED DETECTION OF TARGET EV MARKERS USING THE QUANTUM DOT ASSAY (QDOT ASSAY)

5.1 Quantum dots (Qdot) as detection probes

The assay uses quantum dots as the fluorescent detection probes, which are semiconductor nanoparticles having physical and optical properties making them the useful for high-resolution labeling and imaging (Pathak, Davidson et al. 2007). In addition to having high quantum yield and high extinction coefficient which makes them brighter and more photostable than other fluorescent probes, they have narrow emission spectral peak which prevents spectral overlap mostly seen with other organic fluorophores which plays to the advantage of using them for multiplexing (Pathak, Davidson et al. 2007, Toseland 2013). Quantum dots have a broad excitation spectrum, suggesting that the same excitation wavelength could be used to excite two or more dots. We selected two quantum dots with emission spectra maxima at 605 nm (QD605) and 655 nm (QD655) as the two fluorescent probes for our assay. We ran a preliminary test using a mixture of the same concentration of the quantum dots and excited them at 390nm to measure the signal intensities at 605 and 655 at the same time. Figure 17, shows that the signal intensities were very similar for both the qdots, implying that we could further use them together in our assay.

5.2 Materials and methods

To test the difference of between normalized and not normalized signals for EpCAM and EphA2, we designed the Qdot assay to measure the total signal from the DiO dye, followed with measuring the signal from quantum dot conjugated antibodies, anti-EpCAM-QD605 and anti-EphA2-QD655

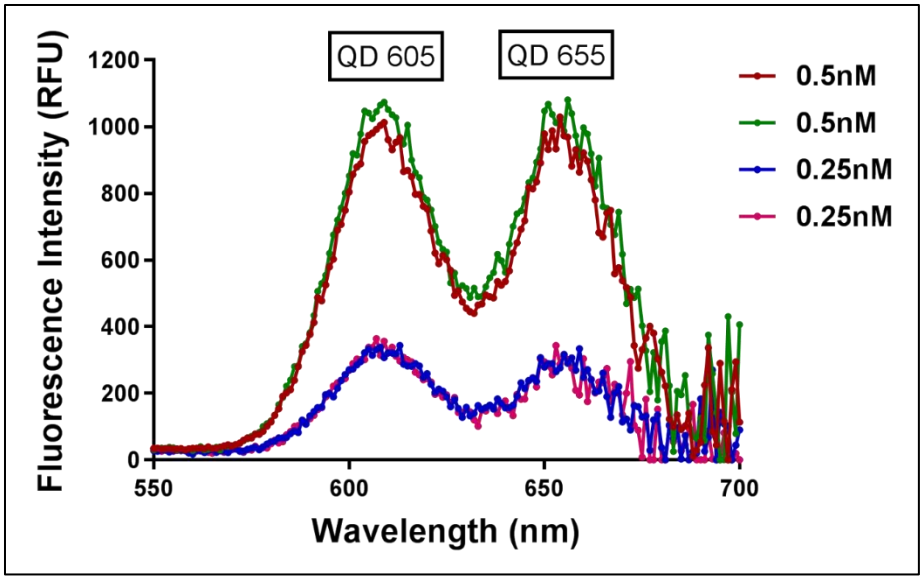

Figure 17. Replicate emission spectra of equal mixtures of QD605 and QD655 particles analyzed at two different concentrations (390 nm excitation).

Day 1:

- High-binding 96-well black-walled, clear-bottom 96-well microplates (Corning 3601) were incubated with 100 µL/well of a 1:500 dilution of anti-CD81 (0.5mg/mL, BioLegend, Clone #5A6) antibody for 12 h at 4°C, then washed twice with PBS

Day 2:

- Then incubated with 200 µL/well of 5% BSA/PBST in 0.02% TritonX-100 for 2 h at room temperature,
- Then aspirated and incubated with 50 µL/well of EV for 12 h at 4°C.

Day 3:

- Sample wells were then washed with PBS for 5 min, incubated for 10 min at 37ºC with a 2.5 μL/mL Vybrant DiO cell-labeling solution (Invitrogen) diluted in PBS (100 μL/well), subjected to three 10 min washes with 0.01% TritonX-100 in PBS, and then read at 470 nm excitation on a fluorescence microplate reader to measure lipid labeling.
- Biotin-labeled anti- EphA2 (0.5mg/mL, R&D system) antibodies were diluted 1:200 in 5% BSA/PBST and added to sample wells (50 μL/well) and incubated for 1 h at 37ºC, then washed three times for 5 min with PBST
- Add 12nM of streptavidin-coated Qdot 655 sample wells (50 μL/well) and incubated for 1 h at 37ºC shaking at 100 rpm, then washed three times for 5 min with PBST
- Block the excess streptavidin regions of the Qdot 655 with biotin (Biotin blocking kit, ThermoFisher Scientific) and incubate covered for 10 mins at 37°C shaking at 100 rpm (50 μL/well). then washed three times for 5 min with PBST
- Biotin-labeled anti-EpCAM (0.5mg/mL; ThermoFisher Scientific, clone #VU-1D9) antibodies were diluted 1:200 in 5% BSA/PBST and added to sample wells (50 μL/well) and incubated for 1 h at 37ºC, then washed three times for 5 min with PBST
- Add 12nM of streptavidin-coated Qdot 605 (Invitrogen) sample wells (50 μL/well) and incubated for 1 h at 37ºC shaking at 100 rpm, then washed three times for 5 min with PBST

- incubated for 1 h at 37ºC, washed three times for 10 min with PBST, and read in a fluorescence microplate reader (390 nm excitation) to quantify DiO (500 nm) and quantum dot (605nm and 665 nm) signal intensity.

5.3 Results and discussions

5.3.1 Total signal for EpCAM-QD605 and EphA2-QD655

Analysis of EV- free serum spiked with serial dilutions of purified PANC-1 and HPNE EVs revealed progressive signal increases after CD81-captured EVs were hybridized with anti-EpCAM-QD605 and anti-EphA2-QD655, in correspondence with input EV concentrations (Figures 18-19). The Qdot assay is designed to first quantitate the number of EVs in the sample in using the DiO signal, followed with measuring the signals at 605nm and 655nm with 390nm excitation. We summarized the standard curves for EpCAM total expression levels on the same number of EV samples revealing a linearity for both HPNE and PANC-1 EVs (Figure 20). The EpCAM expression on HPNE EVs revealed a slope of 5.28×10^{-7}, and for PANC-1 EVs a slope of 4.722×10^{-7} relative fluorescent units (RFU) per input EV, respectively, with robust correlation coefficients ($R^2 = 0.99$ and 0.90). In, the expression for EphA2 on HPNE EVs revealed a slope of 5.14×10^{-7}, and for PANC-1 EVs a slope of 4.69×10^{-7} , relative fluorescent units (RFU) per input EV , respectively, with robust correlation coefficients ($R^2 = 0.98$ and 0.89) (Figure 21). Furthermore, student's t-test analysis on the expressions for EpCAM and EphA2 in PANC-1 vs HPNE EVs demonstrated good ability to discriminate between differences in the expression of these EV biomarkers.

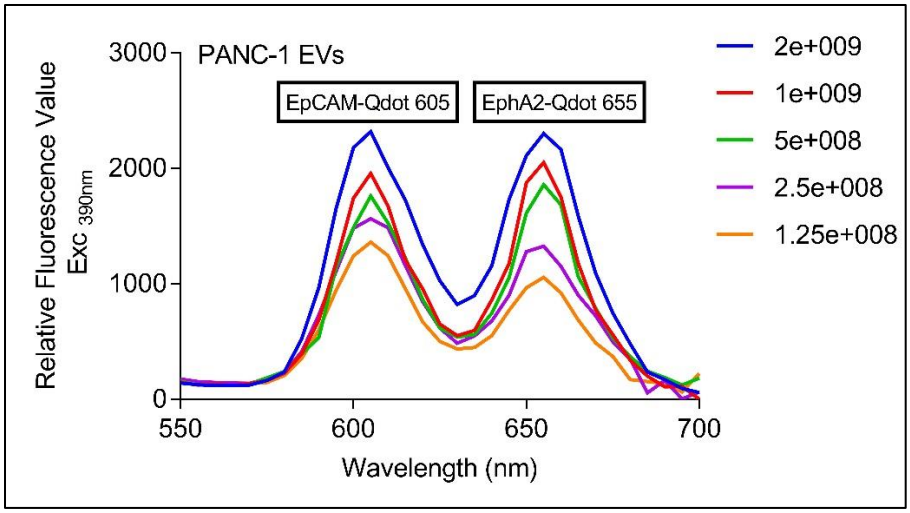

Figure 18. Fluorescence spectra of QD605-EpCAM and QD655-EphA2 on CD81-captured PANC-1 EVs.

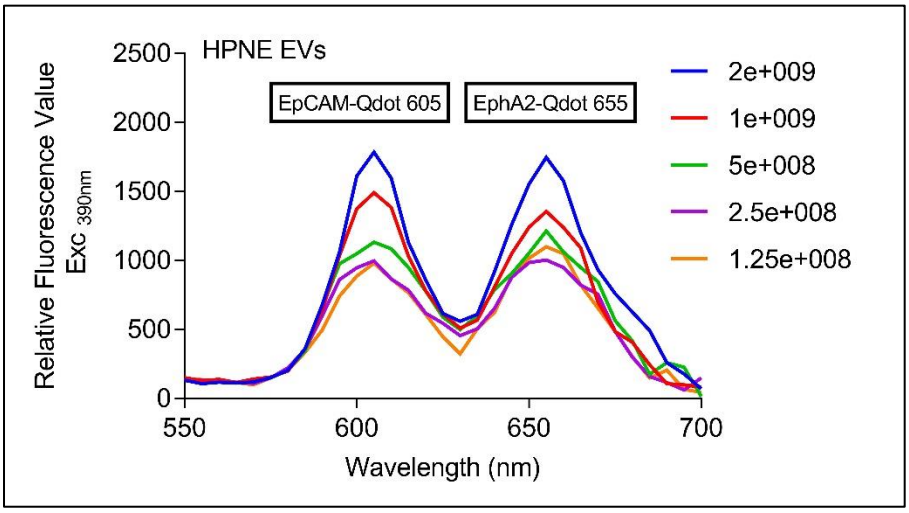

Figure 19. Fluorescence spectra of QD605-EpCAM and QD655-EphA2 on CD81-captured HPNE EVs.

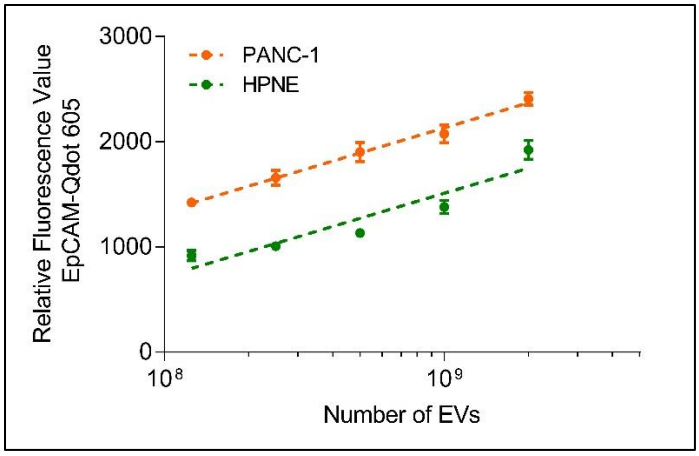

Figure 20. Standard curve for EpCAM expression on HPNE and PANC-1 EVs. Data represents means ± SEM, n=3 replicates/sample

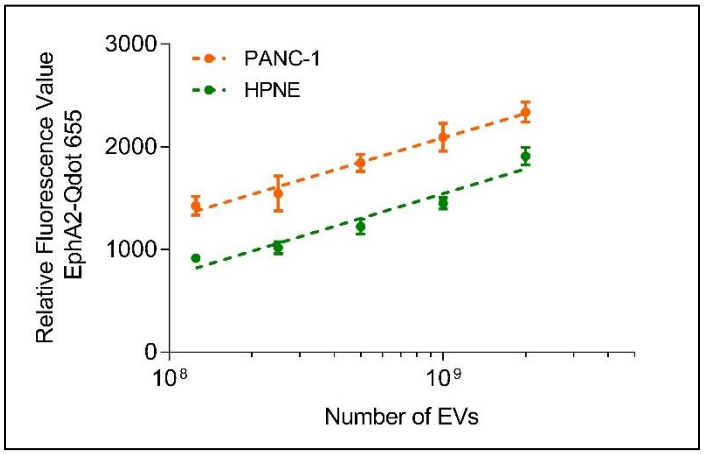

Figure 21. Standard curve for EpCAM expression on HPNE and PANC-1 EVs. Data represents means ± SEM, n=3 replicates/sample

In Table.3, a significant difference was observed in the expression of EpCAM for the same number of EVs with p= 0.001 for 1.25×10^8 (lower sample size) EVs to p=0.01 for 2×10^9 (higher sample size) EVs. Similarly, in Table.4, we observed a significant difference in the expression of EphA2 for the same number of EVs with p= 0.01 for 1.25×10^8 (lower sample size) EVs to p=0.03 for 2×10^9 (higher sample size). These results

thus hold promise for the ability of this approach to detect similar differences in peripheral blood samples of cancer patients, which contain approximately 10^{11} EVs per mL (Kanwar, Dunlay et al. 2014)

HPNE EV	1.25E+08	2.50E+08	5.00E+08	1.00E+09	2.00E+09
vs.					
PANC-1 EV	1.25E+08	2.50E+08	5.00E+08	1.00E+09	2.00E+09
P value	0.001	0.0007	0.0016	0.002	0.01
t, df	t=8.472 df=4	t=9.316 df=4	t=7.643 df=4	t=6.599 df=4	t=4.447 df=4

Table 3. Student's t-test analysis of Quantum dot-measured EV EpCAM expression from equal numbers of HPNE and PANC-1 EVs.

HPNE EV	1.25E+08	2.50E+08	5.00E+08	1.00E+09	2.00E+09
vs.					
PANC-1 EV	1.25E+08	2.50E+08	5.00E+08	1.00E+09	2.00E+09
P value	0.01	0.04	0.005	0.01	0.03
t, df	t=4.427 df=4	t=14.28 df=4	t=11.90 df=4	t=12.09 df=4	t=19.32df=4

Table 4. Student's t-test analysis of Quantum dot-measured EV EphA2 expression from equal numbers of HPNE and PANC-1 EVs.

5.3.2 Normalized signal for EpCAM and EphA2

Notably, this assay was performed using known amounts of EVs spiked in EV free serum, but only highly purified EV samples can be accurately quantified using current methods. We propose that staining with a lipophilic fluorescent dye can be used to assess the relative lipid content of affinity-captured EVs to quantify their abundance and normalize the mean expression of EV biomarkers.

DiO signal did not differ between equal numbers of HPNE and PANC-1 EVs at any point in these concentration curves (Figure 22) These HPNE and PANC-1 EVs dilutions were then analyzed to determine if their EpCAM-QD605 and EphA2-QD655 signals differed after they were normalized against their DiO signal to correct for differing EV concentrations.

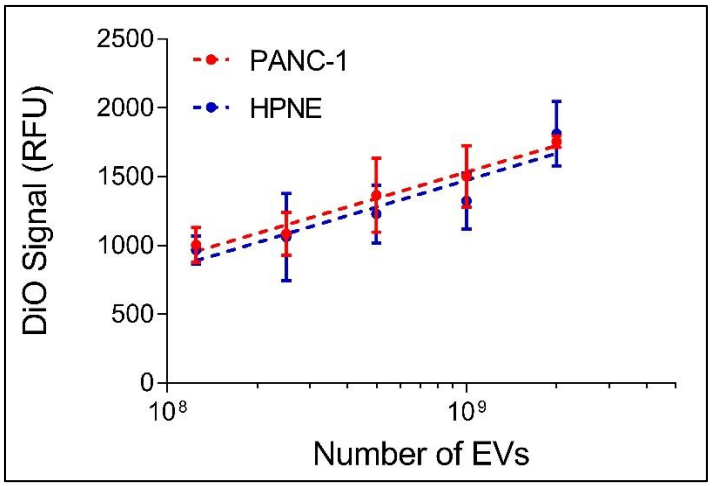

Figure 22. DiO signal from serial dilution samples of PANC-1 and HPNE EVs. Data represents means ± SEM, n=3 replicates/sample

The DiO signal for number of EVs and the Quantum dot signal for the two markers, was used with a simple formula to measure per EV expression levels, where expression of the biomarker per EV = (Signal intensity of the Qdot / Signal intensity of the DiO). The results will reveal the information of the markers on each EV type, implying that the values from the test show a trend with no significant deviation from zero and no significant difference in the data points for different number of EVs within each population. In, we find that biomarker signal, both EpCAM and EphA2 did not significantly vary with input EV number and that the slope of these signals among these samples did not significantly differ from zero (Figures 23-24). These results strongly imply that DiO signal accurately

reflects increasing EV abundance, as previously indicated (Figure 11), and is sufficient to correct for differences in EV number to normalize EV biomarker signals to EV number, eliminating the need for EV purification and NTA quantification, which can introduce variation and require significant amounts of starting sample.

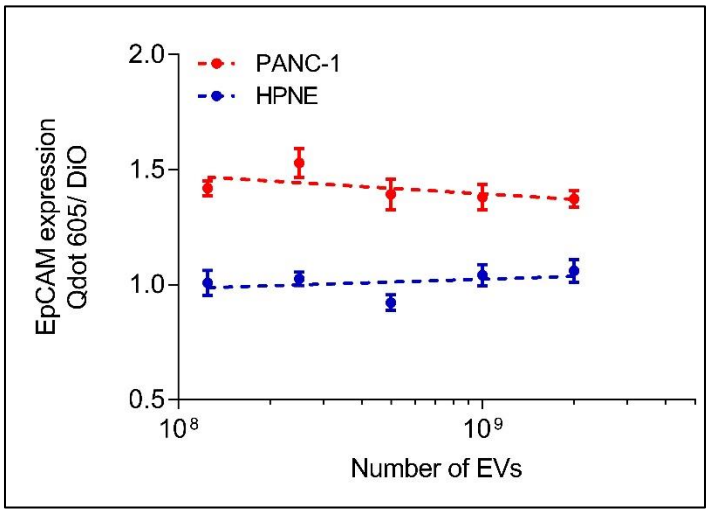

Figure 23. DiO-normalized EpCAM-Qdot 605 signal detected using HPNE and PANC-1 EV concentration standards. Data represents means ± SEM, n=3 replicates/sample

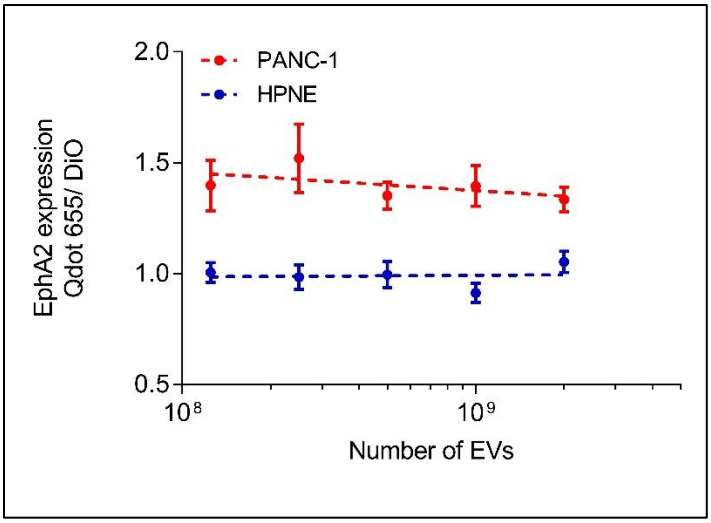

Figure 24. DiO-normalized EphA2-Qdot 655 signal detected using HPNE and PANC-1 EVs concentration standards. Data represents means ± SEM, n=3 replicates/sample

CHAPTER 6 CLINICAL VALIDATION OF THE QDOT ASSAY ON TWO DIFFERENT PANCREATIC CANCER COHORT

6.1 Clinical cohort information

To test the utility of this approach in clinical samples, we investigated two different cohorts one from obtained from subjects enrolled at the Baylor University Medical Center (n=74), the Baylor cohort and the other patients with pancreatic cancer and non-cancer controls enrolled at Weill Cornell Medicine College, the Cornell cohort. We tested whether this assay approach could distinguish pancreatic cancer patients from non-malignant control patients. In this study, we analyzed DiO-normalized anti-EpCAM-QD605 and anti-EphA2-QD655 probe signal on CD81-captured EVs from plasma and serum samples drawn from a cohort of 74 subjects (Table 5) and 32 subjects (Table 6) respectively. The Baylor cohort included healthy non-malignant control subjects, and pancreatic cancer patients with stage I/II, III, or IV tumors (11 – 21 subjects/group) while the Cornell cohort included 20 pancreatic cancer patients and 12 non-malignant controls (e.g. liver injury, pancreatitis and cholangitis).

6.2 Materials and methods

6.2.1 Baylor Cohort clinical samples

Pancreatic cancer and healthy control patient plasma samples were obtained from subjects enrolled at the Baylor University Medical Center. Written informed consent was obtained from all patients prior to participating in the study and the study was approved by the Institutional Review Board at Baylor Scott & White Health (IRB # 015-196). Demographic information including sex, age, and cancer stage is recorded in Table 5.

Samples were added to the quantum dot assay in a randomized order, but investigators were not blind to the group identity of the samples during data processing or analysis.

	Normal Control vs. Pancreatic Cancer			
	Normal Control	Pancreatic Cancer Stages I + II	Pancreatic Cancer Stage III	Pancreatic Cancer Stage IV
Male No. (%)	12 (57.1)	8 (72.7)	14 (66.7)	15 (71.4)
Female No. (%)	9 (42.9)	3 (27.3)	7 (33.3)	6 (28.6)
Age median (range) year	65 (55-74)	68 (52-76)	59 (50-88)	64 (36-83)
CA 19-9 median (range) U/mL		73 (2.8-16910)	56.5 (1.5-1065)	206.1 (0.96-3080)

Note: CA 19-9 values were not recorded for normal controls or 3 pancreatic cancer stage IV patients.

Table 5. Demographic information of pancreatic cancer cohort (N= 21, Control; N=53, Cancer)

	Non- Cancer vs Pancreatic Cancer Cases	
	Non-Cancer	Pancreatic Cancer
Male No. (%)	3 (25)	9 (45)
Female No. (%)	9 (75)	11 (55)
Age, year median (range)	54 (39-77)	72 (52-84)
CA 19-9, U/mL median (range)	15 (3-76)	69 (1-21816)

Note: CA 19-9 values were not recorded for 4 non-cancer controls

Table 6. Demographic information of the pancreatic cancer cohort, which contains 12 non-cancer controls and 20 patients with pancreatic cancer.

6.2.2 Cornell cohort clinical samples

Serum samples were obtained from patients with pancreatic cancer and non-cancer controls enrolled at Weill Cornell Medicine College in accordance with a protocol approved by its Institutional Review Board. Demographic information including sex, age, and CA19-9 level is recorded in Table 6. Samples were added to the quantum dot assay in a randomized order, but investigators were not blind to the group identity of the samples during data processing or analysis.

6.2.3 Statistical Analysis

GraphPad Prism version 8.0.2 (GraphPad Software) was used for all calculations. Statistical analyses were performed using Student's t-tests, one-way ANOVA with Tukey's multiple comparison test as determined by sample distribution and variance. Differences with p-values < 0.05 were considered statistically significant. We wrote a MATLAB program to generate a logistic regression model to fit the clinical samples data and generate probabilities, which was then used to generate the ROC curves. Figures were prepared using GraphPad Prism 8.0.2 (GraphPad Software). All data points are derived from three biological or technical replicates as indicated for each experiment.

6.3 Results and discussions

6.3.1 Baylor Cohort clinical validation

We directly added plasma samples from this cohort to a black 96-well plate coated with anti-CD81 antibody to allow EVs capture, then stained with DiO, hybridized with anti-EpCAM-QD605 and anti-EphA2-QD655, and analyzed on a fluorescent plate reader to quantify the fluorescent signal arising from their lipid labeled EVs and biomarker

expression. No difference in total EV-associated EpCAM or EphA2 expression was detected between the cancer and healthy, non-malignant groups in this cohort (Figure 25 A-B), however, there was a significant difference in the DiO signal for the cancer vs healthy, non-malignant control ($p = 0.0021$) (Figure 26).

On further evaluating the clinical information provided for the samples, we noticed that there was no mention if the healthy subjects had any underlying diseases which can play a role in the amount of EVs released and observed for the healthy controls. Another factor contributing to this could be patient to patient variability, for example a particular known value of EVs in a healthy normal patient could be an increased level in a cancer subjects. Hence we cannot use the number of EVs as a stand-alone diagnostic marker for cancer (Xu, Rai et al. 2018).

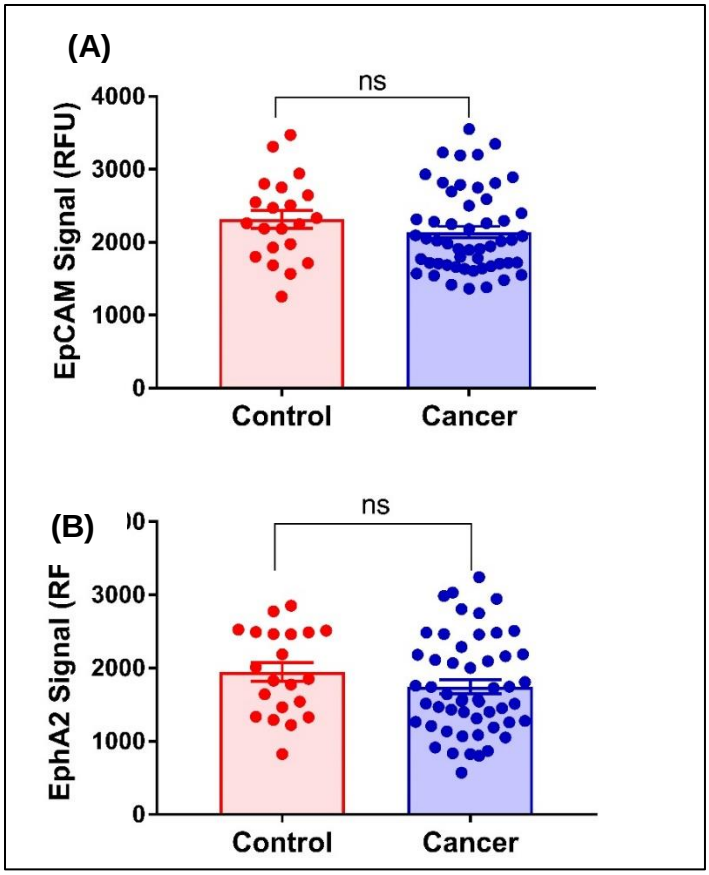

Figure 25. Raw (A) EpCAM and (B) EphA2 expression on CD81-captured plasma EVs from plasma samples of patients with pancreatic cancer (N=53) and their healthy, non-malignant controls (N=21). Data represent means ± SEM (ns = not significant by Student's t-test), n= 2 replicates/sample.

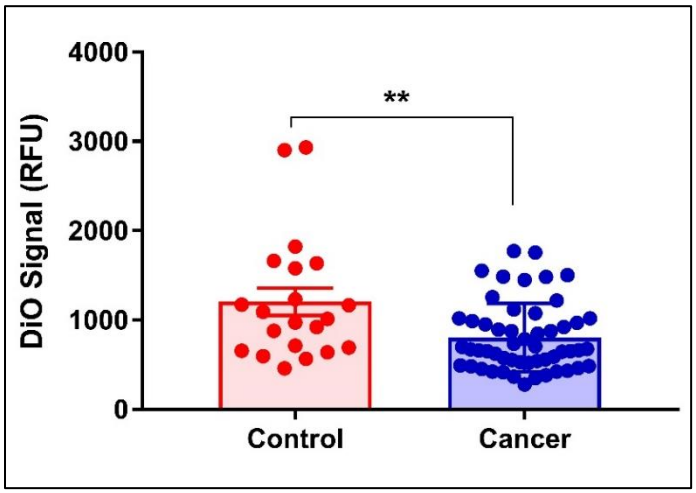

Figure 26. DiO signal from plasma samples drawn from patients with pancreatic cancer and those without cancer. (**$p < 0.01$ by Student's t-test), Data represent means ± SEM, n= 2 replicates/sample.

The assay quantum dot signals (Figure 25 A-B) was then normalized to the EV DiO signal (Figure 26), which revealed both EpCAM and EphA2 expression levels for pancreatic cancer vs control (Figure 27 A-B). On comparing the expression of EpCAM and EphA2 for control to cancer patient we see a significant difference with p-value 0.001 and p-value 0.04 respectively, affirming that per EV protein expression levels for these two biomarkers could help distinguish control and cancer subjects.

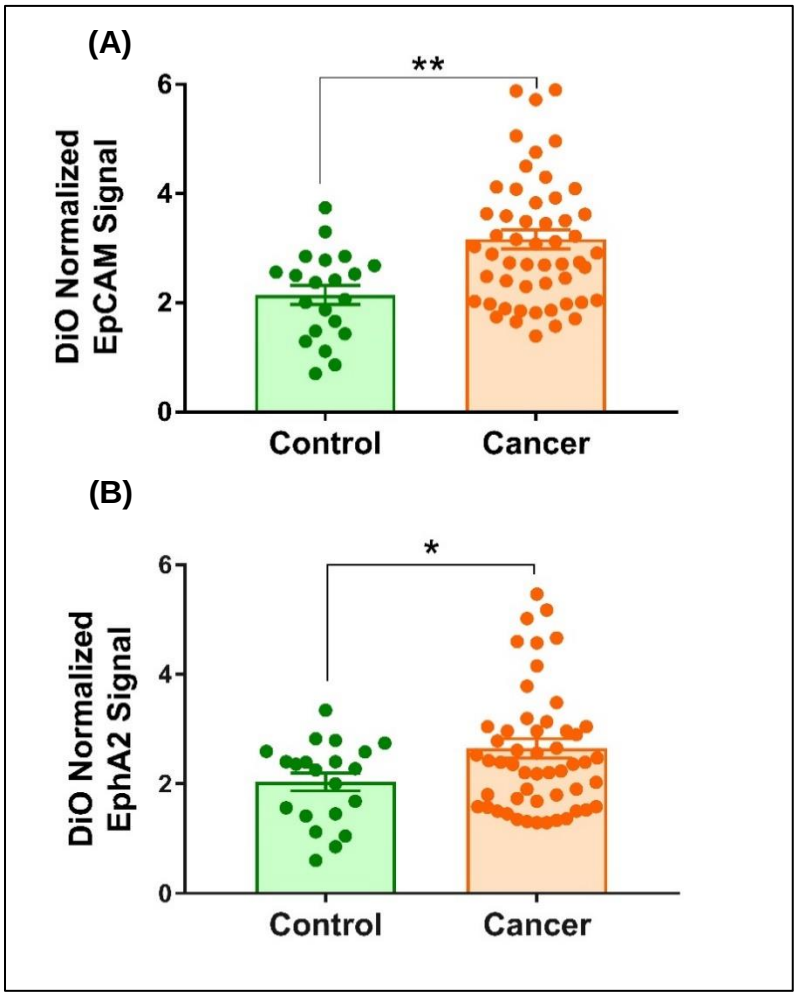

Figure 27. DiO-normalized (A) EpCAM and (B) EphA2 expression on CD81-captured plasma EVs from plasma samples of patients with pancreatic cancer (N=53) and their healthy, non-malignant controls (N=21). Data represent means ± SEM (*p<0.05, and **p<0.01 by Student's t-test), n= 2 replicates/sample.

The receiver operating characteristic (ROC) analyses were performed to evaluate the ability of raw and DiO-normalized signal from these EV biomarkers to differentiate patients with and without pancreatic cancer. No difference was detected for area under the curve (AUC) values for raw (0.59) and DiO-normalized (0.61) EphA2 EV signals (Figure 28B), but found an AUC difference between the normalized (0.75) and raw (0.60) EpCAM EV signals (Figure 28A) that were not improved by combined analysis of both EV biomarkers (Figure 29). Here, the combined markers did not improve the ability to differentiate the cancer from the normal subjects, mainly due to the ability of EphA2 markers for this particular cohort.

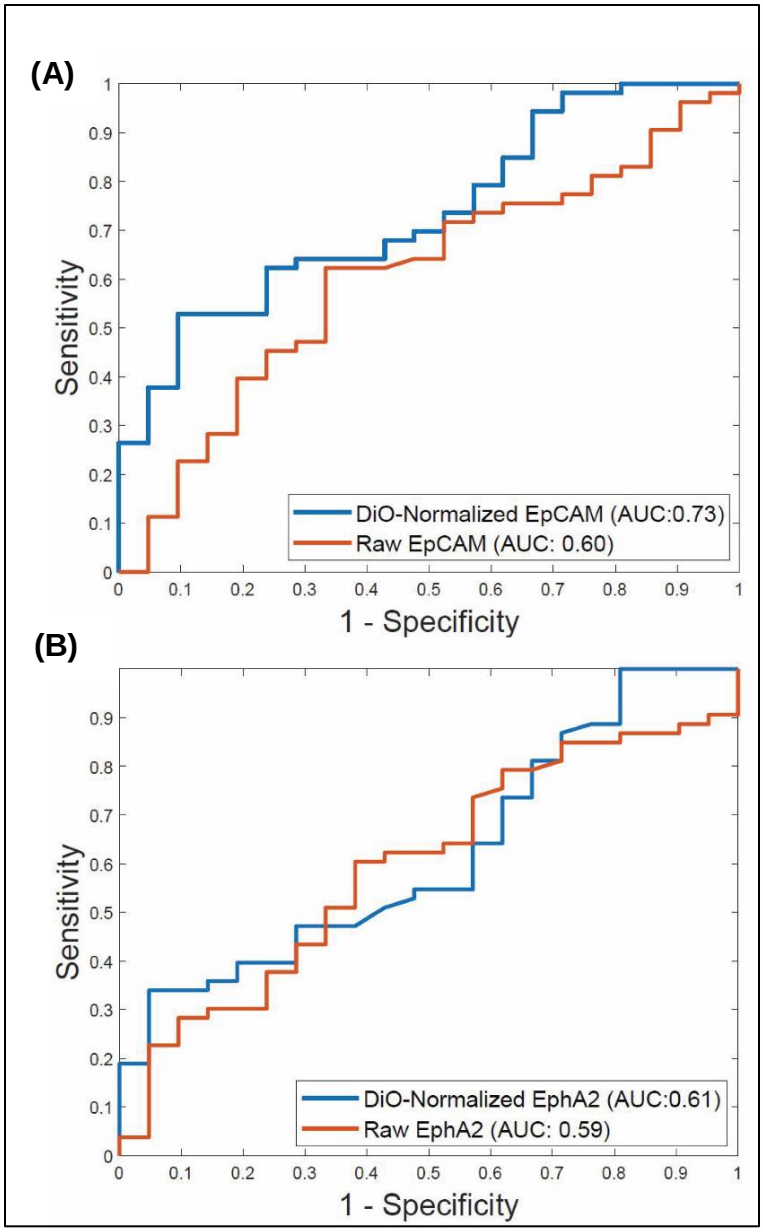

Figure 28. ROC curves of the ability of raw and DiO-normalized (A) EpCAM signal or (B) EphA2 signal to differentiate pancreatic cancer patients from their healthy controls. Researchers performing these analyses were not blinded to sample identity.

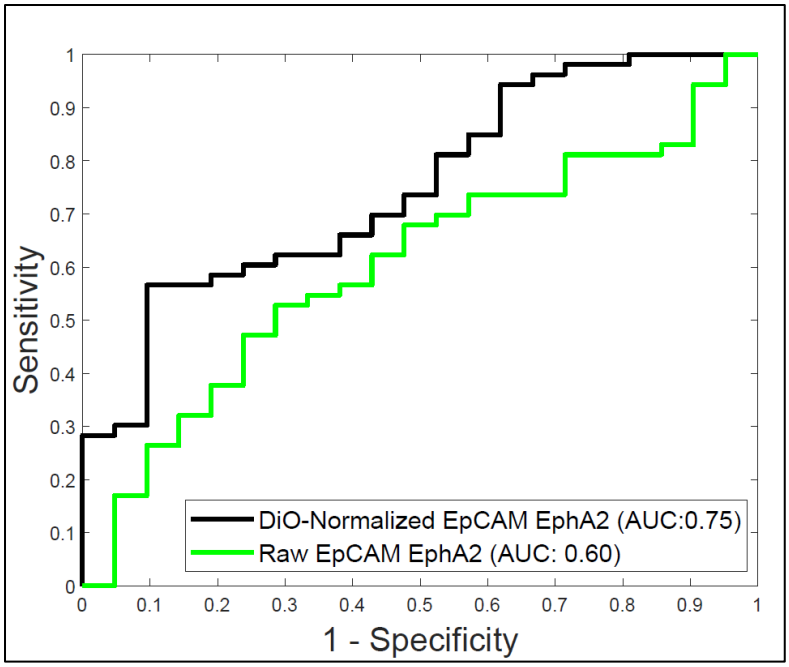

Figure 29. ROC curves of the ability of raw and DiO-normalized data for combined EpCAM and EphA2 signal to differentiate pancreatic cancer patients from their healthy controls. Researchers performing these analyses were not blinded to sample identity

On further analyzing the data (Figure 28B), we can see that the signal did not show a great improvement for raw vs normalized data. One of the reason could be the samples for this cohort, as previously mentioned EphA2 is more of a metastatic marker, and as we did not have any additional clinical information regarding the metastatic status of the cancer patients we could not further analyze the data from the assay to patient history. We performed subgroup analysis by cancer stage that revealed the DiO-normalized EpCAM signal, but not EphA2 signal, significantly differed between patients with stage III or stage IV cancer and non-malignant controls (Figures 30-31).

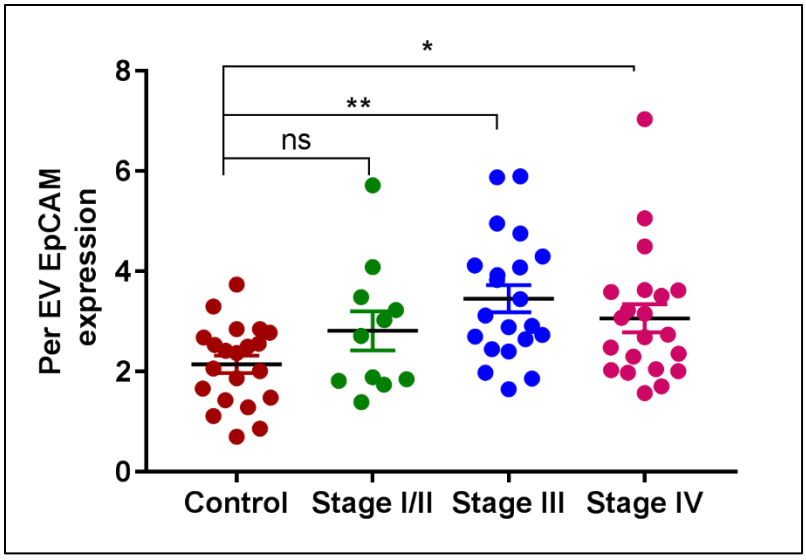

Figure 30. DiO-normalized EpCAM expression on CD81-captured EVs captured from plasma samples of patients with stage I+II (N=11), stage III (N=21), and stage IV (N=21) pancreatic cancer and their healthy, non-malignant controls (N=21). Data represent means ± SEM. ("ns" denotes that the indicated comparisons are not significant when analyzed by 1-way ANOVA with Tukey's post-test)

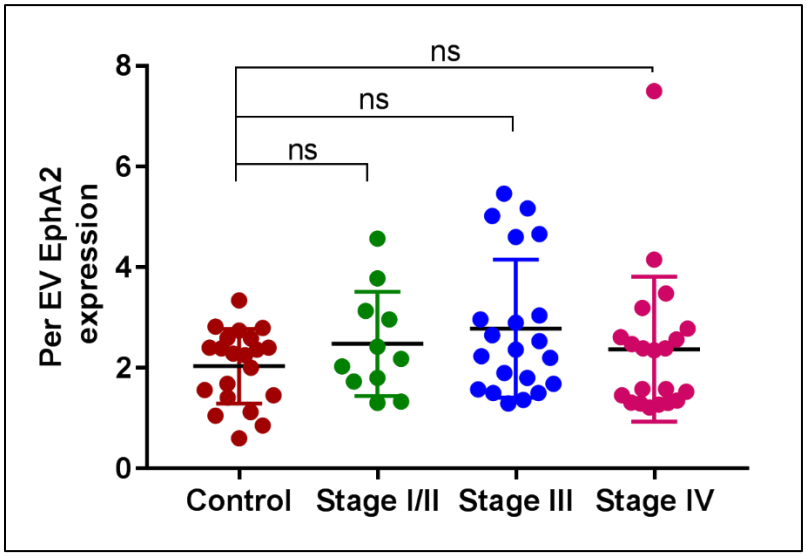

Figure 31. DiO-normalized EphA2 expression on CD81-captured EVs captured from plasma samples of patients with stage I+II (N=11), stage III (N=21), and stage IV (N=21) pancreatic cancer and their healthy, non-malignant controls (N=21). Data represent means ± SEM. ("ns" denotes that the indicated comparisons are not significant when analyzed by 1-way ANOVA with Tukey's post-test)

6.3.2 Cornell cohort

In this study, we analyzed DiO-normalized anti-EpCAM-QD605 and anti-EphA2-QD655 probe signal on CD81-captured EVs from serum samples drawn from a cohort of 32 subjects (Table 6) that included non-cancer control subjects having other disease conditions like liver injury, pancreatitis and cholangitis (n=12) and pancreatic cancer patients (n=20). We directly added serum samples from this cohort to a black 96-well plate coated with anti-CD81 antibody to allow EV capture, then stained with DiO, hybridized with anti-EpCAM-QD605 and anti-EphA2-QD655, and analyzed on a fluorescent plate reader to quantify the fluorescent signal arising from their EV lipid and biomarker expression. There was a significant difference observed in total EV-associated EpCAM ($p=0.02$) and total EV associated EphA2 ($p=0.01$) levels between cancer and, non-cancer groups in this cohort (Figure 32A-B), but no significant difference observed in the DiO signal for the cancer vs non cancer groups (Figure 33).

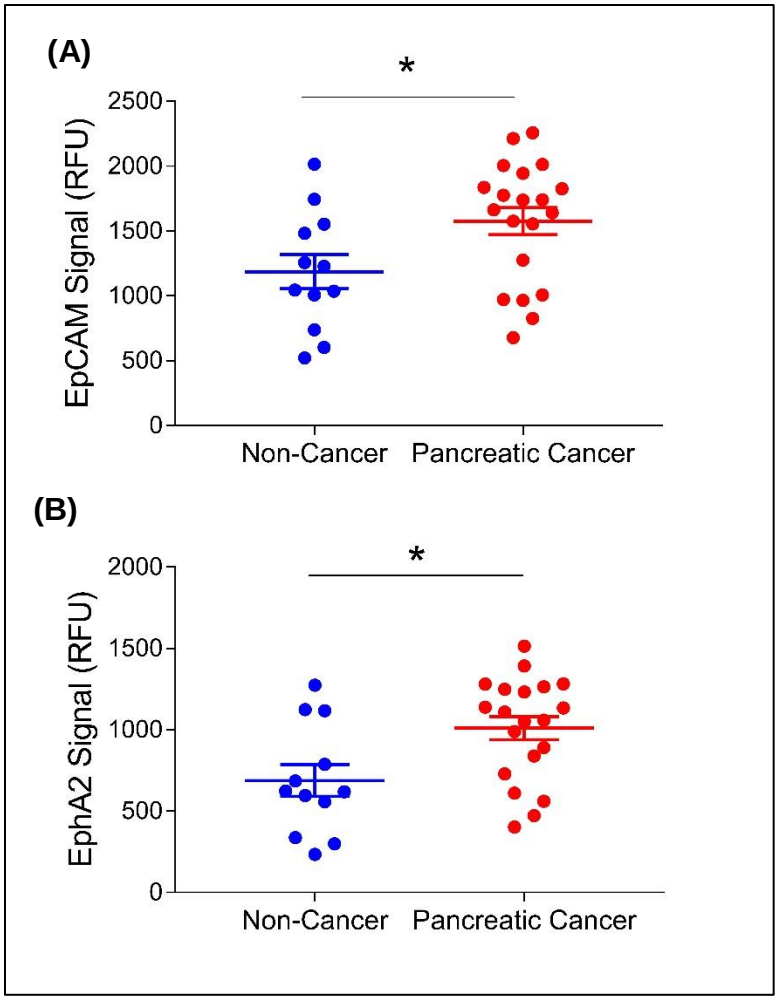

Figure 32. Raw (A) EpCAM and (B) EphA2 expression on CD81-captured serum EVs from serum samples of patients with pancreatic cancer (N=20) and their non-malignant controls (N=12). Data represent means ± SEM, n=3 replicates/sample (*$p<0.05$ by Student's t-test)

However, DiO normalization markedly reduced the biomarker overlap between these groups and increased the statistical significance of their detected EpCAM ($p=0.0002$) and EphA2 ($p<0.0001$) differences (Figure 34A-B). Receiver operating characteristic (ROC) analyses were performed to evaluate the ability of raw and DiO-normalized signal from these EV biomarkers to differentiate patients with and without pancreatic cancer

along with CA19-9 levels which is currently the most extensively studied biomarker and the only one approved by the FDA.

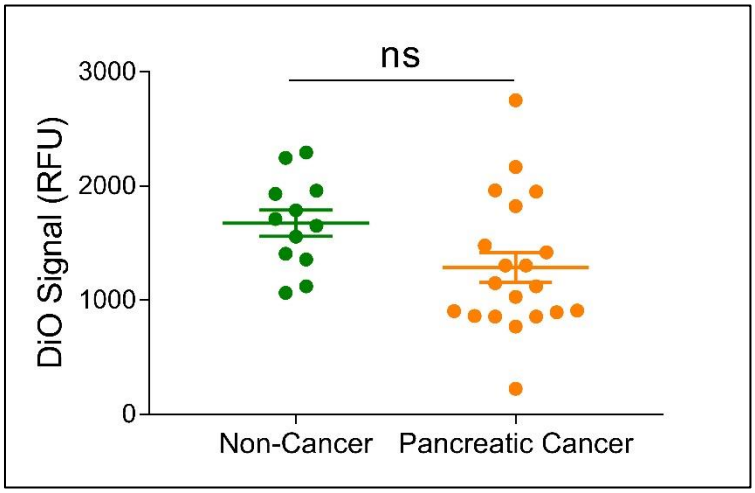

Figure 33. DiO signal from serum samples drawn from patients with pancreatic cancer and those without cancer. (ns = not significant, p >0.05 by Student's t-test), Data represent means ± SEM, n= 3 replicates/sample.

The ROC analyses revealed the ability of raw and DiO-normalized EV biomarker signal to differentiate patients with and without pancreatic cancer found that the area under the curve (AUC) values to distinguish these groups were markedly improved when using normalized versus raw EpCAM (AUC of 0.92 versus 0.72) and EphA2 (AUC of 0.93 versus 0.75) EV signals (Figure 35A-B). Serum levels of CA19-9, the only biomarker approved by the FDA for pancreatic cancer evaluations, exhibited an AUC of 0.74 in this cohort (Goonetilleke and Siriwardena 2007).

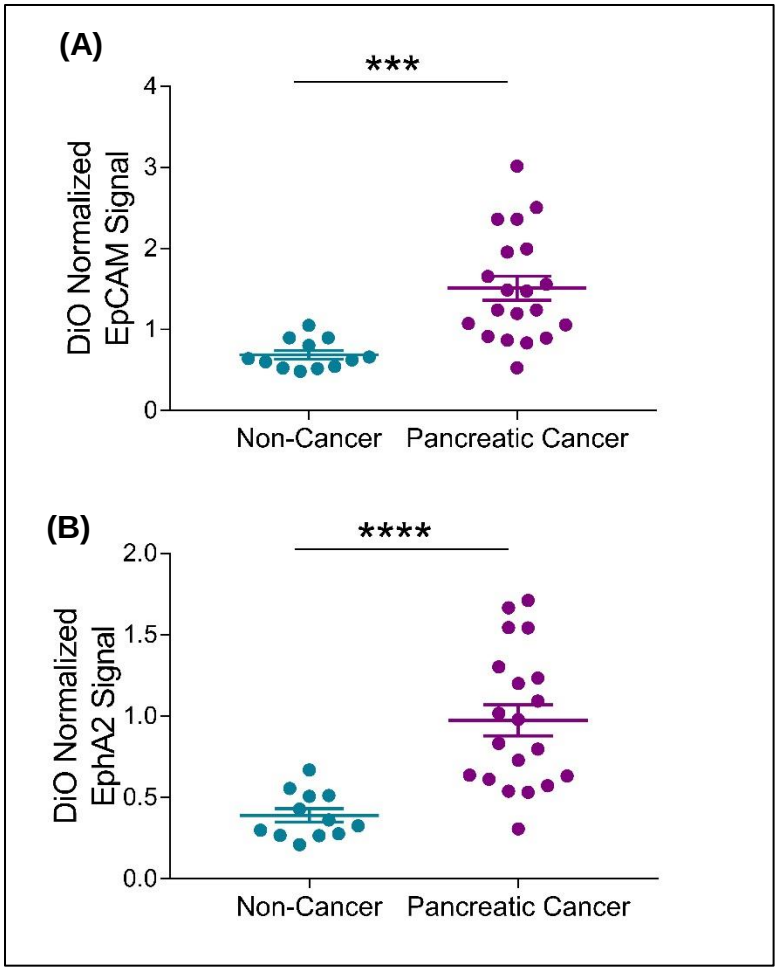

Figure 34. EpCAM and EphA2 expression on EVs captured from patient serum samples. DiO-normalized (A) EpCAM and (B) EphA2 expression on CD81-captured serum EVs from serum samples of patients with pancreatic cancer (N=20) and their non-malignant controls (N=12). Data represent means ± SEM, n=3 replicates/sample (*** $p<0.001$ and **** $p<0.0001$ by Student's t-test)

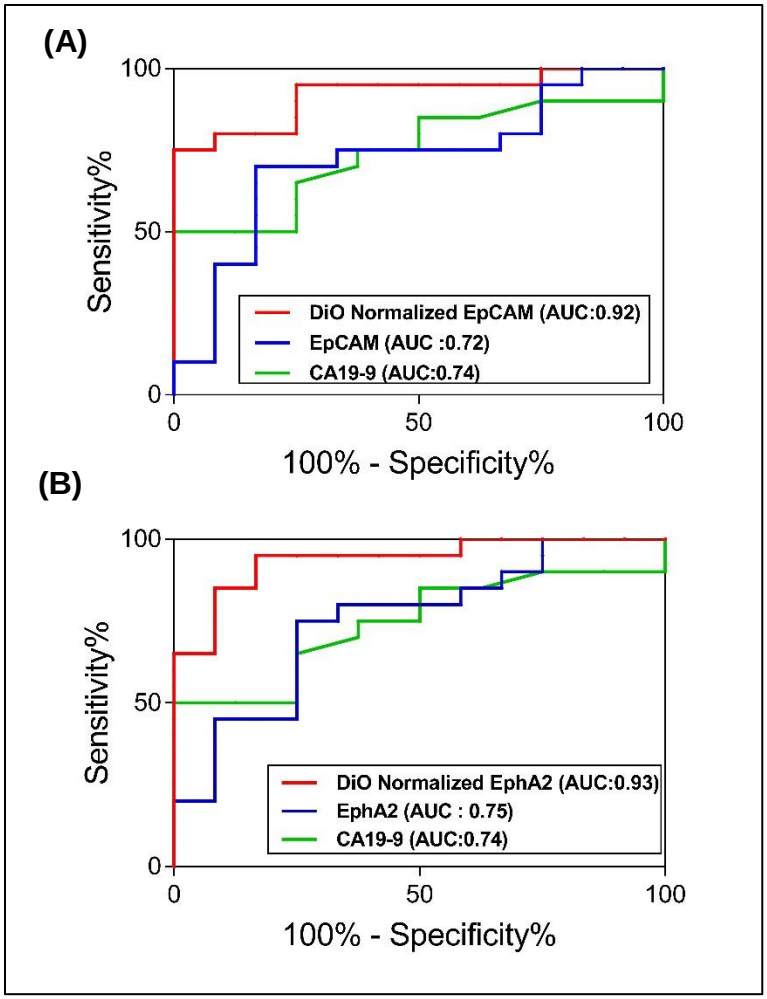

Figure 35. ROC curves of the ability of CA19-9 level, and raw and DiO-normalized (A) EpCAM signal and (B) EphA2 signal to differentiate pancreatic cancer patients from their nonmalignant controls. Researchers performing these analyses were not blinded to sample identity.

Combined ROC analyses performed with either unadjusted or DiO-normalized EpCAM and EphA2 data (Figure 36) produced AUCs greater than those detected with each marker alone (AUCs of 0.77 and 0.95, respectively) but these values could not conclusively determine if these combined analyses improved the ability to distinguish these groups due to the limitations imposed by the cohort size (n=32). However, future studies performed using larger cohorts could exploit the multiplex ability of this assay for improved diagnosis.

Serum levels of CA19-9, the only biomarker approved by the FDA for pancreatic cancer evaluations, exhibited an AUC of 0.74 in this cohort (Goonetilleke and Siriwardena 2007).

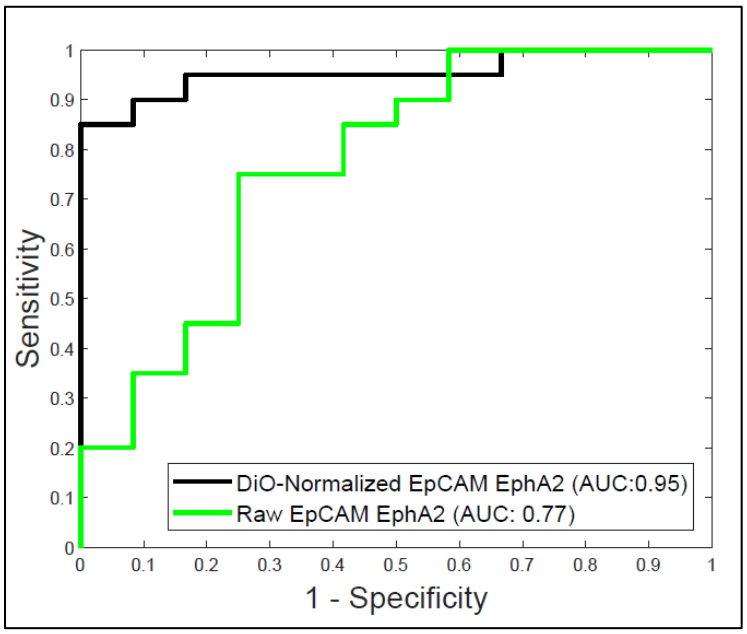

Figure 36. Combined ROC curves indicating the ability of unadjusted and DiO-normalized EpCAM and EphA2 signal to differentiate pancreatic cancer patients from their nonmalignant controls. Researchers performing these analyses were not blinded to sample identity

Based on the clinical information provided for these cancer controls, we performed subgroup analysis by cancer stage/ status that revealed the DiO-normalized EpCAM signal and EphA2 signal, significantly differed between patients with stage I+II and or metastatic cancer and non-malignant controls (Figure 37 and 38). However, these values could not conclusively determine if these markers could be used for early detection of pancreatic cancer and furthermore help in distinguishing non-malignant controls from metastatic cancer due to the limitations imposed by the cohort size. However, future studies performed

using larger cohorts could exploit the capabilities of these individual markers in distinguishing sub groups of cancers from their controls for improved diagnosis.

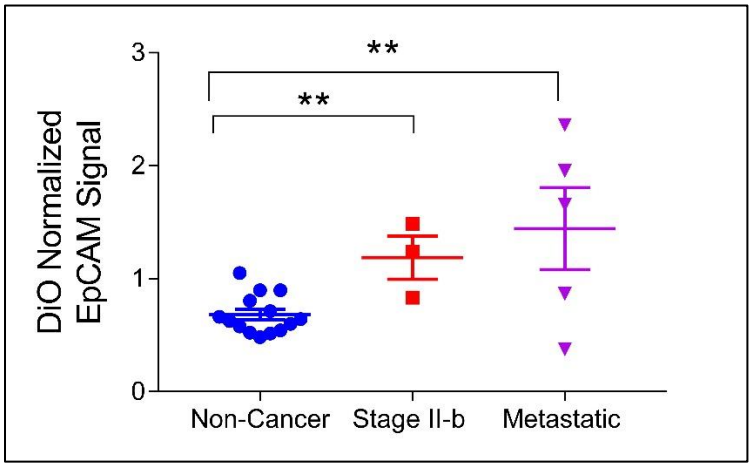

Figure 37. DiO-normalized EpCAM expression on CD81-captured EVs captured from serum samples of patients with stage I+II (N=3) and metastatic (N=5) pancreatic cancer and non-malignant controls (N=12). Data represent means ± SEM, n=3 replicates/sample (**p<0.01 by Student's t-test)

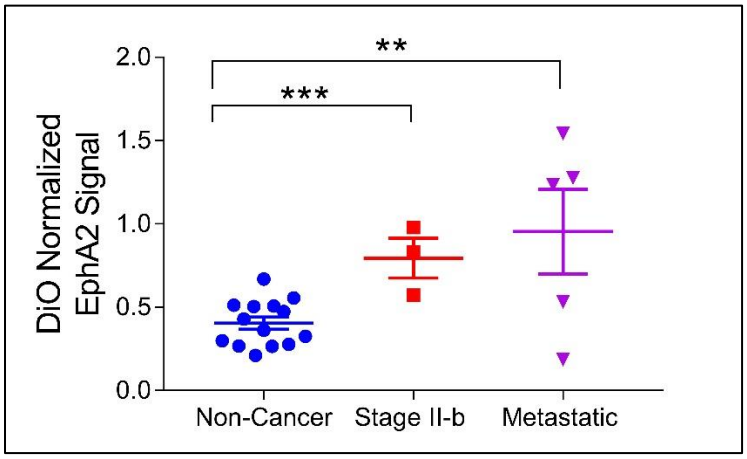

Figure 38. DiO-normalized EphA2 expression on CD81-captured EVs captured from serum samples of patients with stage I+II (N=3) and metastatic (N=5) pancreatic cancer and non-malignant controls (N=12). Data represent means ± SEM, n=3 replicates/sample (**p<0.01 and *** p<0.001 by Student's t-test)

CHAPTER 7 CONCLUSIONS AND FUTURE WORK

7.1. Summary and Conclusion

This proof-of-principle data strongly implies that DiO-normalization to correct for differences in EV abundance may provide additional value to EV biomarker analyses. Quantum dot probes are a key component of this approach, since they are brighter, more photostable, and exhibit narrower emission peaks than most other fluorescent probes (Toseland 2013). These features are critical in visualizing biomarkers present on the limited surface area on an EV and to permit multiplex analyses with minimal signal interference. Standard approaches to correct for differences in EV abundance require normalization against an EV-associated factor or direct quantitation of isolated EVs, both of which are subject to significant variation. The proposed method provides a direct measure of 1) the relative EV abundance in a sample, without requiring a time-consuming and variable EV isolation step, 2) the total expression level of one or more EV biomarker targets, 3) and the average expression of such targets in the captured EV population. This allows one to distinguish between biomarker differences arising from changes in EV abundance or relative biomarker expression, which may reflect different regulatory processes. This can have important implications for certain disease conditions, including cancer, as these processes may require different interventions to address. The potential to simultaneously monitor these different parameters should improve the monitoring of tumor changes during cancer progression and in response to therapy (Lee, Fraser et al. 2018).

One limitation of this approach, however, is that altered abundance of other EVs other than the EV population of interest can influence the normalization process when analyses are performed on the total EV population. This is of concern for mixed EV populations present in clinical samples, and this approach therefore works best when the target EV population can be selectively captured using antibodies specific to a biomarker specific to the disease or tissue of interest. However, it appears that EV biomarker normalization can still improve the diagnostic performance of certain EV biomarkers even in mixed EV populations, as indicated in our proof-of-concept study.

This approach utilizes a streamlined procedure and equipment found in most well-equipped clinical laboratories, reducing one potential barrier for its clinical translation. It also allows multiple EV biomarkers to be analyzed in a single sample, and for the specificity of the assay to be readily modified to analyze different EV biomarkers associated with other disease conditions, including infectious diseases. The proof-of-principle clinical sample analysis conducted for this study analyzed two biomarkers whose expression in EVs is of mounting interest (Klein-Scory, Tehrani et al. 2014, Yang, Im et al. 2017). Altered EpCAM expression is associated with primary tumors and appears to play a critical role in tumor growth and progression (Visvader and Lindeman 2009) while altered EphA2 expression is reported to be associated with tumor metastasis (Duxbury, Ito et al. 2004). Both biomarkers were enriched on EVs isolated from PANC-1 metastatic pancreatic carcinoma cells versus those isolated from HPNE nonmalignant pancreatic tissue cells, and on EVs present in the serum of patients with pancreatic cancer versus their non-malignant controls. Normalization of their EV expression to EV-related DiO signal in these samples markedly reduced the variability of these EV biomarkers in the

nonmalignant controls, decreasing their overlap with the pancreatic cancer patients to greatly improve their ability to distinguish these populations. A ROC analysis performed with both markers, however, was not able to conclusively demonstrate additional diagnostic benefit, despite a potential AUC increase, due to the limited cohort size. Further studies with larger well-defined cohorts are needed to determine if changes in the EV expression of these factors, alone or in combination, can distinguish pancreatic cancer patients with or without metastatic disease or at different cancer stages.

7.2. Future work

7.2.1. EVs as diagnostic markers in infectious disease

EV expression of pathogen-derived factors and changes in the EV abundance of specific host-derived factors can serve as diagnostic biomarkers, indicators of disease progression, and/or capture targets for the enrichment of pathogen-derived EVs for further analysis. Changes in EV composition during disease progression make them excellent biomarker candidates. The first blood-based EV test for cancer diagnosis became commercially available in the US in January 2016, marking a major step in the maturation of EVs as diagnostic factors (Sheridan 2016). The study of EVs for diagnosis of infectious disease is relatively new but shows great promise, particularly for intracellular bacterial pathogens, such as mycobacteria. Diagnosis of these pathogens normally requires culture or molecular analysis of pathogen samples derived from the site of infection and can misdiagnose patients with low pathogen loads. EVs containing pathogen-derived factors are actively secreted from most cells to accumulate in the circulation; some studies indicate that infection increases EV release rates (Singh, Smith et al. 2012, Hu, Gong et al. 2013) although it is not clear if this increase is common to all infections. Most current approaches

that diagnose active tuberculosis cases use sputum samples as the primary diagnostic specimen. However, there are limitations associated with sputum diagnostics and the World Health Organization has issued a call for new approaches that can diagnose active tuberculosis cases using minimally invasive patient samples, such as peripheral blood samples (Ferhan, Jackman et al. 2017).

Several studies have now indicated the potential of EVs from minimally or non-invasive biological samples to detect such infections. Serum EV concentrations in mice infected with *M. bovis* BCG correlated and exhibited similar kinetics with *M. bovis* BCG mycobacterial load, suggesting the potential utility of serum EVs as diagnostic biomarkers for disease burden (Singh, Smith et al. 2012). A subsequent study used liquid-chromatography and tandem mass spectrometry to identify 41 mycobacterial proteins in EVs derived from *Mtb*-infected J774 cells (Giri, Kruh et al. 2010) and in 2014, analysis of serum EVs isolated from patients with active tuberculosis cases detected numerous mycobacterial proteins, indicating that *Mtb*-derived EVs can function as markers of active disease (Kruh-Garcia, Wolfe et al. 2014). Mycobacterial RNA was also detected in EVs derived from *Mtb*-infected macrophages (Singh, Li et al. 2015), implying the potential for analyzing *Mtb* RNA in EVs as a diagnostic marker for active tuberculosis cases.

Nanoparticles are too small for direct detection by conventional flow cytometry, but one company has developed a high-resolution flow cytometer that can directly detect EVs. This specialized machine requires high-power lasers and high-performance photomultiplier tubes, detection of light scattering at customized angles, and the application of fluorescence-based thresholding to distinguish particles of interest from noise (Aras, Shet et al. 2004, van der Vlist, Nolte-'t Hoen et al. 2012). Standard flow

cytometers can, however, analyze multiplex bead-based platforms to detect and analyze aggregate signal derived from multiple EVs after they are bound to micrometer polystyrene capture beads (Koliha, Wiencek et al. 2016). Stimulated emission depletion (STED) microscopy can also be used to measure multiple markers on single EVs, but this approach does not appear suitable for the analysis of rare EV populations without a prior isolation step.

Several groups have recently reported robust on-chip isolation and detection methods to study and profile EVs. In 2014, a group reported the development of a nanoplasmonic EV (nPLEX) sensor consisting of an affinity ligand-modified gold film that contained an array of periodic nanoholes, in which EV binding produced a spectral shift proportional to the number of targeted EVs bound on the array (Im, Shao et al. 2014). In 2015, a second group reported the development of an immunomagnetic EV RNA (iMER) platform for on-chip EV enrichment, RNA isolation, reverse transcription and real-time analysis of distinct RNA targets, which they used for treatment-induced mRNA in glioblastoma multiforme patients (Shao, Chung et al. 2015). In 2017, we published a nanoplasmonic enhanced scattering (nPES) method where EVs are bound to a chip by a pan-specific EV antibody, and hybridized with antibody-labeled nanoparticles specific to a second common EV protein and a disease-specific EV marker so that target EVs produce a shifted nPES signal in direct proportion to their number (Liang, Liu et al. 2017). All these technologies should allow one to modify the EV targets analyzed by changing the affinity of the detection antibody or ligand, and thus should be readily adaptable for any disease for which there is a disease-specific EV biomarker available. None of these approaches are yet available for clinical applications, but they demonstrate the potential of new chip technologies to rapidly

profile disease-specific EVs from human samples after minimal sample preparation.

Mounting evidence indicates pathogen-derived EV factors play important roles in several human diseases, and a better understanding of these mechanisms may provide new insights for future therapeutic development. Several reports indicate that immunomodulatory molecules present in or on EVs can affect pathogen responses through actions to activate or suppress immune responses, and it is possible that increased knowledge of these mechanisms will improve pathogen treatment approaches, including the potential use of EVs to develop more effective vaccines and immunotherapies. Pathogen-specific EV factors are also of great interest as novel disease biomarkers, due to their close association with disease and their potential for greater diagnostic sensitivity and specificity due to their stability in blood and urine. Specific EV biomarkers and means to analyze specific EV subsets have been lacking to date, however The Qdot assay can be easily modified to address different infectious disease conditions by the substitution of different EV biomarker probes, and is limited only by the existence of such probes and the ability to identify EV capture antibodies specific for an EV population of interest.

7.2.2. Clinical Translation

There are tremendous ongoing efforts focused on discovering novel cancer biomarkers for use in clinical practice. However, one of the issues in translation into the clinical setting is the limited knowledge researchers possess of analytical, diagnostic, and regulatory requirements for a clinical assay (Pepe, Etzioni et al. 2001, Fuzery, Levin et al. 2013). As part of our study, we aim to establish a clinically accessible biomarker test that

will help improve diagnostic outcomes. Below is a flow chart elaborating on each process required to study and validate the biomarker assay development (Figure 39)

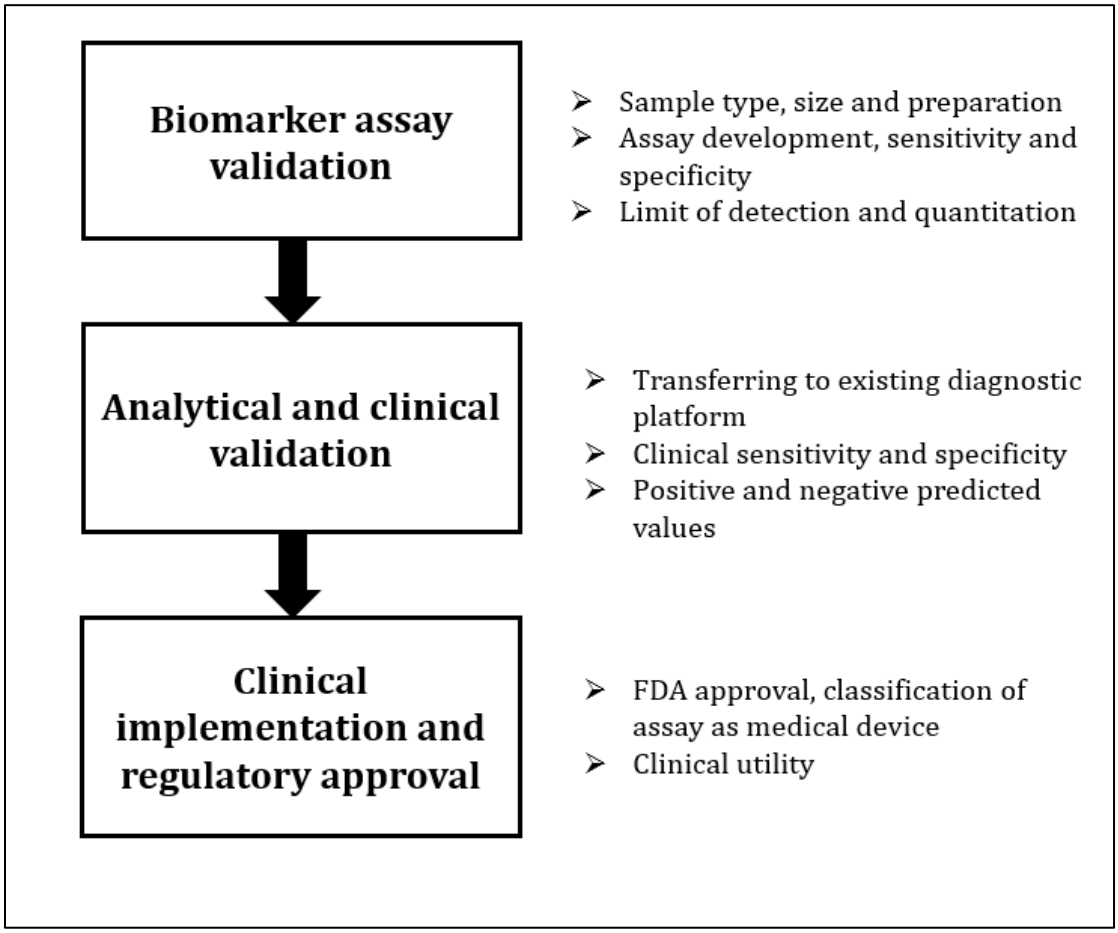

Figure 39. Schematic overview of the different steps for validation and clinical translation of a biomarker assay.

Biomarker assay validation:

- By achieving sensitive EV detection and quantification without the need for a separate pre-purification step. The design will focus on using serum/plasma samples that bind to an EV-specific marker (capture antibody).

- The next step will focus on designing and validating the quantum dot probes for biomarker detection (measuring sensitivity and specificity).
- Determining the sample/cohort to test such as pancreatic cancer patients for different stages, pre-cancer lesion patients, and normal patient samples. Finally, determining the limit of detection for the assay with reliable and reproducible results.

Analytical and clinical validation:

- Determining the robustness of the assay, testing for analytical as well as clinical validation (cohort size).
- Incorporating assay onto a single platform, determining the instruments for readout, easy transition from existing laboratory to a diagnostic platform.
- Designing tests to measure clinical sensitivity and specificity, e.g. distinguishing between normal and diseased patients, determining the diagnostic accuracy and testing clinical performance on a study group that is representative of the target patient population.

Regulatory approval and clinical implementation:

- Protein-based biomarker assay used for diagnostics are considered by the FDA to be medical devices and follow the same regulatory standards as other types of medical devices (Fuzery, Levin et al. 2013).
- The current available FDA approved pancreatic cancer marker CA19-9 followed the 510 (k) FDA pathway. This is for moderate risk, Class II medical devices.

- We would similarly follow the 510 (k) pathway, once the FDA and sponsor (firm submitting the pre-market approval application) have agreed on the intended use; the biomarker test will then be reviewed under 510(k) guidelines.
- Finally, accounting for clinical challenges, handling steps for the assay interpretation of multiplexed data and workflow acceptance by clinicians.

To be successful, one should develop a plan and take into consideration the key steps that are critical in this process, by defining the assay importance both for analytical and clinical performances.

REFERENCES

Admyre, C., B. Bohle, S. M. Johansson, M. Focke-Tejkl, R. Valenta, A. Scheynius and S. Gabrielsson (2007). "B cell-derived exosomes can present allergen peptides and activate allergen-specific T cells to proliferate and produce T(H)2-like cytokines." Journal of Allergy and Clinical Immunology 120(6): 1418-1424.

Admyre, C., S. M. Johansson, S. Paulie and S. Gabrielsson (2006). "Direct exosome stimulation of peripheral human T cells detected by ELISPOT." European Journal of Immunology 36(7): 1772-1781.

Aga, M., G. L. Bentz, S. Raffa, M. R. Torrisi, S. Kondo, N. Wakisaka, T. Yoshizaki, J. S. Pagano and J. Shackelford (2014). "Exosomal HIF1 alpha supports invasive potential of nasopharyngeal carcinoma-associated LMP1-positive exosomes." Oncogene 33(37): 4613-4622.

Alenquer, M. and M. J. Amorim (2015). "Exosome Biogenesis, Regulation, and Function in Viral Infection." Viruses 7(9): 5066-5083.

Ali, S. A., M. B. Huang, P. E. Campbell, W. W. Roth, T. Campbell, M. Khan, G. Newman, F. Villinger, M. D. Powell and V. C. Bond (2010). "Genetic Characterization of HIV Type 1 Nef-Induced Vesicle Secretion." Aids Research and Human Retroviruses 26(2): 173-192.

Alvarez-Erviti, L., Y. Seow, H. Yin, C. Betts, S. Lakhal and M. J. Wood (2011). "Delivery of siRNA to the mouse brain by systemic injection of targeted exosomes." Nat Biotechnol 29(4): 341-345.

Anand, P. K., E. Anand, C. K. E. Bleck, E. Anes and G. Griffiths (2010). "Exosomal Hsp70 Induces a Pro-Inflammatory Response to Foreign Particles Including Mycobacteria." Plos One 5(4).

Andre, F., N. Chaput, N. E. C. Schartz, C. Flament, N. Aubert, J. Bernard, F. Lemonnier, G. Raposo, B. Escudier, D. H. Hsu, T. Tursz, S. Amigorena, E. Angevin and L. Zitvogel (2004). "Exosomes as potent cell-free peptide-based vaccine. I. Dendritic cell-derived exosomes transfer functional MHC class I/peptide complexes to dendritic cells." Journal of Immunology 172(4): 2126-2136.

Andreu, Z. and M. Yanez-Mo (2015). "Tetraspanins in extracellular vesicle formation and function." Frontiers in Immunology 5.

Aqil, M., A. R. Naqvi, A. S. Bano and S. Jameel (2013). "The HIV-1 Nef protein binds argonaute-2 and functions as a viral suppressor of RNA interference." PLoS One 8(9): e74472.

Aras, O., A. Shet, R. R. Bach, J. L. Hysjulien, A. Slungaard, R. P. Hebbel, G. Escolar, B. Jilma and N. S. Key (2004). "Induction of microparticle- and cell-associated intravascular tissue factor in human endotoxemia." Blood 103(12): 4545-4553.

Arenaccio, C., S. Anticoli, F. Manfredi, C. Chiozzini, E. Olivetta and M. Federico (2015). "Latent HIV-1 is activated by exosomes from cells infected with either replication-competent or defective HIV-1." Retrovirology 12.

Arenaccio, C., C. Chiozzini, S. Columba-Cabezas, F. Manfredi, E. Affabris, A. Baur and M. Federico (2014). "Exosomes from Human Immunodeficiency Virus Type 1 (HIV-1)-Infected Cells License Quiescent CD4(+) T Lymphocytes To Replicate HIV-1 through a Nef- and ADAM17-Dependent Mechanism." Journal of Virology 88(19): 11529-11539.

Atay, S. and A. K. Godwin (2014). "Tumor-derived exosomes: A message delivery system for tumor progression." Commun Integr Biol 7(1): e28231.

Beatty, W. L. and D. G. Russell (2000). "Identification of mycobacterial surface proteins released into subcellular compartments of infected macrophages." Infection and Immunity 68(12): 6997-7002.

Beatty, W. L., H. J. Ullrich and D. G. Russell (2001). "Mycobacterial surface moieties are released from infected macrophages by a constitutive exocytic event." European Journal of Cell Biology 80(1): 31-40.

Bhatnagar, S. and J. S. Schorey (2007). "Exosomes released from infected macrophages contain mycobacterium avium glycopeptidolipids and are proinflammatory." Journal of Biological Chemistry 282(35): 25779-25789.

Bhatnagar, S., K. Shinagawa, F. J. Castellino and J. R. S. Schorey (2007). "Exosomes released from macrophages infected with intracellular pathogens stimulate a proinflammatory response in vitro and in vivo." Blood 110(9): 3234-3244.

Bukong, T. N., F. Momen-Heravi, K. Kodys, S. Bala and G. Szabo (2014). "Exosomes from Hepatitis C Infected Patients Transmit HCV Infection and Contain Replication Competent Viral RNA in Complex with Ago2-miR122-HSP90." Plos Pathogens 10(10).

Ceccarelli, S., V. Visco, S. Raffa, N. Wakisaka, J. S. Pagano and M. R. Torrisi (2007). "Epstein-Barr virus latent membrane protein 1 promotes concentration in multivesicular bodies of fibroblast growth factor 2 and its release through exosomes." International Journal of Cancer 121(7): 1494-1506.

Chang, C. C., H. J. Hsu, J. H. Yen, S. Y. Lo and J. W. Liou (2017). "A Sequence in the loop domain of hepatitis C virus E2 protein identified in silico as crucial for the selective binding to human CD81." Plos One 12(5).

Chaput, N., N. E. C. Schartz, F. Andre, J. Taieb, S. Novault, P. Bonnaventure, N. Aubert, J. Bernard, F. Lemonnier, M. Merad, G. Adema, M. Adams, M. Ferrantini, A. F. Carpentier, B. Escudier, T. Tursz, E. Angevin and L. Zitvogel (2004). "Exosomes as potent cell-free peptide-based vaccine. II. Exosomes in CpG adjuvants efficiently prime naive Tc1 lymphocytes leading to tumor rejection." Journal of Immunology 172(4): 2137-2146.

Charlotte, L., M. V. Jose, M. Y. Derek and M. D. Sean (2016). "Microvesicles and exosomes: new players in metabolic and cardiovascular disease." Journal of Endocrinology 228(2): R57-R71.

Chen, G., A. C. Huang, W. Zhang, G. Zhang, M. Wu, W. Xu, Z. L. Yu, J. G. Yang, B. K. Wang, H. H. Sun, H. F. Xia, Q. W. Man, W. Q. Zhong, L. F. Antelo, B. Wu, X. P. Xiong, X. M. Liu, L. Guan, T. Li, S. J. Liu, R. F. Yang, Y. T. Lu, L. Y. Dong, S. McGettigan, R. Somasundaram, R. Radhakrishnan, G. Mills, Y. L. Lu, J. Kim, Y. H. H. Chen, H. D. Dong, Y. F. Zhao, G. C. Karakousis, T. C. Mitchell, L. M. Schuchter, M. Herlyn, E. J. Wherry, X. W. Xu and W. Guo (2018). "Exosomal PD-L1 contributes to immunosuppression and is associated with anti-PD-1 response." Nature 560(7718): 382-+.

Chen, L., Y. Wang, Y. Pan, L. Zhang, C. Shen, G. Qin, M. Ashraf, N. Weintraub, G. Ma and Y. Tang (2013). "Cardiac progenitor-derived exosomes protect ischemic myocardium from acute ischemia/reperfusion injury." Biochem Biophys Res Commun 431(3): 566-571.

Chettimada, S., D. R. Lorenz, V. Misra, S. T. Dillon, R. K. Reeves, C. Manickam, S. Morgello, G. D. Kirk, S. H. Mehta and D. Gabuzda (2018). "Exosome markers associated with immune activation and oxidative stress in HIV patients on antiretroviral therapy." Scientific Reports 8.

Clayton, A., C. L. Harris, J. Court, M. D. Mason and B. P. Morgan (2003). "Antigen-presenting cell exosomes are protected from complement-mediated lysis by expression of CD55 and CD59." Eur J Immunol 33(2): 522-531.

Colombo, M., C. Moita, G. van Niel, J. Kowal, J. Vigneron, P. Benaroch, N. Manel, L. F. Moita, C. Thery and G. Raposo (2013). "Analysis of ESCRT functions in exosome biogenesis, composition and secretion highlights the heterogeneity of extracellular vesicles." Journal of Cell Science 126(24): 5553-5565.

Console, L., M. Scalise and C. Indiveri (2019). "Exosomes in inflammation and role as biomarkers." Clinica Chimica Acta 488: 165-171.

Dabitao, D., J. B. Margolick, J. Lopez and J. H. Bream (2011). "Multiplex measurement of proinflammatory cytokines in human serum: comparison of the Meso Scale Discovery electrochemiluminescence assay and the Cytometric Bead Array." J Immunol Methods 372(1-2): 71-77.

De Toro, J., L. Herschlik, C. Waldner and C. Mongini (2015). "Emerging roles of exosomes in normal and pathological conditions: new insights for diagnosis and therapeutic applications." Frontiers in Immunology 6.

Dragovic, R. A., C. Gardiner, A. S. Brooks, D. S. Tannetta, D. J. P. Ferguson, P. Hole, B. Carr, C. W. G. Redman, A. L. Harris, P. J. Dobson, P. Harrison and I. L. Sargent (2011). "Sizing and phenotyping of cellular vesicles using Nanoparticle Tracking Analysis." Nanomedicine-Nanotechnology Biology and Medicine 7(6): 780-788.

Dreux, M., U. Garaigorta, B. Boyd, E. Decembre, J. Chung, C. Whitten-Bauer, S. Wieland and F. V. Chisari (2012). "Short-Range Exosomal Transfer of Viral RNA from Infected Cells to Plasmacytoid Dendritic Cells Triggers Innate Immunity." Cell Host & Microbe 12(4): 558-570.

Duxbury, M. S., H. Ito, M. J. Zinner, S. W. Ashley and E. E. Whang (2004). "EphA2: a determinant of malignant cellular behavior and a potential therapeutic target in pancreatic adenocarcinoma." Oncogene 23: 1448.

Duxbury, M. S., H. Ito, M. J. Zinner, S. W. Ashley and E. E. Whang (2004). "Ligation of EphA2 by Ephrin A1-Fc inhibits pancreatic adenocarcinoma cellular invasiveness." Biochemical and Biophysical Research Communications 320(4): 1096-1102.

Feng, Z., L. Hensley, K. L. McKnight, F. Hu, V. Madden, L. Ping, S. H. Jeong, C. Walker, R. E. Lanford and S. M. Lemon (2013). "A pathogenic picornavirus acquires an envelope by hijacking cellular membranes." Nature 496(7445): 367-371.

Feng, Z. D., L. Hensley, K. L. McKnight, F. Y. Hu, V. Madden, L. F. Ping, S. H. Jeong, C. Walker, R. E. Lanford and S. M. Lemon (2013). "A pathogenic picornavirus acquires an envelope by hijacking cellular membranes." Nature 496(7445): 367-+.

Ferhan, A. R., J. A. Jackman, J. H. Park, N. J. Cho and D. H. Kim (2017). "Nanoplasmonic sensors for detecting circulating cancer biomarkers." Adv Drug Deliv Rev.

Flanagan, J., J. Middeldorp and T. Sculley (2003). "Localization of the Epstein-Barr virus protein LMP 1 to exosomes." Journal of General Virology 84: 1871-1879.

Fuhrmann, G., A. L. Neuer and I. K. Herrmann (2017). "Extracellular vesicles – A promising avenue for the detection and treatment of infectious diseases?" European Journal of Pharmaceutics and Biopharmaceutics 118(Supplement C): 56-61.

Fuzery, A. K., J. Levin, M. M. Chan and D. W. Chan (2013). "Translation of proteomic biomarkers into FDA approved cancer diagnostics: issues and challenges." Clinical Proteomics 10.

Garcia, E., M. Pion, A. Pelchen-Matthews, L. Collinson, J. F. Arrighi, G. Blot, F. Leuba, J. M. Escola, N. Demaurex, M. Marsh and V. Piguet (2005). "HIV-1 trafficking to the dendritic cell-T-cell infectious synapse uses a pathway of tetraspanin sorting to the immunological synapse." Traffic 6(6): 488-501.

Giri, P. K., N. A. Kruh, K. M. Dobos and J. S. Schorey (2010). "Proteomic analysis identifies highly antigenic proteins in exosomes from M. tuberculosis-infected and culture filtrate protein-treated macrophages." Proteomics 10(17): 3190-3202.

Goonetilleke, K. S. and A. K. Siriwardena (2007). "Systematic review of carbohydrate antigen (CA 19-9) as a biochemical marker in the diagnosis of pancreatic cancer." European Journal of Surgical Oncology (EJSO) 33(3): 266-270.

Gould, S. J., A. M. Booth and J. E. K. Hildreth (2003). "The Trojan exosome hypothesis." Proceedings of the National Academy of Sciences of the United States of America 100(19): 10592-10597.

Gray, L. R., D. Gabuzda, D. Cowley, A. Ellett, L. Chiavaroli, S. L. Wesselingh, M. J. Churchill and P. R. Gorry (2011). "CD4 and MHC class 1 down-modulation activities of nef alleles from brain- and lymphoid tissue-derived primary HIV-1 isolates." Journal of Neurovirology 17(1): 82-91.

Gutzeit, C., N. Nagy, M. Gentile, K. Lyberg, J. Gumz, H. Vallhov, I. Puga, E. Klein, S. Gabrielsson, A. Cerutti and A. Scheynius (2014). "Exosomes Derived from Burkitt's Lymphoma Cell Lines Induce Proliferation, Differentiation, and Class-Switch Recombination in B Cells." Journal of Immunology 192(12): 5852-5862.

Harding, C. V. and W. H. Boom (2010). "Regulation of antigen presentation by Mycobacterium tuberculosis: a role for Toll-like receptors." Nature Reviews Microbiology 8(4): 296-307.

Herreros-Villanueva, M. and L. Bujanda (2016). "Non-invasive biomarkers in pancreatic cancer diagnosis: what we need versus what we have." Annals of Translational Medicine 4(7).

Hidalgo , M. (2010). "Pancreatic Cancer." New England Journal of Medicine 362(17): 1605-1617.

Honig, M. G. and R. I. Hume (1989). "Dil and diO: versatile fluorescent dyes for neuronal labelling and pathway tracing." Trends Neurosci 12(9): 333-335, 340-331.

Hood, J. L., R. S. San and S. A. Wickline (2011). "Exosomes released by melanoma cells prepare sentinel lymph nodes for tumor metastasis." Cancer Res 71(11): 3792-3801.

Hoshino, A., B. Costa-Silva, T. L. Shen, G. Rodrigues, A. Hashimoto, M. T. Mark, H. Molina, S. Kohsaka, A. Di Giannatale, S. Ceder, S. Singh, C. Williams, N. Soplop, K. Uryu, L. Pharmer, T. King, L. Bojmar, A. E. Davies, Y. Ararso, T. Zhang, H. Zhang, J. Hernandez, J. M. Weiss, V. D. Dumont-Cole, K. Kramer, L. H. Wexler, A. Narendran, G. K. Schwartz, J. H. Healey, P. Sandstrom, K. J. Labori, E. H. Kure, P. M. Grandgenett, M. A. Hollingsworth, M. de Sousa, S. Kaur, M. Jain, K. Mallya, S. K. Batra, W. R. Jarnagin, M. S. Brady, O. Fodstad, V. Muller, K. Pantel, A. J. Minn, M. J. Bissell, B. A. Garcia, Y. Kang, V. K. Rajasekhar, C. M. Ghajar, I. Matei, H. Peinado, J. Bromberg and D. Lyden (2015). "Tumour exosome integrins determine organotropic metastasis." Nature 527(7578): 329-+.

Hu, G., A. Y. Gong, A. L. Roth, B. Q. Huang, H. D. Ward, G. Zhu, N. F. LaRusso, N. D. Hanson and X. M. Chen (2013). "Release of Luminal Exosomes Contributes to TLR4-Mediated Epithelial Antimicrobial Defense." Plos Pathogens 9(4).

Hurwitz, S. N., D. Nkosi, M. M. Conlon, S. B. York, X. Liu, D. C. Tremblay and D. G. Meckes (2017). "CD63 Regulates Epstein-Barr Virus LMP1 Exosomal Packaging, Enhancement of Vesicle Production, and Noncanonical NF-kappa B Signaling." Journal of Virology 91(5).

Hwang, I. Y., X. F. Shen and J. Sprent (2003). "Direct stimulation of naive T cells by membrane vesicles from antigen-presenting cells: Distinct roles for CD54 and B7 molecules." Proceedings of the National Academy of Sciences of the United States of America 100(11): 6670-6675.

Ibsen, S. D., J. Wright, J. M. Lewis, S. Kim, S. Y. Ko, J. Ong, S. Manouchehri, A. Vyas, J. Akers, C. C. Chen, B. S. Carter, S. C. Esener and M. J. Heller (2017). "Rapid Isolation and Detection of Exosomes and Associated Biomarkers from Plasma." Acs Nano 11(7): 6641-6651.

Im, H., H. L. Shao, Y. I. Park, V. M. Peterson, C. M. Castro, R. Weissleder and H. Lee (2014). "Label-free detection and molecular profiling of exosomes with a nano-plasmonic sensor." Nature Biotechnology 32(5): 490-U219.

Imrich, S., M. Hachmeister and O. Gires (2012). "EpCAM and its potential role in tumor-initiating cells." Cell adhesion & migration 6(1): 30-38.

Izquierdo-Useros, N., M. Naranjo-Gomez, I. Erkizia, M. C. Puertas, F. E. Borras, J. Blanco and J. Martinez-Picado (2010). "HIV and Mature Dendritic Cells: Trojan Exosomes Riding the Trojan Horse?" Plos Pathogens 6(3).

Kalluri, R. (2016). "The biology and function of exosomes in cancer." Journal of Clinical Investigation 126(4): 1208-1215.

Kanwar, S. S., C. J. Dunlay, D. M. Simeone and S. Nagrath (2014). "Microfluidic device (ExoChip) for on-chip isolation, quantification and characterization of circulating exosomes." Lab on a Chip 14(11): 1891-1900.

Keerthikumar, S., L. Gangoda, M. Liem, P. Fonseka, I. Atukorala, C. Ozcitti, A. Mechler, C. G. Adda, C. S. Ang and S. Mathivanan (2015). "Proteogenomic analysis reveals exosomes are more oncogenic than ectosomes." Oncotarget 6(17): 15375-15396.

Keller, S., J. Ridinger, A. K. Rupp, J. W. Janssen and P. Altevogt (2011). "Body fluid derived exosomes as a novel template for clinical diagnostics." J Transl Med 9: 86.

King, H. W., M. Z. Michael and J. M. Gleadle (2012). "Hypoxic enhancement of exosome release by breast cancer cells." BMC Cancer 12: 421.

Klein-Scory, S., M. M. Tehrani, C. Eilert-Micus, K. A. Adamczyk, N. Wojtalewicz, M. Schnolzer, S. A. Hahn, W. Schmiegel and I. Schwarte-Waldhoff (2014). "New insights in the composition of extracellular vesicles from pancreatic cancer cells: implications for biomarkers and functions." Proteome Science 12.

Klibi, J., T. Niki, A. Riedel, C. Pioche-Durieu, S. Souquere, E. Rubinstein, S. Le Moulec, J. Guigay, M. Hirashima, F. Guemira, D. Adhikary, J. Mautner and P. Busson (2009). "Blood diffusion and Th1-suppressive effects of galectin-9-containing exosomes released by Epstein-Barr virus-infected nasopharyngeal carcinoma cells." Blood 113(9): 1957-1966.

Koliha, N., Y. Wiencek, U. Heider, C. Jungst, N. Kladt, S. Krauthauser, I. C. Johnston, A. Bosio, A. Schauss and S. Wild (2016). "A novel multiplex bead-based platform highlights the diversity of extracellular vesicles." J Extracell Vesicles 5: 29975.

Kowal, J., G. Arras, M. Colombo, M. Jouve, J. P. Morath, B. Primdal-Bengtson, F. Dingli, D. Loew, M. Tkach and C. Thery (2016). "Proteomic comparison defines novel markers to characterize heterogeneous populations of extracellular vesicle subtypes." Proc Natl Acad Sci U S A 113(8): E968-977.

Kozak, D., W. Anderson, R. Vogel, S. Chen, F. Antaw and M. Trau (2012). "Simultaneous size and zeta-potential measurements of individual nanoparticles in dispersion using size-tunable pore sensors." ACS Nano 6(8): 6990-6997.

Kruh-Garcia, N. A., L. M. Wolfe, L. H. Chaisson, W. O. Worodria, P. Nahid, J. S. Schorey, J. L. Davis and K. M. Dobos (2014). "Detection of Mycobacterium tuberculosis peptides in the exosomes of patients with active and latent M. tuberculosis infection using MRM-MS." PLoS One 9(7): e103811.

Lee, K., K. Fraser, B. Ghaddar, K. Yang, E. Kim, L. Balaj, E. A. Chiocca, X. O. Breakefield, H. Lee and R. Weissleder (2018). "Multiplexed Profiling of Single Extracellular Vesicles." ACS nano 12(1): 494-503.

Lee, Y., S. El Andaloussi and M. J. Wood (2012). "Exosomes and microvesicles: extracellular vesicles for genetic information transfer and gene therapy." Hum Mol Genet 21(R1): R125-134.

Lenassi, M., G. Cagney, M. Liao, T. Vaupotic, K. Bartholomeeusen, Y. Cheng, N. J. Krogan, A. Plemenitas and B. M. Peterlin (2010). "HIV Nef is secreted in exosomes and triggers apoptosis in bystander CD4+ T cells." Traffic 11(1): 110-122.

Lenassi, M., G. Cagney, M. F. Liao, T. Vaupotic, K. Bartholomeeusen, Y. F. Cheng, N. J. Krogan, A. Plemenitas and B. M. Peterlin (2010). "HIV Nef is Secreted in Exosomes and Triggers Apoptosis in Bystander CD4(+) T Cells." Traffic 11(1): 110-122.

Lener, T., M. Gimona, L. Aigner, V. Borger, E. Buzas, G. Camussi, N. Chaput, D. Chatterjee, F. A. Court, H. A. del Portillo, L. O'Driscoll, S. Fais, J. M. Falcon-Perez, U. Felderhoff-Mueser, L. Fraile, Y. S. Gho, A. Gorgens, R. C. Gupta, A. Hendrix, D. M. Hermann, A. F. Hill, F. Hochberg, P. A. Horn, D. de Kleijn, L. Kordelas, B. W. Kramer, E. M. Kramer-Albers, S. Laner-Plamberger, S. Laitinen, T. Leonardi, M. J. Lorenowicz, S. K. Lim, J. Lotvall, C. A. Maguire, A. Marcilla, I. Nazarenko, T. Ochiya, T. Patel, S. Pedersen, G. Pocsfalvi, S. Pluchino, P. Quesenberry, I. G. Reischl, F. J. Rivera, R. Sanzenbacher, K. Schallmoser, I. Slaper-Cortenbach, D. Strunk, T. Tonn, P. Vader, B. W. M. van Balkom, M. Wauben, S. El Andaloussi, C. Thery, E. Rohde and B. Giebel (2015). "Applying extracellular vesicles based therapeutics in clinical trials - an ISEV position paper." Journal of Extracellular Vesicles 4.

Li, M., E. Zeringer, T. Barta, J. Schageman, A. Cheng and A. V. Vlassov (2014). "Analysis of the RNA content of the exosomes derived from blood serum and urine and its potential as biomarkers." Philosophical transactions of the Royal Society of London. Series B, Biological sciences 369(1652): 20130502.

Li, M., E. Zeringer, T. Barta, J. Schageman, A. G. Cheng and A. V. Vlassov (2014). "Analysis of the RNA content of the exosomes derived from blood serum and urine and its potential as biomarkers." Philosophical Transactions of the Royal Society B-Biological Sciences 369(1652).

Liang, K., F. Liu, J. Fan, D. Sun, C. Liu, C. J. Lyon, D. W. Bernard, Y. Li, K. Yokoi, M. H. Katz, E. J. Koay, Z. Zhao and Y. Hu (2017). "Nanoplasmonic quantification of tumour-derived extracellular vesicles in plasma microsamples for diagnosis and treatment monitoring." Nature Biomedical Engineering 1: 0021.

Lindberg, R. A. and T. Hunter (1990). "cDNA cloning and characterization of eck, an epithelial cell receptor protein-tyrosine kinase in the eph/elk family of protein kinases." Mol Cell Biol 10(12): 6316-6324.

Loosen, S. H., U. P. Neumann, C. Trautwein, C. Roderburg and T. Luedde (2017). "Current and future biomarkers for pancreatic adenocarcinoma." Tumor Biology 39(6).

Luketic, L., J. Delanghe, P. T. Sobol, P. C. Yang, E. Frotten, K. L. Mossman, J. Gauldie, J. Bramson and Y. H. Wan (2007). "Antigen presentation by exosomes released from peptide-pulsed dendritic cells is not suppressed by the presence of active CTL." Journal of Immunology 179(8): 5024-5032.

Mack, M., A. Kleinschmidt, H. Bruhl, C. Klier, P. J. Nelson, J. Cihak, J. Plachy, M. Stangassinger, V. Erfle and D. Schlondorff (2000). "Transfer of the chemokine receptor CCR5 between cells by membrane-derived microparticles: A mechanism for cellular human immunodeficiency virus 1 infection." Nature Medicine 6(7): 769-+.

Mahon, R. N., O. J. Sande, R. E. Rojas, A. D. Levine, C. V. Harding and W. H. Boom (2012). "Mycobacterium tuberculosis ManLAM inhibits T-cell-receptor signaling by interference with ZAP-70, Lck and LAT phosphorylation." Cellular Immunology 275(1-2): 98-105.

Matsuo, H., J. Chevallier, N. Mayran, I. Le Blanc, C. Ferguson, J. Faure, N. S. Blanc, S. Matile, J. Dubochet, R. Sadoul, R. G. Parton, F. Vilbois and J. Gruenberg (2004). "Role of LBPA and Alix in multivesicular liposome formation and endosome organization." Science 303(5657): 531-534.

McKnight, K. L., L. Xie, O. Gonzalez-Lopez, E. E. Rivera-Serrano, X. Chen and S. M. Lemon (2017). "Protein composition of the hepatitis A virus quasi-envelope." Proc Natl Acad Sci U S A 114(25): 6587-6592.

Meckes, D. G., Jr., H. P. Gunawardena, R. M. Dekroon, P. R. Heaton, R. H. Edwards, S. Ozgur, J. D. Griffith, B. Damania and N. Raab-Traub (2013). "Modulation of B-cell exosome proteins by gamma herpesvirus infection." Proc Natl Acad Sci U S A 110(31): E2925-2933.

Meckes, D. G., Jr., K. H. Shair, A. R. Marquitz, C. P. Kung, R. H. Edwards and N. Raab-Traub (2010). "Human tumor virus utilizes exosomes for intercellular communication." Proc Natl Acad Sci U S A 107(47): 20370-20375.

Melo, S. A., L. B. Luecke, C. Kahlert, A. F. Fernandez, S. T. Gammon, J. Kaye, V. S. LeBleu, E. A. Mittendorf, J. Weitz, N. Rahbari, C. Reissfelder, C. Pilarsky, M. F. Fraga, D. Piwnica-Worms and R. Kalluri (2015). "Glypican-1 identifies cancer exosomes and detects early pancreatic cancer." Nature 523: 177.

Melo, S. A., H. Sugimoto, J. T. O'Connell, N. Kato, A. Villanueva, A. Vidal, L. Qiu, E. Vitkin, L. T. Perelman, C. A. Melo, A. Lucci, C. Ivan, G. A. Calin and R. Kalluri (2014). "Cancer Exosomes Perform Cell-Independent MicroRNA Biogenesis and Promote Tumorigenesis." Cancer Cell 26(5): 707-721.

Mendt, M., S. Kamerkar, H. Sugimoto, K. M. McAndrews, C. C. Wu, M. Gagea, S. Yang, E. V. R. Blanko, Q. Peng, X. Ma, J. R. Marszalek, A. Maitra, C. Yee, K. Rezvani, E. Shpall, V. S. LeBleu and R. Kalluri (2018). "Generation and testing of clinical-grade exosomes for pancreatic cancer." JCI Insight 3(8).

Mittelbrunn, M., C. Gutierrez-Vazquez, C. Villarroya-Beltri, S. Gonzalez, F. Sanchez-Cabo, M. A. Gonzalez, A. Bernad and F. Sanchez-Madrid (2011). "Unidirectional transfer of microRNA-loaded exosomes from T cells to antigen-presenting cells." Nature Communications 2.

Montecalvo, A., W. J. Shufesky, D. B. Stolz, M. G. Sullivan, Z. L. Wang, S. J. Divito, G. D. Papworth, S. C. Watkins, P. D. Robbins, A. T. Larregina and A. E. Morelli (2008). "Exosomes as a short-range mechanism to spread alloantigen between dendiritic cells during T cell allorecognition." Journal of Immunology 180(5): 3081-3090.

Morse, M. A., J. Garst, T. Osada, S. Khan, A. Hobeika, T. M. Clay, N. Valente, R. Shreeniwas, M. A. Sutton, A. Delcayre, D. H. Hsu, J. B. Le Pecq and H. K. Lyerly (2005). "A phase I study of dexosome immunotherapy in patients with advanced non-small cell lung cancer." J Transl Med 3: 9.

Mudali, S. V., B. J. Fu, S. S. Lakkur, M. D. Luo, E. E. Embuscado and C. A. Iacobuzio-Donahue (2006). "Patterns of EphA2 protein expression in primary and metastatic pancreatic carcinoma and correlation with genetic status." Clinical & Experimental Metastasis 23(7-8): 357-365.

Muntasell, A., A. C. Berger and P. A. Roche (2007). "T cell-induced secretion of MHC class II-peptide complexes on B cell exosomes." Embo Journal 26(19): 4263-4272.

Nagashima, S., S. Jirintai, M. Takahashi, T. Kobayashi, Tanggis, T. Nishizawa, T. Kouki, T. Yashiro and H. Okamoto (2014). "Hepatitis E virus egress depends on the exosomal pathway, with secretory exosomes derived from multivesicular bodies." J Gen Virol 95(Pt 10): 2166-2175.

Narayanan, A., S. Iordanskiy, R. Das, R. Van Duyne, S. Santos, E. Jaworski, I. Guendel, G. Sampey, E. Dalby, M. Iglesias-Ussel, A. Popratiloff, R. Hakami, K. Kehn-Hall, M. Young, C. Subra, C. Gilbert, C. Bailey, F. Romerio and F. Kashanchi (2013). "Exosomes Derived from HIV-1-infected Cells Contain Trans-activation Response Element RNA." Journal of Biological Chemistry 288(27): 20014-20033.

Nguyen, D. G., A. Booth, S. J. Gould and J. E. K. Hildreth (2003). "Evidence that HIV budding in primary macrophages occurs through the exosome release pathway." Journal of Biological Chemistry 278(52): 52347-52354.

Nolte-'t Hoen, E. N. M., S. I. Buschow, S. M. Anderton, W. Stoorvogel and M. H. M. Wauben (2009). "Activated T cells recruit exosomes secreted by dendritic cells via LFA-1." Blood 113(9): 1977-1981.

Nuzhat, Z., V. Kinhal, S. Sharma, G. E. Rice, V. Joshi and C. Salomon (2017). "Tumour-derived exosomes as a signature of pancreatic cancer - liquid biopsies as indicators of tumour progression." Oncotarget 8(10): 17279-17291.

Osteikoetxea, X., B. Sodar, A. Nemeth, K. Szabo-Taylor, K. Paloczi, K. V. Vukman, V. Tamasi, A. Balogh, A. Kittel, E. Pallinger and E. I. Buzas (2015). "Differential detergent sensitivity of extracellular vesicle subpopulations." Organic & Biomolecular Chemistry 13(38): 9775-9782.

Pant, S., H. Hilton and M. E. Burczynski (2012). "The multifaceted exosome: biogenesis, role in normal and aberrant cellular function, and frontiers for pharmacological and biomarker opportunities." Biochem Pharmacol 83(11): 1484-1494.

Parolini, I., C. Federici, C. Raggi, L. Lugini, S. Palleschi, A. De Milito, C. Coscia, E. Iessi, M. Logozzi, A. Molinari, M. Colone, M. Tatti, M. Sargiacomo and S. Fais (2009). "Microenvironmental pH Is a Key Factor for Exosome Traffic in Tumor Cells." Journal of Biological Chemistry 284(49): 34211-34222.

Pathak, S., M. C. Davidson and G. A. Silva (2007). "Characterization of the functional binding properties of antibody conjugated quantum dots." Nano Letters 7(7): 1839-1845.

Pawliczek, T. and C. M. Crump (2009). "Herpes simplex virus type 1 production requires a functional ESCRT-III complex but is independent of TSG101 and ALIX expression." J Virol 83(21): 11254-11264.

Pegtel, D. M., K. Cosmopoulos, D. A. Thorley-Lawson, M. A. J. van Eijndhoven, E. S. Hopmans, J. L. Lindenberg, T. D. de Gruijl, T. Wurdinger and J. M. Middeldorp (2010). "Functional delivery of viral miRNAs via exosomes." Proceedings of the National Academy of Sciences of the United States of America 107(14): 6328-6333.

Pepe, M. S., R. Etzioni, Z. D. Feng, J. D. Potter, M. L. Thompson, M. Thornquist, M. Winget and Y. Yasui (2001). "Phases of biomarker development for early detection of cancer." Journal of the National Cancer Institute 93(14): 1054-1061.

Pfeffer, S., M. Zavolan, F. A. Grasser, M. C. Chien, J. J. Russo, J. Y. Ju, B. John, A. J. Enright, D. Marks, C. Sander and T. Tuschl (2004). "Identification of virus-encoded microRNAs." Science 304(5671): 734-736.

Pileri, P., Y. Uematsu, S. Campagnoli, G. Galli, F. Falugi, R. Petracca, A. J. Weiner, M. Houghton, D. Rosa, G. Grandi and S. Abrignani (1998). "Binding of hepatitis C virus to CD81." Science 282(5390): 938-941.

Qazi, K. R., U. Gehrmann, E. D. Jordo, M. C. I. Karlsson and S. Gabrielsson (2009). "Antigen-loaded exosomes alone induce Th1-type memory through a B cell-dependent mechanism." Blood 113(12): 2673-2683.

Raab-Traub, N. and D. P. Dittmer (2017). "Viral effects on the content and function of extracellular vesicles." Nat Rev Microbiol.

Raiborg, C. and H. Stenmark (2009). "The ESCRT machinery in endosomal sorting of ubiquitylated membrane proteins." Nature 458(7237): 445-452.

Rajagopal, C. and K. B. Harikumar (2018). "The Origin and Functions of Exosomes in Cancer." Frontiers in Oncology 8.

Ramakrishnaiah, V., C. Thumann, I. Fofana, F. Habersetzer, Q. W. Pan, P. E. de Ruiter, R. Willemsen, J. A. A. Demmers, V. S. Raj, G. Jenster, J. Kwekkeboom, H. W. Tilanus, B. L. Haagmans, T. F. Baumert and L. J. W. van der Laan (2013). "Exosome-mediated transmission of hepatitis C virus between human hepatoma Huh7.5 cells." Proceedings of the National Academy of Sciences of the United States of America 110(32): 13109-13113.

Raposo, G., H. W. Nijman, W. Stoorvogel, R. Leijendekker, C. V. Harding, C. J. M. Melief and H. J. Geuze (1996). "B lymphocytes secrete antigen-presenting vesicles." Journal of Experimental Medicine 183(3): 1161-1172.

Raposo, G. and W. Stoorvogel (2013). "Extracellular vesicles: Exosomes, microvesicles, and friends." Journal of Cell Biology 200(4): 373-383.

Ratajczak, J., K. Miekus, M. Kucia, J. Zhang, R. Reca, P. Dvorak and M. Z. Ratajczak (2006). "Embryonic stem cell-derived microvesicles reprogram hematopoietic progenitors: evidence for horizontal transfer of mRNA and protein delivery." Leukemia 20(5): 847-856.

Raymond, A. D., T. C. Campbell-Sims, M. Khan, M. Lang, M. B. Huang, V. C. Bond and M. D. Powell (2011). "HIV Type 1 Nef Is Released from Infected Cells in CD45(+) Microvesicles and Is Present in the Plasma of HIV-Infected Individuals." Aids Research and Human Retroviruses 27(2): 167-178.

Rodrigues, M., J. Fan, C. Lyon, M. H. Wan and Y. Hu (2018). "Role of Extracellular Vesicles in Viral and Bacterial Infections: Pathogenesis, Diagnostics, and Therapeutics." Theranostics 8(10): 2709-2721.

Rozmyslowicz, T., M. Majka, J. Kijowski, S. L. Murphy, D. O. Conover, M. Poncz, J. Ratajczak, G. N. Gaulton and M. Z. Ratajczak (2003). "Platelet- and megakaryocyte-

derived microparticles transfer CXCR4 receptor to CXCR4-null cells and make them susceptible to infection by X4-HIV." Aids 17(1): 33-42.

Sadeghipour, S. and R. A. Mathias (2017). "Herpesviruses hijack host exosomes for viral pathogenesis." Semin Cell Dev Biol 67: 91-100.

Sarker, S., K. Scholz-Romero, A. Perez, S. E. Illanes, M. D. Mitchell, G. E. Rice and C. Salomon (2014). "Placenta-derived exosomes continuously increase in maternal circulation over the first trimester of pregnancy." Journal of Translational Medicine 12.

Savina, A., M. Furlan, M. Vidal and M. I. Colombo (2003). "Exosome release is regulated by a calcium-dependent mechanism in K562 cells." Journal of Biological Chemistry 278(22): 20083-20090.

Schaefer, M. R., E. R. Wonderlich, J. F. Roeth, J. A. Leonard and K. L. Collins (2008). "HIV-1 Nef targets MHC-I and CD4 for degradation via a final common beta-COP-dependent pathway in T cells." Plos Pathogens 4(8).

Schnell, U., V. Cirulli and B. N. Giepmans (2013). "EpCAM: structure and function in health and disease." Biochim Biophys Acta 1828(8): 1989-2001.

Schorey, J. S. and S. Bhatnagar (2008). "Exosome function: From tumor immunology to pathogen biology." Traffic 9(6): 871-881.

Schorey, J. S. and C. V. Harding (2016). "Extracellular vesicles and infectious diseases: new complexity to an old story." J Clin Invest 126(4): 1181-1189.

Segura, E., S. Amigorena and C. Thery (2005). "Mature dendritic cells secrete exosomes with strong ability to induce antigen-specific effector immune responses." Blood Cells Molecules and Diseases 35(2): 89-93.

Shao, H. L., J. Chung, K. Lee, L. Balaj, C. Min, B. S. Carter, F. H. Hochberg, X. O. Breakefield, H. Lee and R. Weissleder (2015). "Chip-based analysis of exosomal mRNA mediating drug resistance in glioblastoma." Nature Communications 6.

Shao, H. L., H. Im, C. M. Castro, X. Breakefield, R. Weissleder and H. H. Lee (2018). "New Technologies for Analysis of Extracellular Vesicles." Chemical Reviews 118(4): 1917-1950.

Sharma, S., F. Zuniga, G. E. Rice, L. C. Perrin, J. D. Hooper and C. Salomon (2017). "Tumor-derived exosomes in ovarian cancer - liquid biopsies for early detection and real-time monitoring of cancer progression." Oncotarget 8(61): 104687-104703.

Sheridan, C. (2016). "Exosome cancer diagnostic reaches market." Nat Biotechnol 34(4): 359-360.

Shi, M., C. Q. Liu, T. J. Cook, K. M. Bullock, Y. C. Zhao, C. Ginghina, Y. F. Li, P. Aro, R. Dator, C. M. He, M. J. Hipp, C. P. Zabetian, E. Peskind, S. C. Hu, J. F. Quinn, D. R. Galasko, W. A. Banks and J. Zhang (2014). "Plasma exosomal alpha-synuclein is likely CNS-derived and increased in Parkinson's disease." Acta Neuropathologica 128(5): 639-650.

Singh, P. P., L. Li and J. S. Schorey (2015). "Exosomal RNA from Mycobacterium tuberculosis-Infected Cells Is Functional in Recipient Macrophages." Traffic 16(6): 555-571.

Singh, P. P., V. L. Smith, P. C. Karakousis and J. S. Schorey (2012). "Exosomes Isolated from Mycobacteria-Infected Mice or Cultured Macrophages Can Recruit and Activate Immune Cells In Vitro and In Vivo." Journal of Immunology 189(2): 777-785.

Sun, D., X. Zhuang, X. Xiang, Y. Liu, S. Zhang, C. Liu, S. Barnes, W. Grizzle, D. Miller and H. G. Zhang (2010). "A novel nanoparticle drug delivery system: the anti-inflammatory activity of curcumin is enhanced when encapsulated in exosomes." Mol Ther 18(9): 1606-1614.

Tamai, K., M. Shiina, N. Tanaka, T. Nakano, A. Yamamoto, Y. Kondo, E. Kakazu, J. Inoue, K. Fukushima, K. Sano, Y. Ueno, T. Shimosegawa and K. Sugamura (2012). "Regulation of hepatitis C virus secretion by the Hrs-dependent exosomal pathway." Virology 422(2): 377-385.

Taylor, D. D. and C. Gercel-Taylor (2008). "MicroRNA signatures of tumor-derived exosomes as diagnostic biomarkers of ovarian cancer." Gynecologic Oncology 110(1): 13-21.

Taylor, D. D. and C. Gercel-Taylor (2008). "MicroRNA signatures of tumor-derived exosomes as diagnostic biomarkers of ovarian cancer." Gynecol Oncol 110(1): 13-21.

Thakur, B. K., H. Zhang, A. Becker, I. Matei, Y. Huang, B. Costa-Silva, Y. Zheng, A. Hoshino, H. Brazier, J. Xiang, C. Williams, R. Rodriguez-Barrueco, J. M. Silva, W. Zhang, S. Hearn, O. Elemento, N. Paknejad, K. Manova-Todorova, K. Welte, J. Bromberg, H. Peinado and D. Lyden (2014). "Double-stranded DNA in exosomes: a novel biomarker in cancer detection." Cell Research 24: 766.

Thery, C., S. Amigorena, G. Raposo and A. Clayton (2006). "Isolation and characterization of exosomes from cell culture supernatants and biological fluids." Curr Protoc Cell Biol Chapter 3: Unit 3 22.

Thery, C., L. Duban, E. Segura, P. Veron, O. Lantz and S. Amigorena (2002). "Indirect activation of naive CD4(+) T cells by dendritic cell-derived exosomes." Nature Immunology 3(12): 1156-1162.

Thompson, C. A., A. Purushothaman, V. C. Ramani, I. Vlodavsky and R. D. Sanderson (2013). "Heparanase regulates secretion, composition, and function of tumor cell-derived exosomes." J Biol Chem 288(14): 10093-10099.

Tian, Y., S. Li, J. Song, T. Ji, M. Zhu, G. J. Anderson, J. Wei and G. Nie (2014). "A doxorubicin delivery platform using engineered natural membrane vesicle exosomes for targeted tumor therapy." Biomaterials 35(7): 2383-2390.

Toseland, C. P. (2013). "Fluorescent labeling and modification of proteins." J Chem Biol 6(3): 85-95.

Utsugi-Kobukai, S., H. Fujimaki, C. Hotta, M. Nakazawa and M. Minami (2003). "MHC class I-mediated exogenous antigen presentation by exosomes secreted from immature and mature bone marrow derived dendritic cells." Immunology Letters 89(2-3): 125-131.

Vaidyanathan, R., R. H. Soon, P. Zhang, K. Jiang and C. T. Lim (2019). "Cancer diagnosis: from tumor to liquid biopsy and beyond." Lab on a Chip 19(1): 11-34.

Valadi, H., K. Ekstrom, A. Bossios, M. Sjostrand, J. J. Lee and J. O. Lotvall (2007). "Exosome-mediated transfer of mRNAs and microRNAs is a novel mechanism of genetic exchange between cells." Nature Cell Biology 9(6): 654-U672.

van der Pol, E., A. N. Boing, P. Harrison, A. Sturk and R. Nieuwland (2012). "Classification, Functions, and Clinical Relevance of Extracellular Vesicles." Pharmacological Reviews 64(3): 676-705.

van der Vlist, E. J., E. N. Nolte-'t Hoen, W. Stoorvogel, G. J. Arkesteijn and M. H. Wauben (2012). "Fluorescent labeling of nano-sized vesicles released by cells and subsequent quantitative and qualitative analysis by high-resolution flow cytometry." Nat Protoc 7(7): 1311-1326.

van Niel, G., G. D'Angelo and G. Raposo (2018). "Shedding light on the cell biology of extracellular vesicles." Nature Reviews Molecular Cell Biology 19: 213.

Verweij, F. J., M. A. J. van Eijndhoven, E. S. Hopmans, T. Vendrig, T. Wurdinger, E. Cahir-McFarland, E. Kieff, D. Geerts, R. van der Kant, J. Neefjes, J. M. Middeldorp and D. M. Pegtel (2011). "LMP1 association with CD63 in endosomes and secretion via exosomes limits constitutive NF-kappa B activation." Embo Journal 30(11): 2115-2129.

Visvader, J. E. and G. J. Lindeman (2009). "EpCAM and solid tumour fractionation." Nature Reviews Cancer 9(2): 144-144.

Vogel, R., G. Willmott, D. Kozak, G. S. Roberts, W. Anderson, L. Groenewegen, B. Glossop, A. Barnett, A. Turner and M. Trau (2011). "Quantitative sizing of nano/microparticles with a tunable elastomeric pore sensor." Anal Chem 83(9): 3499-3506.

Watanabe, T., E. M. Sorensen, A. Naito, M. Schott, S. Kim and P. Ahlquist (2007). "Involvement of host cellular multivesicular body functions in hepatitis B virus budding." Proc Natl Acad Sci U S A 104(24): 10205-10210.

Whiteside, T. L. (2016). "Tumor-Derived Exosomes and Their Role in Cancer Progression." Advances in Clinical Chemistry, Vol 74 74: 103-141.

Wiley, R. D. and S. Gummuluru (2006). "Immature dendritic cell-derived exosomes can mediate HIV-1 trans infection." Proceedings of the National Academy of Sciences of the United States of America 103(3): 738-743.

Williams, C., R. Rodriguez-Barrueco, J. M. Silva, W. J. Zhang, S. Hearn, O. Elemento, N. Paknejad, K. Manova-Todorova, K. Welte, J. Bromberg, H. Peinado and D. Lyden (2014). "Double-stranded DNA in exosomes: a novel biomarker in cancer detection." Cell Research 24(6): 766-769.

Willms, E., H. J. Johansson, I. Mager, Y. Lee, K. E. Blomberg, M. Sadik, A. Alaarg, C. I. Smith, J. Lehtio, S. El Andaloussi, M. J. Wood and P. Vader (2016). "Cells release subpopulations of exosomes with distinct molecular and biological properties." Sci Rep 6: 22519.

Witwer, K. W., E. I. Buzas, L. T. Bemis, A. Bora, C. Lasser, J. Lotvall, E. N. Nolte-'t Hoen, M. G. Piper, S. Sivaraman, J. Skog, C. Thery, M. H. Wauben and F. Hochberg (2013). "Standardization of sample collection, isolation and analysis methods in extracellular vesicle research." J Extracell Vesicles 2.

Xu, R., A. Rai, M. S. Chen, W. Suwakulsiri, D. W. Greening and R. J. Simpson (2018). "Extracellular vesicles in cancer - implications for future improvements in cancer care." Nature Reviews Clinical Oncology 15(10): 617-638.

Yachida, S., S. Jones, I. Bozic, T. Antal, R. Leary, B. J. Fu, M. Kamiyama, R. H. Hruban, J. R. Eshleman, M. A. Nowak, V. E. Velculescu, K. W. Kinzler, B. Vogelstein and C. A. Iacobuzio-Donahue (2010). "Distant metastasis occurs late during the genetic evolution of pancreatic cancer." Nature 467(7319): 1114-U1126.

Yang, C. J., M. A. Ruffner, S. H. Kim and P. D. Robbins (2012). "Plasma-derived MHC class II+ exosomes from tumor-bearing mice suppress tumor antigen-specific immune responses." European Journal of Immunology 42(7): 1778-1784.

Yang, H. J., T. J. Huang, C. F. Yang, L. X. Peng, R. Y. Liu, G. D. Yang, Q. Q. Chu, J. L. Huang, N. Liu, H. B. Huang, Z. Y. Zhu, C. N. Qian and B. J. Huang (2013). "Comprehensive profiling of Epstein-Barr virus-encoded miRNA species associated with specific latency types in tumor cells." Virology Journal 10.

Yang, K. S., H. Im, S. Hong, I. Pergolini, A. F. del Castillo, R. Wang, S. Clardy, C.-H. Huang, C. Pille, S. Ferrone, R. Yang, C. M. Castro, H. Lee, C. F. del Castillo and R. Weissleder (2017). "Multiparametric plasma EV profiling facilitates diagnosis of pancreatic malignancy." Science Translational Medicine 9(391).

Yu, J. L., L. May, V. Lhotak, S. Shahrzad, S. Shirasawa, J. I. Weitz, B. L. Coomber, N. Mackman and J. W. Rak (2005). "Oncogenic events regulate tissue factor expression in colorectal cancer cells: implications for tumor progression and angiogenesis." Blood 105(4): 1734-1741.

Yu, X., S. L. Harris and A. J. Levine (2006). "The regulation of exosome secretion: a novel function of the p53 protein." Cancer Res 66(9): 4795-4801.

Yuana, Y., R. I. Koning, M. E. Kuil, P. C. Rensen, A. J. Koster, R. M. Bertina and S. Osanto (2013). "Cryo-electron microscopy of extracellular vesicles in fresh plasma." J Extracell Vesicles 2.

Zelinski, D. P., N. D. Zantek, J. C. Stewart, A. R. Irizarry and M. S. Kinch (2001). "EphA2 overexpression causes tumorigenesis of mammary epithelial cells." Cancer Research 61(5): 2301-2306.

Zhang, J., G. Randall, A. Higginbottom, P. Monk, C. M. Rice and J. A. McKeating (2004). "CD81 is required for hepatitis C virus glycoprotein-mediated viral infection." Journal of Virology 78(3): 1448-1455.

Zhang, X., X. Yuan, H. Shi, L. J. Wu, H. Qian and W. R. Xu (2015). "Exosomes in cancer: small particle, big player." Journal of Hematology & Oncology 8.

APPENDIX A

MATLAB CODE FOR ROC FOR SINGLE MARKERS AND COMBINED MARKERS

A MATLAB CODE FOR ROC FOR SINGLE MARKERS AND COMBINED MARKERS

```
Close all;

Clear all;

load ('ROCcombinedvalues053019.mat');

%% Individual

% Marker 1

range_control = 1:12;

range_cancer = 1:20;

range_cancer2 = 13:32;


M1_norm = [ZhaoClinicalMeryl2 {range_control,'Control'} ;
ZhaoClinicalMeryl2{range_cancer, 'Cancer'}];

pred_ind = M1_norm;

Y = []; Y(range_control,1) = 0; Y(range_cancer2,1) = 1; % Combining control and
cancer in a single variable and indication with 0 and 1.

mdl_ind1 = fitglm (pred_ind,Y,'Distribution','binomial','Link','logit');

labels = strings ; labels(range_control,1) = 'Control'; labels(range_cancer2,1) = 'Cancer';

scores_ind = mdl_ind1.Fitted.Probability;

[X_ind1,Y_ind1,T_ind1, AUC_ind1] = perfcurve(labels,scores_ind,'Cancer');


% Un - normalized data

M1_unnorm = [ZhaoClinicalMeryl2{range_control,'Control2'} ;
ZhaoClinicalMeryl2{range_cancer, 'Cancer2'}];


pred_ind2 = M1_unnorm;

mdl_ind2 = fitglm(pred_ind2,Y,'Distribution','binomial','Link','logit');


labels = strings ; labels(range_control,1) = 'Control'; labels(range_cancer2,1) = 'Cancer';

scores_ind2 = mdl_ind2.Fitted.Probability;
```

```
[X_ind2,Y_ind2,T_ind2,AUC_ind2] = perfcurve(labels,scores_ind2,'Cancer');


figure();

plot(X_ind1, Y_ind1,'LineWidth',2); hold on;

plot(X_ind2,Y_ind2, 'LineWidth',2);

legend('DiO-Normalized EpCAM (AUC:0.95)','Raw EpCAM (AUC:
0.77)','FontSize',12);

set(gca,'FontSize',9);

ylabel('Sensitivity','FontSize',16);

xlabel('1 - Specificity','FontSize',16);

% title('ROC Curve Analysis-EpCAM');



% Marker 2

M2_norm = [ZhaoClinicalMeryl2{range_control,'Control1'}
;ZhaoClinicalMeryl2{range_cancer, 'Cancer1'}];

pred_ind3 = M2_norm;

Y = []; Y(range_control,1) = 0; Y(range_cancer2,1) = 1;

mdl_ind3 = fitglm(pred_ind3,Y,'Distribution','binomial','Link','logit');

labels = strings ; labels(range_control,1) = 'Control'; labels(range_cancer2,1) = 'Cancer';

scores_ind3 = mdl_ind3.Fitted.Probability;

[X_ind3,Y_ind3,T_ind3, AUC_ind3] = perfcurve(labels,scores_ind3,'Cancer');


% Un - normalized data

M2_unnorm = [ZhaoClinicalMeryl2{range_control,'Control3'}

ZhaoClinicalMeryl2{range_cancer, 'Cancer3'}];



pred_ind4 = M2_unnorm;

mdl_ind4 = fitglm(pred_ind4,Y,'Distribution','binomial','Link','logit');
```

```
labels = strings ; labels(range_control,1) = 'Control'; labels(range_cancer2,1) = 'Cancer';
scores_ind4 = mdl_ind4.Fitted.Probability;
[X_ind4,Y_ind4,T_ind4,AUC_ind4] = perfcurve(labels,scores_ind4,'Cancer');

figure();
plot(X_ind3, Y_ind3, 'LineWidth',2); hold on;
plot(X_ind4,Y_ind4,'LineWidth',2);
legend('DiO-Normalized EphA2 (AUC:0.97)','Raw EphA2 (AUC: 0.82)','FontSize',12);
set(gca,'FontSize',9);
ylabel('Sensitivity','FontSize',16);
xlabel('1 - Specificity','Fontsize',16);
% title('ROC Curve Analysis EphA_2');

%% Combined Markers
% Reorganize data
M1_norm = [ZhaoClinicalMeryl2{range_control,'Control'} ;
ZhaoClinicalMeryl2{range_cancer, 'Cancer'}];
M2_norm = [ZhaoClinicalMeryl2{range_control,'Control1'}
;ZhaoClinicalMeryl2{range_cancer, 'Cancer1'}];
pred = [M1_norm M2_norm];
Y = []; Y(range_control,1) = 0; Y(range_cancer2,1) = 1;
mdl_comb1 = fitglm(pred,Y,'Distribution','binomial','Link','logit');
labels = strings ; labels(range_control,1) = 'Control'; labels(range_cancer2,1) = 'Cancer';
scores = mdl_comb1.Fitted.Probability;
[X_norm,Y_norm,T_norm, AUC_norm] = perfcurve(labels,scores,'Cancer');

% Un - normalized data
M1_unnorm = [ZhaoClinicalMeryl2{range_control,'Control2'} ;
ZhaoClinicalMeryl2{range_cancer, 'Cancer2'}];
```

```
M2_unnorm = [ZhaoClinicalMeryl2{range_control,'Control3'} ;
ZhaoClinicalMeryl2{range_cancer, 'Cancer3'}];

pred2 = [M1_unnorm M2_unnorm];

mdl_comb2 = fitglm(pred2,Y,'Distribution','binomial','Link','logit');

labels = strings ; labels(range_control,1) = 'Control'; labels(range_cancer2,1) = 'Cancer';

scores_2 = mdl_comb2.Fitted.Probability;

[X_unnorm,Y_unnorm,T_unnorm,AUC_unnorm] = perfcurve(labels,scores_2,'Cancer');


figure();

plot(X_norm, Y_norm, 'LineWidth',2,'Color','k'); hold on;

plot(X_unnorm,Y_unnorm,'LineWidth',2,'Color','g');

legend('DiO-Normalized EpCAM EphA2 (AUC:0.95)','Raw EpCAM EphA2 (AUC:
0.77)','FontSize',12);

set(gca,'FontSize',9);

ylabel('Sensitivity','FontSize',16);

xlabel('1 - Specificity','FontSize',16);

% title('ROC Curve Analysis - Combined');
```